HIV-1 Reverse Transcriptase: Determinants and Impact of the Translocational Equilibrium with Implications for Drug Resistance

Brian James Scarth

Department of Microbiology and Immunology

McGill University, Montréal

February 2011

Thesis submitted to McGill University in

partial fulfillment of the degree of Doctor of Philosophy

Abstract

The process of translocation by the reverse transcriptase (RT) of human immunodeficiency virus-1 (HIV-1) is a critical step in the incorporation of nucleotides by this polymerase, with functional consequences with respect to both the mechanism of action and resistance to inhibitors of RT. The work contained in this thesis describes the characterization of molecular determinants of the RT translocational equilibrium, and the functional consequences of this equilibrium. Amino acid substitutions F61A and A62V of the fingers subdomain are shown to have opposite effects on the translocational equilibrium with F61A leading to a strong post-translocation bias, and A62V causing increases in the pre-translocation conformation. These effects are related to the activity of the pyrophosphate analogue foscarnet. The impact of the nucleic acid sequence on the translocational equilibrium is also investigated with respect to incorporation and excision of nucleotides. A post-translocation bias is observed for the majority of sequences tested and corresponds to higher efficiency of nucleotide incorporation under pre-steady state conditions with defined sequences. Pre-translocation bias is associated with increased efficiency of excision of chain-terminated nucleotides. Mechanisms for observed differences between pre- and post-translocation sequences and implications for mechanisms of drug resistance are discussed. Finally, this thesis includes the characterization of the mechanism of novel drug resistance-conferring mutation Q151L. Resistance by Q151L to the investigational inhibitor GS-9148 is determined to be increased discrimination by pre-steady state kinetic analysis.

Résumé

Le processus de translocation de la transcriptase inverse (TI) du virus d'immunodéficience humaine-1 (VIH-1) est une étape critique de l'incorporation de nucléotides lors du processus de polymerization. Cette translocation de la TI affecte le mécanisme d'action ainsi que la resistance aux inhibiteurs de cette derniere. Les travaux contenus dans cette thèse décrivent la caractérisation des déterminants moléculaires qui affecte l'équilibre de la translocation de la TI et les consequences fonctionnelles de cet équilibre. Les substitutions des acides aminés F61A et A62V du sous-domaine des doigts ont des effets opposés sur l'équilibre. En effet, la mutation F61A confère une forte tendance vers la post-translocation tandis que la mutation A62V entraîne des augmentations de la conformation pré-translocation. Ces effets sont liés à l'activité de l'analogue de pyrophosphate foscarnet. L'impact de la séquence d'acides nucléiques sur l'équilibre de la translocation est également étudiée à l'égard de l'incorporation et de l'excision de nucléotides. Un biais de post-translocation est observé pour la majorité des séquences testées et correspond à une plus grande efficacité de l'incorporation de nucléotides dans des conditions pre-stationnaires avec des séquences bien définies. Un biais de pré-translocation est associé à une efficacité accrue de l'excision des analogues de nucléotides qui sont utilisés comme anti-rétroviraux dû a leur capacité à bloquer la polymerization suite à leur incorporation par la TI. Les mécanismes des différences observées entre les sequence post-translocation et pré-translocation ainsi que les implications pour les mécanismes de résistance aux médicaments sont discutés. Enfin, cette thèse inclut la caractérisation du mécanisme de résistance de

nouveaux médicaments conférant la mutation Q151L. En effet, l'analyse cinétique pre-stationnaire a demontré que la résistance par Q151L à l'inhibiteur expérimental GS-9148 est causé par une augmentation de la discrimination entre cet inhibiteur et le nucléotide naturel.

Preface

This thesis was written in accordance with McGill University's "Guidelines for Thesis Preparation." The format of this thesis conforms to the "Manuscript-based thesis" option, which states:

"Candidates have the option of including, as part of the thesis, the text of one or more papers submitted, or to be submitted, for publication, or the clearly duplicated text (not the reprints) of one or more published papers. These texts must conform to the "Guidelines for Thesis Preparation" with respect to font size, line spacing and margin sizes and must be bound together as an integral part of the thesis."

Manuscripts included in this thesis:

Scarth, BJ, McCormick, S, Götte, M. Effects of Mutations F61A and A62V in the Fingers Subdomain of HIV-1 Reverse Transcriptase on the Translocational equilibrium. ***Journal of Molecular Biology*** 2011 Jan 14;405(2):349-60

Scarth, BJ, Götte, M. Impact of the Translocational equilibrium of HIV-1 Reverse Transcriptase on Nucleotide Incorporation and Excision. Manuscript in preparation.

Scarth, BJ, White, KL, Chen, JM, Lansdon, EB, Swaminathan, S, Miller, MD, Götte, M. Mechanism of resistance to GS-9148 by the Q151L mutation in HIV-1 Reverse Transcriptase. Manuscript in review for publication in ***Antimicrobial Agents and Chemotherapy***

The contribution of co-authors to published or submitted articles appears in the section "CONTRIBUTIONS OF AUTHORS". The journal of submission and

information from published articles can be found on the title page of the concerned chapters.

Other manuscripts not included in this thesis but to which a significant contribution was made are listed as follows:

Dash C, **Scarth BJ**, Badorrek C, Götte M, Le Grice SF Examining the ribonuclease H primer grip of HIV-1 reverse transcriptase by charge neutralization of RNA/DNA hybrids. Nucleic Acids Research. 2008 Nov;36(20):6363-71.

Ehteshami M, **Scarth BJ**, Tchesnokov EP, Dash C, Le Grice SF, Hallenberger S, Jochmans D, Götte M. Mutations M184V and Y115F in HIV-1 reverse transcriptase discriminate against "nucleotide-competing reverse transcriptase inhibitors". Journal of Biological Chemistry. 2008 Oct 31;283(44):29904-11.

*Ehteshami M, *Beilhartz GL, ***Scarth BJ,** Tchesnokov EP, McCormick S, Wynhoven B, Harrigan PR, Götte M. Connection domain mutations N348I and A360V in HIV-1 reverse transcriptase enhance resistance to 3'-azido-3'-deoxythymidine through both RNase H-dependent and -independent mechanisms. Journal of Biological Chemistry. 2008 Aug 8;283(32):22222-32.
*contributed equally as co-first author

Acknowledgements

I would like to thank my supervisor Dr. Matthias Götte for accepting me into his lab to pursue my PhD. Matthias has guided me through my development as a scientist and I only hope that as I move forward I can bring honor to his name in whatever I do. During difficult times I may not have endured if it were not for having a supervisor whom I respect so greatly and received such support from.

I would next like to thank Suzanne McCormick for her immeasurable help through the years. Without Sue, I would never have been able to do the work I have done. Words cannot express the gratitude I feel.

I would like to thank Dr. Bruno Marchand and Dr. Jerome Deval for their early help in teaching me the techniques that I used for this work, and in particular Dr. Marchand for his development of the site-specific footprinting technique that formed the foundation of much of my work.

I would also like to thank all the members of the Götte lab, past and present, for their thoughtful comments and for creating an environment that fosters intellectual discovery without ever feeling like work. Thank you to Dr. Claudia Dibrammo, Dr. Egor Tchesnocov, Dr. Konstanin Ivanov, Dimitri Coustinous, Dr. Stephen Barry, Dr. Maryam Ehteshami, Greg Beilhartz, Megan Powdrill, Colins Vasquez, Mia Biondi, Jean Bernachez, Svea Rawe, Chris Ablanas, Jenaya Rikard, Anupriya Kulkarni, James Holdon, Dr. Robert Kozak, Dr. Nicolas Bennet and Anick Auger.

I thank Leslie Ribiero for her thoughtful editing for the introduction of this thesis.

I thank Anick Auger for translating the abstract to French.

I thank Greg Beilhartz for thoughtful comments. I also thank Greg for his partnership through the years. We began in the lab on the same day and while I am finishing slightly sooner than he is, I couldn't have done it without him.

I thank Dr. Maryam Ehteshami for her beautiful voice. The music we made together while working side by side was surely inspiration to all around us.

I thank Chris LeSage for help implementing the java script used in chapter three and hosting of this software.

I thank Dr. Egor Tchesnokov for guidance in experimental endeavors and for his continued support in this regard even beyond his time in the lab.

I thank the Murphy family for helping me land in Montreal and making me feel at home in a new city.

Finally, I dedicate this work to my parents Peter and Eleanor Scarth. For giving me both roots and wings. Roots to keep me grounded through tough times. Wings to soar above everything, and explore new worlds.

This work is also dedicated to my siblings, Bruce, Leslie, John, Rosanne, Dawn and Jeff. With your support I always knew I could do this.

Last I want to dedicate this work to my niece and nephews, Owen, Emily, Jake and Ashton. Stay in school all of you, but not necessarily as long as I have.

Contributions of Authors

For all manuscripts included in this thesis WT and mutant enzymes were generated by Suzanne McCormick.

Scarth, BJ, McCormick, S, Götte, M. Effects of Mutations F61A and A62V in the Fingers Subdomain of HIV-1 Reverse Transcriptase on the Translocational equilibrium. ***Journal of Molecular Biology*** 2011 Jan 14;405(2):349-60

This manuscript appears as chapter two in this thesis and was written by BJS and MG. All experiments were performed by BJS with the exception of IC50 determinations using a filter-based assay (Figure 2.3 c and within results text) which were performed by SM.

Scarth, BJ, Götte, M. Impact of the Translocational equilibrium of HIV-1 Reverse Transcriptase on Nucleotide Incorporation and Excision. *Manuscript in preparation.*

This manuscript appears as chapter three in this thesis and was written by BJS and MG. All experiments were performed by BJS.

Scarth, BJ, White, KL, Chen, JM, Lansdon, EB, Swaminathan, S, Miller, MD, Götte, M. Mechanism of resistance to GS-9148 by the Q151L mutation in HIV-1 Reverse Transcriptase Manuscript in review for publication in ***Antimicrobial Agents and Chemotherapy***

This manuscript appears in chapter four of this thesis and was written by BJS, KLW, MDM and MG. All experiments were performed by BJS with the exception of molecular modeling (Figure 4.3) which was performed by SS, JMC and EBL at Gilead.

Frequently used Abbreviations

AIDS – Acquired Immunodeficiency Syndrome

HIV – Human Immunodeficiency Virus

RT – Reverse Transcriptase

NRTI – Nucleoside Analogue Reverse Transcriptase Inhibitor

NNRTI – Non-nucleoside Analogue Reverse Transcriptase Inhibitor

PFA – Foscarnet, Phosphonoformic Acid

TAM – Thymidine-analogue associated Mutation

dNTP – deoxynucleotide triphosphate

ddNTP – dideoxynucelotide triphosphate

ATP – Adenosine Triphosphate

AZT – Zidovudine

TNF – Tenofovir

DEC – Dead-end complex

PPT – Polypurine Tract

PBS – Primer Binding Site

P-site – Priming Site

N-site – Nucleotide Binding Site

k_{pol} – Catalytic Rate of Polymerization

k_{pyro} – Catalytic Rate of Pyrophosphorolysis

K_D – Dissociation Constant

List of Figures and Tables

Table of Contents

Chapter 1 - Introduction

1.1 Preface

The acquired immunodeficiency syndrome (AIDS) epidemic is a global public health concern related to infection with the human immunodeficiency virus (HIV). Estimates made by the world health organization (WHO) in 2009 place the number of people world wide infected with HIV at 33.3 million [1]. In the same year there were an estimated 2.6 million new HIV infections and 1.8 million AIDS related deaths. This epidemic was first officially identified in July of 1981, through an outbreak of pneumocystis carinii pneumonia (PCP) among gay men, reported in the Centre for Disease Control's (CDC) morbidity and mortality weekly report [2]. In the following years the identification of HIV and its etiological link to AIDS would prompt the intense investigation of available and novel therapies targeting HIV infection [3; 4; 5; 6; 7; 8]. The development of modern highly active antiretroviral therapy (HAART), that is now the standard of care in the developed world, and wherever access to treatment is available, has been estimated to have saved more than 3 million years of life [9]. Challenges to the effective use of HAART include drug toxicity and proper adherence [10; 11; 12]. Failure to achieve complete suppression of viral replication leads to the selection of drug resistant strains of HIV and treatment failure [13]. HIV research related to mechanisms of action and resistance to therapies serve to inform developments of novel treatments and treatment choice in response to the rapidly evolving virus.

This chapter covers central concepts related to the link between HIV and AIDS, and HIV virology. Focus is given to the viral reverse transcriptase (RT), which is critically required for viral replication and has been the subject of the work

contained in this thesis. The role of RT in the viral life cycle is discussed with emphasis given to the clinically available and novel mechanisms of RT inhibition and the development of drug resistance by the virus.

1.2 AIDS and HIV

Prior to the discovery of HIV, AIDS was defined as the presence of one of 27 AIDS defining symptoms or opportunistic infections that are not found in the absence of immune suppression [14]. Upon the discovery of HIV as the probable cause of AIDS, the precise mechanism of immune depletion was not understood. Immune suppression in HIV infection is the result of a combination of killing of CD4+ T-lymphocytes and macrophages, the primary targets of HIV infection, by HIV as well as the destruction of infected cells by the host's immune response [15; 16]. Despite the unfortunate persistence of AIDS denialism among a minority of fringe researchers and misguided AIDS activist groups, a wealth of evidence exists detailing the etiological link between HIV and AIDS [17; 18; 19]. In order to prove the link between putative pathogenic agents and a particular disease, a widely accepted test is that the agent fulfils Koch's postulates [19]. The basic tenets of Koch's postulates are as follows:

1. Epidemiological association: the suspected cause must be strongly associated with the disease.
2. Isolation: the suspected pathogen can be isolated – and propogated – outside the host.
3. Transmission pathogenesis: transfer of the suspected pathogen to an uninfected host, man or animal produces the disease in that host.

HIV fulfils each of these postulates as the etiological cause of AIDS [19]. The first postulate is fulfilled in part by retrospective studies of frozen blood samples from a U.S. cohort of gay men, which found the presence of HIV antibodies as early as 1978, immediately preceding the first reports of AIDS in gay men in California and New York [2; 20]. In a Canadian cohort of 715 homosexual men, researchers observed that every case of AIDS occurred in individuals who were HIV seropositive with no AIDS-defining illnesses observed in those who remained negative for HIV antibodies [21]. Epidemiological association is also seen in a direct positive association among HIV infected individuals between plasma viral RNA concentration and likelihood of developing AIDS [22]. With respect to the second postulate, studies of improved culturing and detection techniques also found that HIV could be isolated from all patients with AIDS defining symptoms, or, who were antibody positive without AIDS defining symptoms [23; 24].

The third postulate has been fulfilled through laboratory accidents in which workers, who had no other risk factors, developed AIDS after becoming HIV infected through exposure to concentrated, cloned HIV [25; 26; 27]. HIV infection was also seen to be the sole cause of the development of AIDS in the case of a Florida dentist who infected 6 patients during invasive oral surgeries [28; 29]. The third postulate is fulfilled with respect to the transmission of HIV to animals, with transmission of HIV-2 seen to cause AIDS-like disease in baboons[30]. Additional experiments in certain humanized mouse strains demonstrate the link between HIV infection and immune depletion. Mice containing a mutation at the SCID (severe combined

immunodeficiency) locus lack B- and T-lymphocytes, and may have their immune system reproducibly reconstituted by implantation of human peripheral blood lymphocytes (hPBLs) [31]. Infection of hPBL-SCID mice with HIV leads to AIDS-like disease including CD4+ T-lymphocyte depletion [32; 33].

With the link between HIV and AIDS a firmly accepted fact, surveillance of HIV infection is now central to efforts to understand the spread of the epidemic globally [34]. The CDC currently sets criteria for HIV infection as a positive result from an HIV antibody screening test confirmed by a positive result from a supplemental HIV antibody test, or, a positive result or report of a detectable quantity of HIV nucleic acid, HIV p24 antigen or isolation of HIV [35]. HIV infection is then classified into three stages with the following criteria set for both adults and adolescents (>13 years). Stage 1 HIV infection is defined by the absence of any AIDS defining conditions and either CD4+ T-lymphocyte count >500 cells/ml or CD4+ T-lymphocyte percentage of total lymphocytes of >29. Stage 2 HIV infection is defined as the absence of AIDS defining conditions and either a CD4+ T-lymphocyte count of 200-499 cells/ml or CD4+ T-lymphocyte percentage of total lymphocytes of 14-28. Stage 3 infection of HIV, or clinical AIDS, is defined as a CD4+ T-lymphocyte count of <200 cells/ml or CD4+ T-lymphocyte percentage of total lymphocytes of <14 or the presence of any of 27 AIDS defining conditions. The presence of an AIDS defining condition supercedes CD4+ T-lymphocyte count or percentage when establishing the stage of HIV infection [35]. Similar definitions are used for the establishment of HIV infection in children and infants without a classification system based on the number or percentage of CD4+ T-lymphocytes [35].

1.3 HIV virology

HIV is a lentivirus of the *retroviridae* family. Each virion caries two copies of a positive stranded RNA genome tightly bound to nucleocapsid (NC) proteins within a conical capsid enclosed within a matrix composed of the viral matrix protein (MA, p17). Also carried within the capsid are the viral enzymes RT, integrase (IN) and protease (PR) required for various stages of the viral life cycle (Figure 1.1). The matrix and capsid is enclosed in the viral envelope, composed of a lipid bilayer from the outer membrane of the host cell from which the virion was produced. The envelope of HIV contains host cellular proteins and the viral protein Env. Env is composed of three molecules of gp120, and, a stem consisting of three molecules of gp41 anchoring the Env structure to the viral envelope [36]. The surface of gp120 is highly variable, which aids in immune evasion by the virus [37; 38]. During a new round of infection this glycoprotein complex attaches to the CD4 receptor on the surface of the target cell in addition to either the CCR5 or CXCR4 co-receptor, the β- and α-chemokine receptors, respectively [39; 40]. Binding of the virion to the target cell, either macrophage or CD4+ T-lymphoctye, leads to fusion of the viral envelope with the cell membrane and release of the capsid into the cytoplasm [41]. This process, termed viral entry, is inhibited by the fusion inhibitor Enfuvirtide (T-20), a 20 amino acid synthetic peptide [42], as well as the small molecule CCR5 antagonist miraviroc [43]. Co-receptor use determines the effectiveness of miraviroc, which is ineffective against CXCR4 tropic viruses [44].

Following entry into the cytoplasm the capsid begins to breakdown and the process of reverse transcription begins [45]. The virally encoded RT carries out a

complex process of reverse transcription via RNA- and DNA-dependant DNA polymerization with precisely co-ordinated RNase H activities (discussed in detail in subsequent sections). Following reverse transcription a pre-integration complex (PIC) composed of the proviral DNA, the viral proteins IN, MA, Vpr and host proteins is carried to the nucleus and through nuclear pores [46; 47]. Within the nucleus IN carries out the integration of proviral DNA into the host chromosome producing a permanent infection. This process is targeted by the small molecule inhibitor raltegravir [48]. Multiple factors including the chromatin organization at the site of integration determine whether infection results in a latent, non-productive infection or the production of new virions [49].

In an active infection the viral genome is transcribed to mRNA, which is spliced to a number of different forms for the production of different viral proteins (discussed in the following section). These mRNAs are sent to the cytoplasm and translated by the host ribosomes. The final steps of the viral life cycle include the assembly and budding of new viral particles. The maturation of polyproteins into their functional form is carried out by PR, an aspartyl protease [50]. Maturation is targeted by small molecule inhibitors of PR, which mimic the PR cleavage substrate [51]. Due to their common mechanism of action, resistance to any of the first generation of PR inhibitors prevents the use of the entire class [52]. Crystallographic studies have led to the development of next generation PR inhibitors that overcome these challenges [8; 52; 53]. Maturation can also be targeted by small molecule inhibitors that interfere with capsid formation, however no such inhibitor is currently clinically approved [54].

1.3.1 HIV gene products, genome organization and gene expression

The expression of the HIV genome is closely related to its organization (Figure 1.2). The complete HIV genome is approximately 9.8 kilobases in length with both ends flanked by long terminal repeat (LTR) regions [55]. Differential splicing and post-translational modification of genes found in the central region of the genome leads to the production of at least nine proteins. The products of the HIV genome can be divided into three classes:

1. Structural proteins, Gag, Pol and Env
2. Regulatory proteins, Tat and Rev
3. Accessory proteins, Vpu, Vpr, Vif and Nef

1.3.1.1 Structural Proteins

The unspliced *gag* gene product gives rise to the 55-kD Gag precursor protein p55. The N-terminus of p55 is myristoylated during translation leading to association of p55 with the cytoplasmic aspect of cellular membranes [56]. Membrane associated Gag polyprotein recruits two copies of the viral RNA genome and other viral and host proteins triggering the budding of the viral protein from the surface of the cell. p55 is cleaved by PR during maturation, following budding, into MA (p17), CA (p24), NC (p9) and p6 [57]. MA proteins primarily play a role in stabilizing the viral particle, though a subset is involved in recruitment of the viral DNA as a karyophilic signal on MA is recognized by host nuclear import machinery [47]. The CA protein forms the conical core of the viral particle described in the above section. NC recognizes a packaging signal of four stem loops on the 5' end of the viral RNA and mediates its incorporation into virions [58]. NC has also been shown to facilitate reverse

transcription [59; 60]. Finally, p6 mediates the incorporation of Vpr into budding virions through interactions between Vpr and p55 Gag [61].

The viral enzymes RT, IN, and PR are expressed within a Gag-Pol fusion protein [62]. During maturation PR cleaves the Pol polypeptide from the Gag-Pol precursor (p160) and further subdivides it into the functional proteins PR (p10), RT (p66), RNase H (p15), and IN (p31). The RNase H portion of RT is further removed from approximately 50% of the p66 proteins leading to the formation of p66/p51 heterodimers of RT in its active form.

The 160 kD Env (gp160) is expressed from a singly spliced mRNA and is cleaved by a cellular protease to generate the gp41 and gp120 components of the Env protein complex found on the surface of virions. The addition of 25 to 30 complex N-linked carbohydrate side chains at asparagine residues is required for infectivity [39]. The gp41 moiety serves as an anchor through a transmembrane domain while the gp120 moiety is held on the surface of virions through noncovalent interactions with gp41. There are five hypervariable regions designated V1-V5 whose amino acid sequence varies between isolates. Tropism between CCR5 and CXCR4 co-receptors is mediated through sequences in the V3 and V1/V2 loops of gp120, which are targets of neutralizing antibodies that block HIV-1 infectivity [37; 38; 63]. Finally, gp120 interacts with the protein DC-SIGN, expressed on the surface of dendritic cells, which increases efficiency of infection of CD4+ T-lymphocytes [64].

1.3.1.2 Regulatory Proteins

Tat, a transcriptional transactivator, is essential for HIV-1 replication and is found in 72 and 101 amino acid forms expressed by fully spliced early mRNAs or

late incompletely spliced mRNAs respectively [65]. Unlike conventional transcription factors, which bind DNA, Tat is an RNA binding protein [66]. Tat binds to the transactivation response element (TAR) in the 5' terminus of HIV RNAs and promotes the elongation phase of HIV-1 transcription [67]. This increases transcription at least 1000-fold and allows for the production of full-length transcripts rather than the short (~100 nucleotide) transcripts produced in the absence of Tat binding.

Rev is a 13-kD sequence-specific RNA binding protein produced from fully spliced mRNAs, encoded by two exons [68]. The accumulation of Rev within the nuclei and nucleoli of infected cells induces the transition from the early to late phase of HIV gene expression [69]. Rev binds to a secondary structure within the second intron of HIV called the Rev response element (RRE) [70]. The binding of Rev to the RRE leads to the export of unspliced and incompletely spliced viral RNAs to the cytoplasm. Unspliced RNAs that contain introns are normally retained in the nucleus. As Rev is itself the product of a fully spliced mRNA, the effect of Rev on the export of unspliced mRNA creates a negative feedback loop whereby the increased levels of Rev lead to decreased levels of RNA available for complete splicing and in turn decreased Rev expression [71].

Rev requires multimerization to function and is believed to exist as a homo-tetramer [72; 73]. Rev binding with the RRE is mediated through an arginine-rich domain while a separate effector domain serves as a specific nuclear export signal (NES) [74; 75]. Export of viral RNA by Rev does not occur through the normal pathway associated with cellular mRNAs but rather the pathway typically used by small nuclear RNAs (snRNAs) and ribosomal 5s RNA [75]. Proviruses that lack Rev function

do not express viral late genes and are therefore replication incompetent, not producing virions.

1.3.1.3 Accessory Proteins

The accessory proteins Nef, Vif, Vpr, and Vpu are not critically required in all *in vitro* systems but do represent critical virulence factors *in vivo*. Expression of Nef is independent from Rev as it is expressed from a multiply spliced mRNA. Vif, Vpr and Vpu are all Rev-dependant as they are expressed from incompletely spliced mRNA in the late phase of HIV gene expression.

Nef

Nef, a 27-kD myristoylated protein encoded by a single exon, is the first HIV protein to accumulate to detectable levels in a cell following HIV infection [69]. Nef acts post-transcriptionally to down regulate cell-surface expression of CD4 by increasing CD4 endocytosis and lysosomal degredation [76; 77]. The effect of Nef on CD4 promotes Env incorporation and virion budding [78; 79]. Nef also serves to protect HIV infected cells from the host immune response by down regulating the expression of Class 1 MHC, a host protein that serves to alert the immune system of a viral infection [80]. Nef is also seen to have pleiomorphic effects on T cell activation depending on the context of expression [81]. Nef separately increases the infectivity of HIV when packaged in the virion, though this effect is genetically distinct from the above roles as mutations are observed that affect individual activities of Nef [78].

Vpr

Vpr is incorporated into virions by association with the carboxyl-terminal region of p55 Gag or p6 in the proteolytically processed protein [61]. Vpr acts as a nucleocytoplasmic transporter by directly tethering the viral genome to the nuclear pore [46]. Vpr is present in the PIC and has been demonstrated to bind to the nuclear pore complex [82]. By mediating nuclear import of the PIC, Vpr plays a role in the ability of HIV to infect non-dividing cells.

Vpu

Vpu is a 16-kD polypeptide found primarily in the internal membranes of the cell [83]. Vpu is expressed from Env encoding mRNAs through a separate, less efficient translation initiation codon leading to tenfold decreased expression relative to Env. Vpu serves two distinct but related functions, the down-modulation of CD4 and the enhancement of viron release through antagonism of host antivirulance factor tetherin at the cell surface [84; 85; 86]. The down-modulation of CD4 is related to virion release as an accumulation of CD4 in the endoplasmic reticulum leads to the formation of Env-CD4 complexes in this cellular compartment, which interferes with virion assembly [79; 87].

Vif

Vif is a 23-kD polypeptide essential for viral replication of HIV in peripheral blood lymphocytes, macrophages and certain cell lines [88]. Infective vif-negative virus can be produced from other cell lines that lack the host restriction factor APOBEC3G [89]. APOBEC3G is a cytidine deaminase that is packaged within assembling virions,

causing G->A hypermutation in the viral genome, rendering the produced virion replication deficient. Vif interferes with the packaging of APOBEC3G suppressing its antiviral effect [89].

1.3.1.4 Regulation of gene expression

The expression of the HIV genome occurs at the level of transcription as well as translation. Early and late gene expression is mediated by Rev, as described above [55; 69; 71]. The early genes, *tat*, *rev*, and *nef* are Rev-independent and expressed from fully spliced mRNAs. The late genes, *gag*, *pol*, *env*, *vpr*, *vpu*, and *vif* are expressed from incompletely spliced or unspliced mRNAs and require Rev for export to the cytoplasm for translation.

Transcription of the HIV genome is mediated by a single promoter in the 5' LTR which generates a 9-kb primary transcript encoding all nine HIV genes. This transcript may be spliced to as many as 30 distinct mRNAs or packaged into virion particles as the viral RNA genome [90]. The LTRs of the HIV genome contain U3, R, and U5 subregions [91]. The U3 or unique 3' sequence located at the 3' end of each LTR contains most of the cis-acting DNA elements that serve as binding sites for cellular transcription factors. The R subregion is a 100 bp central region of each LTR. Transcription begins at the first base of the R region with polyadenylation occurring immediately following the last base of R. The Tat binding site and packaging sequences of HIV are located in the U5 or unique 5' sequence which is 180-bp in length. The 3' end of the U5 contains a lysyl tRNA binding site. The binding of a lysyl tRNA serves as the primer during reverse transcription [92].

The LTR of HIV contains DNA binding sites for both inducible and constitutively expressed transcription factors including but not limited to the NF-kB family of inducible transcription factors and SP-1, Lef and Ets, which are constitutively expressed [93; 94; 95]. Initial transcription leads primarily to the production of short transcripts, though some full-length transcripts are produced allowing for the production of Tat [96]. Tat, as described above, enhances the elongation phase of transcription increasing the amount of full-length transcripts produced.

Different gene products of HIV can be found in the same transcript in different reading frames, with reading frame choice determined by differential efficiencies of initiation codon usage and proximity of the initiation codon to the 5' end of the mRNA [97]. As described above, the role of Rev is to export unspliced and partially spliced mRNAs to the cytoplasm. The different gene products of HIV can be divided into three size classes according to the level of splicing. Unspliced RNA can be used to generate the Gag and Gag-pol precursor as well as the packaged proviral RNA. Partially spliced mRNAs result from the use of a 5' splice donor site nearest to the 5' end of the HIV RNA genome with any of the splice acceptor sites in the central region. These mRNAs retain the second intron of HIV and can potentially express Env, Vif, Vpu, Vpr and the single exon from of Tat. Fully spliced RNA are Rev independent and do not contain either intron, these include Rev, Nef and the two exon form of Tat, as mentioned above.

1.4 Reverse Transcriptase

The RT of HIV-1 was the first target of antiretroviral therapies against this virus [98]. RT is responsible for conversion of the single stranded viral RNA genome

into the double stranded DNA that is subsequently integrated into the host chromosome. The complex process of reverse transcription involves RNA dependent DNA polymerization, DNA dependant DNA polymerization and RNase H degradation of RNA from RNA/DNA intermediates [92]. Each of these activities of RT is essential to viral replication and cannot be carried out by any host factor, making RT an attractive and effective drug target.

All clinically approved pharmaceutical inhibitors of RT target the DNA polymerization process. Two main classes of RT DNA polymerization inhibitors are the non-nucleoside analogue RT inhibitors (NNRTIs) and the nucleoside analogue RT inhibitors (NRTIs). NNRTIs are structurally diverse compounds that bind allosterically to an inducible hydrophobic pocket near the polymerase active site where they interfere with the chemical step of nucleotide incorporation [99]. This binding is non-competitive with respect to the binding of the natural dNTP substrate [100]. NRTIs are composed of modified nucleosides and one nucleotide that bind at the polymerase active site and compete with dNTPs for incorporation [51]. NRTIs inhibit subsequent polymerization as obligate chain terminators, due to their lack of a 3' OH group.

Once incorporated, NRTIs represent a complete block to the process of reverse transcription, and by extension, the viral life cycle. Unfortunately, the chemistry of incorporation is not strictly irreversible. Under certain conditions the reaction can be reversed with RT accepting PPi, the product released during the forward reaction or a PPi donor molecule such as cellular ATP as substrates to excise the ultimate nucleotide or NRTI from the primer terminus [101; 102]. The excision of

NRTIs allows for RT to efficiently rescue DNA polymerization, overcoming inhibition.

DNA polymerization by RT occurs in cycles of nucleotide incorporation. A single cycle consists of the binding of RT to a nucleic acid substrate, binding of a nucleotide or NRTI at the active site, conformational change leading to phosphodiester bond formation, release of PPi, and translocation along the nucleic acid substrate to free the active site. The last step in the cycle, translocation, changes the position of the active site by a single nucleotide. The proper positioning of the active site is essential for the incorporation or excision of dNTP and NRTI substrates. The translocation state of RT also plays a major role in the mechanisms of additional polymerase active site inhibitors of RT including the indolopyridones (INDOPYs), of the recently described nucleotide competing RT inhibitor class (NcRTIs), and the pyrophosphate analogue foscarnet (PFA) [103; 104]. This section covers current and future inhibitors of RT polymerization with regard to their mechanism and site of action and discusses inhibitors with novel mechanisms of action. Focus is given to inhibitors acting at the active site in the context of the translocation state of the enzyme.

1.4.1 Structure and Function of HIV-1 Reverse Transcriptase

1.4.1.1 Structure of HIV-1 RT

The active form of RT is a heterodimer composed of the p66 and p51 subunits derived from post-translational cleavage of the Gag-Pol encoded polyprotein. The polymerase and RNase H activities of RT both reside in the p66 subunit with p51 serving a more structural role. The p66 subunit is separated into two distinct

functional domains, each with separate active sites carrying out their respective polymerase and RNase H activities. The polymerase domain resembles a human right hand and is further divided into fingers (residues 1-85 and 118-155), palm (residues 86-117 and 1156-237) and thumb (residues 238-318) subdomains with a connection domain (residues 319-426) serving as the link to the RNase H domain (residues 427-560) [105]. p51 is a truncated form of p66 lacking its carboxyl terminal RNase H domain (Figure 1.3).

Nucleic acid substrates bind along the nucleic acid binding cleft that spans the RNase H and polymerase domains of p66, with some structural contribution from the connection domain and thumb of p51. The two active sites are located between 17-18 base pairs apart and can simultaneously engage the nucleic acid substrate when the 3' OH of the primer terminus is properly positioned in the polymerase active site [106]. Important residues in the polymerase active site include the catalytic carboxylates in the palm of p66 (D110, D185 and D186) that bind two divalent metal ions (Mg^{2+}) required for catalysis. Proper positioning of the β- and γ- phosphates of a bound nucleotide involve R72 and K65 respectively [107] while Q151 interacts directly with the 3' OH of incoming dNTPs [108].

1.4.1.2 Reverse Transcription

Reverse transcription by RT is a complex process that requires the coordinated polymerase and RNase H activities of RT as well as strand transfer and strand displacement synthesis directed by specific sequences in the HIV genome (Figure 1.4) [92]. Reverse transcription by RT begins by the selective binding of the $tRNA^{lys}$ to the PBS sequence followed by the initiation of the RNA-dependent DNA-

polymerization of (-) strand synthesis. (-) strand synthesis continues to the 5' cap, resulting in minus-strand-strong-stop DNA (-ssDNA). The Rnase H activity of RT removes the RNA template allowing the newly synthesized DNA to undergo a strand transfer reaction to the 3' end complementary R (repeat) sequence of the 3' LTR. This strand transfer reaction may occur intra or intermolecularly as there are two copies of the RNA genome present. Synthesis of (-) strand DNA then proceeds to the 5' end of the PBS, which is now the 5' end of the template due to the removal of the R and U5 by RNase H. The elongation of the (-) strand occurs simultaneously with the polymerase dependent RNase H degradation of the RNA template. (+) strand synthesis is primed by specific RNase H resistant PPT sequences at the border of the U3 domain of the 3' LTR and in the center of the genome where the RNA template has not been degraded. (+) strand synthesis beginning at the 3' PPT proceeds until the first modified base in the tRNA primer, which along with the secondary structure of the PBS sequence, act as stop signals for plus-strand strong-stop DNA (+ssDNA). The primer tRNA is then removed by RNase H activities allowing a second strand transfer such that the copied tRNA bases of the (+)ssDNA pair with the copied PBS on the (-)strand DNA. Elongation then continues to the central termination sequence (CTS) downstream of the cPPT. Approximately 100 nt of (+) strand DNA initiated from the cPPT is displaced with cellular enzymes presumed to remove the displaced sequence and seal the (+) strand to yield double-stranded linear DNA with an LTR at each end.

1.4.1.3 Nucleotide incorporation and translocation

Cycles of nucleotide incorporation begin with either the binding of RT to its nucleic acid substrate or a pre-formed binary complex resulting from the previous cycle. In either case RT must slide on its nucleic acid substrate in order to bring the 3' end of the primer into the correct position at the polymerase active site [109]. The active site is divided into two sites, the priming and the nucleotide binding sites (P- and N-sites respectively). When the 3' end of the primer is located in the P-site, the N-site is available for nucleotide binding (Figure 1.5). Crystallographic studies indicate that the binding of nucleotide in the N-site and the formation of a ternary complex induces a conformational change in the fingers domain, closing this domain over the bound nucleotide [107]. Phosphodiester bond formation occurs through a general mechanism involving the coordination of two divalent metal ions by the catalytic residues in the palm [110; 111]. Metal A coordinates the nucleophilic attack of the 3' OH of the primer terminus on the α-phosphate of the incoming nucleotide. Metal B is likely involved in the release of the PPi reaction product. Immediately following the release of PPi RT exists as a pre-translocation binary complex with the N-site occupied by the newly formed 3' primer terminus. Subsequent incorporation is not possible until the enzyme moves on its nucleic acid substrate freeing the N-site.

Translocation is a rapid process that is not kinetically defined [112]. Pre-steady state kinetic studies, however, with defined, short primer/templates do suggest different populations among the initially formed binary complexes [113]. Reported biphasic dissociation kinetics have also pointed to the existence of different nucleoprotein complexes [114]. The different populations of complexes described in

these kinetics studies could conceivably represent pre- and post-translocated complexes.

A 'translocation track' in RT has been proposed where movement of modular elements against each other cause contacts with the nucleic acid to break and reform allowing for the translocation of the enzyme along its substrate [115]. It has been suggested that the energy driving translocation is derived from the cleavage of the incoming dNTP [116]. Such a model of translocation, wherein bond formation or release of reaction products such as PPi are energetically required, is termed an active or power-stroke model of translocation. Alternatively, in passive models, thermal energy in the form of random Brownian motion is sufficient to propel translocation in both directions and directionality is achieved by the binding of the next nucleotide to drive the forward reaction. Support for these various models of translocation have been established in different RNA polymerases and will be discussed further.

Both active and passive models have support in the form of structural and biochemical data, respectively, for the single subunit bacteriophage T7 RNA polymerase (T7 RNAP) [117; 118; 119; 120; 121]. An active model is supported by crystal structures revealing conformational changes between pre- and post-translocated complexes [119; 120]. The pre-translocated complex is only observed with bound PPi, supporting a mechanism whereby the dissociation of PPi drives the conformational change to the post-translocated state [118]. In contrast to these findings, exonuclease mapping experiments with T7 RNAP have shown that binding of the next nucleotide causes a single nucleotide shift in the protection pattern [121]. These experiments were performed with chain-terminated primers and, therefore, incorporation and PPi

release could not be responsible for the observed movement of the enzyme. These results support a passive model whereby T7 RNAP translocation is driven by nucleotide binding.

A third and more complex ratchet model has been suggested based on structural and biochemical data garnered from studies on the multi-subunit E. Coli RNAP [121]. A bridge helix (F-bridge) located in close proximity to the polymerase active site is seen in both bent and straight conformations in structures of RNAPII [119]. The authors propose that oscillation between these conformations would drive the forward motion of the translocation process. Additionally, biochemical studies have shown that binding of templated nucleotides to sites beyond the catalytic n+1 position up to n+3, and not nucleotide hydrolysis, is responsible for translocation [120; 122].

While 3 models of translocation have been identified in various other RNA polymerases, an active model for translocation has been proposed for HIV-1 RT based on studies of crystal structures. The crystal structures in these studies have captured RT in conformations with a bound nucleotide and structures of RT trapped in the pre- and post-translocated conformations with primer/templates terminated with 3'-azido-3'-deoxythymidine monophosphate (Zidovudine; AZT) [107; 123]. Comparison of these structures revealed that nucleotide binding leads to a displacement of the YMDD motif within the active site. This movement is compared to the 'loading of a springboard' and it is suggested that the 'release of the springboard' following catalysis provides the energy required for translocation. However, the unidirectional nature of this active model is difficult to reconcile with the fact that excision of incorporated NRTIs occurs. As such, RT must have a

mechanism to return the 3' end of the primer to the N-site in order to allow for the chemistry of excision.

In a passive model of translocation, both RT N- and P- sites would be accessible to the 3' end of the primer and could explain the ability of RT to perform the excision reaction. This model of translocation is supported by observations of stalled complexes using FRET [124] and both site-specific [104; 125; 126] and DNase I [127] footprinting techniques. Single molecule FRET-based experiments reveal two populations that differ by 5Å, conceivably representing pre- and post-translocation complexes [124]. The presence of dNTP and PPi differentially favor the two conformations, as would be expected for the different states of translocation. Pyrophosphorolysis, however, could not be ruled out under the reaction conditions.

Different methods of site-specific footprinting have allowed for the direct monitoring of the position of RT on its nucleic acid substrate by specific cleavage at single nucleotide resolution [125; 128]. This level of resolution allows these experiments to clearly differentiate between pre- and post-translocated complexes. One variety of site-specific footprinting utilizes divalent Fe^{2+} to produce cleavage fragments at positions -18/-19 and -17/-18 of the template for pre- and post-translocation complexes respectively (Figure 1.5). The reaction is mediated by the binding of Fe^{2+} ions at or near the RNase H active site [128]. Oxidation of the bound metal ions leads to the generation of hydroxyl radicals responsible for the site-specific cleavage of the template. A metal free method of site-specific footprinting has also been developed [125]. This method involves treatment of RT:DNA/DNA complexes with potassium peroxynitrate (KOONO), which reacts with the sulfur of C280 in p66 to produce local

hydroxyl radicals. The ability to track a single residue, C280, provides this technique with greater resolution than Fe^{2+} footprinting or DNase I protection experiments that can give multiple overlapping cuts for adjacent positions [125; 127]. In KOONO footprinting, as the enzyme moves between pre- and post-translocation conformations, a single cut is produced at template positions -8 or -7 respectively (Figure 1.5).

Site-specific footprinting experiments with stalled RT:DNA/DNA complexes in the presence of the next complementary nucleotide reveal a shift from pre- to post-translocation conformations. Comparison of Fe^{2+} and KOONO techniques revealed that both the RNase H and polymerase domains (C280) move together, with identical responses to dNTP binding-induced transition from the pre- to post-translocation conformation [125]. Similar experiments with the PPi analogue PFA have revealed the stabilization of the pre-translocation conformation [104]. Similar results have been observed for both the binding of complementary dNTP and PFA using DNase I and exonuclease protection assays [127]. In all of these experiments, incorporation was prevented by the use of chain terminated primers, therefore the movement of the RT:DNA/DNA complex could not be energetically linked to catalysis or PPi release. These observations support a passive model of translocation in HIV-1 RT driven by the binding of the next complementary dNTP.

1.4.2 Mechanisms of inhibition and drug resistance at the polymerase active site

1.4.2.1 NRTIs

NRTIs comprise the backbone of highly active antiretroviral therapy (HAART). Analogues of each natural dNTP are represented among the eight NRTIs clinically approved for use. Pyrimidine analogues include the thymidine analogues AZT and 2', 3'-didehydro-2', 3'-dideoxythymidine (stavudine; d4T) together with cytidine analogues 2',3'-dideoxycytidine (zalcitabine; ddC), (-)-β-L-2',3'-dideoxy-3' thiacytidine (lamivudine; 3TC) and (-)-β-L-2',3'-dideoxy-5-fluoro-3' thiacytidine (emtricitabine; FTC). Purine analogues include the inosine analogue 2', 3' dideoxyinosine (didanosine; ddI) (which is converted to ddATP in its active form) and tenfovir dioproxil fumarate (TDF; prodrug of the nucleotide analogue tenofovir; TFV) along with the carbocyclic nucleoside analogue abacavir (ABC) which is converted to an analogue of guanine in its active form (Figure 1.6). Each approved NRTI lacks a 3' OH group and acts as an obligate chain terminator. Once phosphorylated to their active form NRTIs compete with dNTPs for binding to post-translocated RT complexes and incorporation. The chemical nature of the incorporated NRTI has been shown to affect the ability of RT to translocate after incorporation. Such effects on translocation have implications in drug resistance mechanisms and are discussed in detail in the following section.

1.4.2.2 NRTI resistance

Resistance to NRTIs occurs through two general mechanisms. The first mechanism of resistance is achieved by preventing the incorporation of NRTIs through mutations that increase discrimination against the NRTI for the natural substrate. An example of this mechanism is found with treatments containing 3TC that select for the mutation M184V/I. This mutation increases discrimination against

3TC through a steric clash with the oxathiolane ring [129]. The second general mechanism of resistance to NRTIs involves their excision from the 3' end of the primer followed by rescue of DNA synthesis, discussed in detail following a discussion of discrimination based mechanisms of resistance.

1.4.2.2.1 Mutations Conferring Resistance to NRTIs by Discrimination

Mutations that confer resistance by discrimination are all located within or very near the polymerase active site and selectively interfere with either the binding or catalytic step of incorporation of NRTIs.

K65R

K65R is selected for by tenofovir containing regimens and confers cross resistance to ddI, ABC, 3TC , FTC and ddC [130]. K65R has been shown to modulate susceptibility to tenofovir through increased discrimination as well as decreased excision [131]. Kinetics studies indicate that discrimination is the result of a decreased rate of incorporation (k_{pol}) of inhibitors relative to the natural substrate [132; 133; 134; 135; 136; 137; 138]. Resistance to ddC is also associated with decreased binding of the inhibitor [132]. Structural studies reveal that K65R leads to the formation of a molecular platform through guanidium stacking with the conserved R72 [139]. This interaction restricts the structural adaptability of the enzyme.

K70E

The K70E mutation is a less common resistance conferring mutation that appears in patients who have failed regimens containing ABC, TNF and 3TC [140]. The

biochemical evidence suggests that K70E causes increased discrimination through decreases in the rate of incorporation of NRTIs rather than changes in binding affinity [135]. K70E is also seen to significantly antagonize the excision of AZT by TAMs containing RT [135], structural interpretation suggests this is caused by a disruption of the proper positioning of the bound ATP [141].

L74V

The L74V mutation appears in regimens containing ABC or ddI [142; 143]. L74 interacts with the template at position n+1 [107]. Discrimination is seen to be the result of a decreased rate of incorporation of ddATP, the relevant substrate in resistance to ddI [144], with this mutation also acting as an antagonist towards the excision reaction [145; 146].

V75I

V75I appears in response to regimens containing acyclovir, a nucleoside analog used in the treatment of herpes simplex virus [147], as well as regimens containing d4T as an accessory mutation in the Q151M complex (discussed shortly) [148; 149; 150]. V75I reduces the rate of incorporation of acyclovir without affecting binding of the inhibitor [151], and is antagonistic to the excision reaction [150].

V75T

V75T is selected for in the presence of d4T [152] and increases discrimination against the inhibitor through a small decrease in the affinity of the enzyme for the inhibitor [153].

Q151M

The Q151M mutation is the primary mutation usually seen in conjunction with a number of accessory mutations representing the Q151M complex [148; 154; 155; 156]. This complex is associated with broad cross-resistance to a number of NRTIs including AZT, d4T, ddI, ddC, and ABC [157]. Q151M disrupts an electrostatic network between the incoming dNTP and conserved residues in the polymerase active site leading to decreased rates of incorporation without affecting binding [156]. The lack of a 3'OH group by NRTIs is thought to further disrupt this network leading to discrimination. Interestingly, though the mechanism of resistance by Q151M is related to the general lack of a 3'OH g by NRTIs, tenofovir generally remains active against this mutant. A recent report, however, found that the addition of K70Q to the complex adds tenofovir resistance to Q151M multi-drug resistance, by selectively affecting the binding of the inhibitor [158].

M184V

The M184V mutation is rapidly selected in regimens containing either 3TC or FTC [159] and is also seen to confer resistance to ABC [160]. Under the selective pressure of 3TC of FTC the mutation M184I rapidly emerges first as the result of a single point mutation but is later replaced by M184V. M814V is seen to negatively affect viral

fitness [133; 161] and increase fidelity [162; 163] through increased steric demand at the active site [163]. Together with its role as an antagonist of the excision reaction, these properties of M184V have been used to suggest a possible clinical benefit to the mutation [164; 165].

The mechanism of discrimination by M184V is understood to be the result of a steric clash between the beta branched amino acid valine and the oxathiolane rings of 3TC and FTC [129]. Kinetic data offer conflicting reports of this effect being manifested as diminished binding [166; 167] or catalytic rate [168], which may be due to the different nucleic acid sequences used in the conflicting studies. A study by Gao *et. al.* determined through binding assays that M184V could bind 3TC but that the binding resulted in a strained conformation which is not catalytically competent [129].

1.4.2.2.2 Mutations Conferring Resistance to NRTIs by Increased Excision

Resistance via the excision mechanism is associated with the accumulation of a series of mutations near the polymerase active site [169]. These mutations are referred to as thymidine analogue associated mutations (TAMs) due to their initial association with thymidine analogues AZT and d4T. Classical TAMs include M41L, D67N, K70R, L210W, T215F/Y and K219Q/E [169; 170; 171; 172; 173; 174]. In phenotypic drug susceptibility assays, TAMs confer the highest level of resistance to AZT with lower levels seen with d4T and other NRTIs [175].

In 1998 the first reports were made of increased excision of AZT by TAMs-containing RT in the presence of either PPi [101] or NTPs [102]. PPi is the natural product of the incorporation reaction and an efficient substrate for the reverse reaction under appropriate conditions. Alternatively ATP can bind to RT as a PPi donor resulting in

the release of a dinucleotide tetraphosphate. Although PPi is a more efficient substrate for the excision reaction, it is ATP that has been shown to selectively increase the rate of excision in the context of TAMs. If the mechanism of resistance by TAMs were to increase the population of excision competent pre-translocated complexes, both PPi- and ATP-mediated reactions would benefit from increased rates of excision. Structural studies have suggested interactions between specific TAMs and ATP that help to explain its role in the context of this resistance pathway.

Boyer *et al* 2001 predicted through modeling experiments that the TAM T215F/Y can stack with the base moiety of ATP through pi-pi interactions [176]. This interaction may be involved in increased binding of ATP [177], though increased binding is not consistently reported [178]. A recent study supports these early models and reveals that extensive interaction between bound ATP and primary TAMs T215Y and K70R creates a high affinity binding site, while in the WT enzyme, ATP binds away from the site of TAMs mutations in a number of different conformations [141]. Crystal structures of AZT terminated primers in the pre- and post-translocated conformations also support the prediction by Boyer *et al* of a steric clash between incorporated AZT at the 3' primer terminus and an incoming dNTP in the post-translocation conformation [123; 179]. Thus, AZT primarily mediates the effect on translocation in this context while the selectivity for ATP as the PPi source is mediated by interactions between TAMs and the base moiety of ATP.

The effect of AZT on the translocational equilibrium has direct functional consequences for excision. As mentioned earlier the excision reaction can only take place when the 3' end of the primer resides in the N-site. A change in conformation

from pre- to post-translocation moves the scissile bond out of position preventing the excision reaction [123]. Moreover, post-translocated complexes that accept binding of an incoming nucleotide form stable closed complexes [180]. When a chain terminator is present at the 3' end of the primer these "dead-end complexes" (DECs) are incapable of both incorporation and excision reactions (Figure 1.7). Footprinting experiments have confirmed biochemically that AZT terminated primers preferentially reside in the pre-translocation conformation in the absence of dNTP and require higher concentrations of dNTP to trap a post-translocated complex than primers terminated with ddTTP [125]. This finding suggests that since AZT stalls RT predominantly in the pre-translocation conformation, the susceptibility of the complex to excision is increased, promoting resistance. The effect of the 3' azido group was also seen when comparing AZA terminated primers with those terminated with ddATP, though the effect was greater with AZT than AZA. The importance of the base moiety has separately been shown in a study that found the 3' azido group was not the primary determinant of resistance; in this study resistance was conferred to pyrimidines but not purines [181].

Decreased resistance to other NRTIs conferred by TAMs is usually explained by increased DEC formation as these NRTIs can form stable complexes at concentrations of dNTP within the physiological range [182]. For example, TAMs do not confer high-level resistance to tenofovir in phenotypic drug susceptibility assays [183] even though this NtRTI has been shown to be efficiently excised *in vitro* [126]. While both AZT and tenofovir were readily excised, differences in the translocational equilibrium allowed the excision of tenofovir to be blocked at much lower

concentration of dNTP [126]. These effects were enhanced for the novel NtRTI GS-9148 when compared to tenofovir [184]. GS-9148 and tenofovir are related adenosine analogue phosphonate containing NtRTIs. GS-9148 differs from tenofovir in its sugar moiety and has been shown to maintain activity against TAMs in phenotypic susceptibility assays [185]. GS-9148 terminated primers were shown to facilitate the transition from pre- to post-translocation leading to suppression of excision by DEC formation at lower concentrations of dNTP then with tenofovir [184]. These findings help to explain the results of phenotypic assays, however, the conditions found in such assays may not fully represent the conditions *in vivo* and excision may persist in cell types with still lower dNTP concentrations [186; 187].

An additional factor that has been seen to affect both translocation and excision is the nucleic acid sequence context. Site-specific footprinting has shown that the sequence context alone can influence the translocational equilibrium with certain sequences inducing either heavily pre- or post-translocational equilibriums and others inducing mixtures of the two [125; 188]. Sequences on which RT exhibits decreased access to the pre-translocated conformation are seen to be deficient at the excision reaction [125]. In a separate study the sequence context was seen to heavily affect rates of excision [189]. Although the authors did not correlate their results with the translocational equilibrium, it is conceivable that the effects are related. It has been shown that AZT terminated primers are able to overcome sequence specific effects while d4T remained susceptible to them [190]. This provides further explanation for effects seen in phenotypic drug susceptibility assays in which the sequence context of the entire genome is reflected. Sequences that favor the pre-translocation

conformation would be resistant to dead-end complex formation for d4T while AZT would resist binding of the next nucleotide at all positions.

Additional mutations in RT can broaden cross-resistance to other NRTIs. For example, dipeptide insertions following position 69 of RT accumulate in viruses that already contain TAMs and are associated with high levels of excision [191; 192; 193; 194; 195; 196; 197; 198; 199]. Footprinting experiments have shown that RT containing M41L/69ss/T215Y required higher concentrations of dNTP to induce a shift from pre- to post-translocation conformations relative to WT, increasing the breadth of conditions under which excision would not be inhibited by DEC formation [125]. Individual mutations further enhance the effects of the 69ss insertion. The A62V mutation is also associated with the 69ss insertion complex and is implicated as a key mutation in conferring high-level excision activity [198]. Structural analyses indicate that A62V and M41L affect the resistance mechanism through a coordinated effect on the positioning of the β-3 β-4 hairpin loop [198]. Comparison of the translocational equilibrium in the absence of dNTPs between enzymes containing M41L/69ss/T215Y revealed no change relative to WT, while the addition of A62V resulted in an increase in pre-translocated complexes [188]. The increase in pre-translocated complexes could further facilitate the excision reaction.

Excision of NRTIs is therefore a general resistance mechanism that is seen to differentially affect NRTIs in part based on their susceptibility to DEC formation. By preventing the binding of the next nucleotide, AZT remains the most susceptible to this mechanism. While the remaining NRTIs are protected from the excision reaction by DEC formation, HIV-1 RT will select for resistance via discrimination in this

context. Interestingly, mutations that confer resistance via discrimination have been shown to negatively affect the excision reaction. These interactions are discussed in the following section.

1.4.2.2.3 Suppression of NRTI Excision by Incompatible Resistance Mechanisms

Mutations conferring resistance to the pyrophosphate analogue foscarnet (discussed in a following section) [200] and to NRTIs via discrimination, as mentioned, are antagonistic to the excision reaction and cause sensitization to AZT in the context of TAMs [135; 150; 201; 202; 203; 204]. It is possible that these effects could be mediated through changes to the translocational equilibrium. Considering the location of residues such as M184, which is near the primer terminus, and L74 which is within contact distance of the template [107]; an effect on the translocational equilibrium was investigated. However, foot-printing experiments with and without the incoming nucleotide indicate that neither of these mutations has an effect on the translocational equilibrium [146].

Recently the substitution V75I was shown to suppress both ATP- and PPi-mediated excision of thymidine analogues when placed in multiple genetic backgrounds with minimal effects on the translocational equilibrium [150]. V75I interacts with template nucleotide n+1 during ternary complex formation [107] and, as mentioned above, exerts its effect in both the Q151M complex and acyclovir resistance by increased discrimination [150; 151]. In their recent study Matamoros *et al* found that in certain genetic contexts V75I slightly increased the amount of pre-translocated complexes available for excision, however, a decrease in excision efficiency was the dominant phenotype [150].

While a mutation, which causes an increase in the proportion of post-translocation complexes, would theoretically act to antagonize the excision reaction, this is not the mechanism of antagonism seen in practice. This is not entirely surprising when considering the selective pressure that has lead to the development of these mutations. They cannot have been selected to antagonize the excision reaction, as that would be of no fitness benefit to the virus, it is merely a side effect of their mechanisms of discrimination. Intuitively, an increased proportion of post-translocation complexes would not, in itself, serve to increase discrimination.

1.4.2.3 NRTIs with Novel Mechanisms of Action - Non-obligate and Delayed Chain Terminators

Although all of the currently available NRTIs discussed to this point act as obligate chain terminators, polymerization by RT can be effectively inhibited by NRTIs acting through additional mechanisms. Such non-obligate and delayed chain terminators may act at the site of incorporation as effective chain terminators through inhibition of translocation or from within an extended primer by disrupting later incorporation events.

1.4.2.3.1 EFdA

2'-deoxy-4'-C-ethynyl-2-fluoroadenosine (EFdA) (Figure 1.8), is among a group of 4'-substituted NRTIs that require a 3'OH group for activity and are therefore classified as non-obligate chain terminators. Since the first report of 4'-azido-thymidine in 1992 a wide range of molecules of this class have been synthesized [161; 205]. EFdA stands out as the most potent of those synthesized with EC50 values in the remarkable sub nM range [161]. Once incorporated, EFdA inhibits

polymerization at the polymerase active site as a chain terminator by preventing the translocation of RT [206]. Modeling suggests that the 4'ethynyl fits into a hydrophobic pocket on RT. This translocation deficient mechanism of chain termination prevents binding of the next nucleotide and subsequent incorporation despite the presence of a 3'OH group at the primer terminus (Figure 1.9). The translocation block can be seen in site-specific footprinting experiments. EFdA is able to remain active against NRTI resistant strains containing TAMs while being efficiently excised. This is a result of the extremely high level of potency and the ability of excised EFdA to be efficiently reincorporated. EFdA selects for resistance mutations M184V, I142V and T165R [206]. Modeling predicts the mechanism to be discrimination by steric conflict through M184V with I142V and T165R seen to augment this effect.

1.4.2.3.2 Delayed Chain Terminators

Delayed chain terminators (DCTs) allow for subsequent incorporation of dNTPs by the presence of a 3'OH. Only after additional nucleotides are incorporated do these inhibitors exert their effect, presumably through steric interference between the primer/template and the nucleic acid binding cleft in the immediate vicinity of the polymerase active site. This mechanism of action is particularly effective in the context of resistance by excision as the DCT responsible for the block is effectively shielded from the excision reaction. North methanocarba-nucleotide triphosphates (N-MCN-TPs) exhibit inhibition via a delayed chain terminator mechanism *in vitro* as a result of their locked North or 2-endo conformation [207]. This block occurs after two to three subsequent rounds of nucleotide incorporation. This mechanism exploits the normal conversion from North to South that occurs in the nucleic acid substrate of

RT [115]. However, due to their inability to serve as substrates for cellular kinases N-MCN-TPs are not phosphorylated and exhibit no antiviral activity *in vivo*. Delayed chain termination has also been demonstrated for a nucleoside analogue inhibitor of hepatitis B virus RT, entecavir (ETV) (Figure 1.10), that weakly inhibits HIV-1 RT [208]. ETV was shown to block DNA polymerization by both enzymes, inducing strong pausing three nucleotides after its incorporation into the primer [209]. ETV-MP is efficiently excised by RT when present at the 3' primer terminus; however delayed chain termination serves to protect the inhibitor from excision even in the context of major NRTI resistance-conferring mutations. RNase H mapping experiments revealed exclusively polymerase-independent cuts, suggesting that delayed chain termination is achieved through a repulsion of the 3' primer terminus from the polymerase competent mode (Figure 1.11). The total amount of RNase H cutting is unaffected, indicating that overall binding is not affected. It appears as though the incorporated delayed chain terminator affects the equilibrium between sliding and primer recognition [109]. ETV was also shown to inhibit synthesis when present in the template strand (Figure 1.11). This base pair confounding mechanism of action has also been reported for the broad spectrum viral inhibitors cidofovir and (S)-9-[3-hydroxy-(2-phosphonomethoxy) propyl] adenine ([S]-HPMPA) in the context of the vaccinia virus DNA polymerase [210]. Cidofovir is also able to serve as a delayed chain terminator of this enzyme at position n+1, as well as inhibiting the (3'→5') exonuclease proofreading activity [211]. This is particularly interesting, as this mechanism is not shared by [S]-HPMPA despite the compounds differing only in the structure of their base moeity. Although cidofovir and [S]-HPMPA are not active

against HIV in the forms used in these studies [212] alkoxyalkyl ester derivatives of [S]-HPMPA have been shown to inhibit both WT and drug resistant forms of HIV [213]. The mechanism of inhibition by these alkoxyalkyl derivatves remains to be determined as either DCT or base pair confounding from the template strand.

1.4.2.4 Foscarnet (PFA)

The PPi analogue foscarnet (PFA) (Figure 1.12) is a polymerase active site inhibitor of RT that acts through a mechanism distinct from that of NRTIs. The use of PFA is limited to salvage therapy due to problems with associated with its clinical use including poor bioavailability [214] and adverse effects [215; 216]. The use of PFA in salvage therapy revealed a relationship to the excision of AZT by TAMs [200]. In these patients treatment with PFA can produce initially favourable results with the majority of NNRTI and NRTI resistance mutations conferring no resistance to PFA. PFA resistance conferring mutations, however, eventually develop which cause increased susceptibility to AZT [217]. The mechanism of resensitization to AZT by PFA resistance-conferring mutations has been determined to be reduction of the excision reaction [200; 218; 219].

The relationship between AZT sensitization and PFA resistance was linked to the translocational equilibrium by characterization of the specific mechanism of action of PFA [104]. Inhibition with PFA on long templates was seen at 'hot-spots' along the template. These positions exhibit a strong bias toward the pre-translocation conformation in site-specfic footprinting experiments. PFA binding at these sequences results in the formation of stable closed complexes while sequences heavily biased to post-translocation are literally resistant to PFA binding. The binding

of PFA increases in the presence of divalent metal ions which points to a PFA binding site at the active site. Binding of PFA and the natural dNTP substrate are, therefore, mutually exclusive (Figure 1.13).

In agreement with an overlapping binding site of PFA and PPi, resistance to PFA occurs in the context of mutations that directly interact with the β and γ phosphates of the incoming nucleotide such as K65R [220] and R72A [221]. Resistance to PFA and sensitization to AZT can also occur through a decrease in the amount of pre-translocated complexes as seen with E89K. E89 is located in the palm adjacent to template position n-2, relatively removed from the putative PPi/PFA binding site [107]. E89K affects the translocational equilibrium by disrupting the normal distribution between pre- and post-translocated conformations, causing the enzyme to slide beyond this typical register [104]. Without the pre-translocated conformation PFA cannot exert its inhibitory effect nor can RT carry out the excision of AZT.

Similarly mutations F61A and A62V in the fingers domain of RT that decrease and enhance the stability of pre-translocation complexes, respectively, were shown to affect both binding and inhibition by PFA [188]. The substitution F61A does not occur naturally and is known to negatively affect DNA synthesis [222; 223; 224; 225]. A62V has been implicated as a compensatory mutation in the multi-drug resistant Q151M complex [154], and can partially restore replication deficits found with K65R [137], and, as mentioned earlier, confers high-level excision activity in 69ss containing complexes [196]. Site-specific footprinting experiments with binary RT complexes showed that F61A strongly favors a post-translocation conformation while A62V favors a pre-translocation conformation. Further, A62V was shown to increase the

proportion of pre-translocated complexes when placed on multiple drug resistant backgrounds including the Q151M and 69ss containing complexes. These effects on translocation were associated with strong resistance to PFA with F61A-containing RT, and, increased susceptibility with A62V-containing RT, in binding and inhibition assays [188].

1.4.2.5 Nucleotide Competing RT Inhibitors (NcRTIs) at the Polymerase Active Site

A novel class of RT inhibitors has recently been described [103; 226]. These compounds are not nucleotide analogues and are not incorporated as chain terminators. Instead these compounds bear more structural resemblance to NNRTIs. Unlike NNRTIs, however, they block polymerization by competing with dNTPs for binding at the polymerase active site of RT. Due to their unique mechanism of action, these compounds have been termed nucleotide competing RT inhibitors (NcRTIs). Of the NcRTIs so far identified there are two families of molecules, the first, the INDOPYs including INDOPY-1 (Figure 1.14), are polymerase active site inhibitors. The second class of NcRTIs, the 4-dimethylamino-6-vinylpyrimidines (DAVPs) bind a novel site near the polymerase active site and are discussed in the context of NNRTIs in the following section. Studies with INDOPY-1 revealed that this compound binds to post-translocated RT complexes, creating stable closed complexes, analogous to DEC formation seen with dNTP binding to RT containing a chain-terminated primer/template (Figure 1.13). Unlike dNTP binding, INDOPY-1 binding is not directed by the templated nucleotide. Instead the presence of a pyrimidine (preferentially TTP) at the 3' primer terminus directs binding of

INDOPY-1 [103]. Resistance conferring mutations map to the polymerase active site and overlap with NRTI resistance conferring mutations M184V and Y115F [227]. M184V and Y115F confer resistance by discrimination whereby the enzyme preferentially binds dNTP over INDOPY-1 relative to WT. In contrast, K65R has been shown to confer hypersusceptibility to INDOPY-1 through decreased binding of dNTP with increased binding of the NcRTI [227]. The mutation F61A, which results in a heavy bias to the post-translocated conformation, also confers a large increase in susceptibility to INDOPY-1, indicating the importance of translocation conformation in the binding and inhibition by INDOPY-1.

1.4.3 NNRTIs

The use of multiple inhibitors that act through distinct mechanisms of action is necessary to prevent treatment failure through cross-resistance and is an important aspect of current therapy. To this end most therapies include one or two active NRTIs paired with either a protease inhibitor (PI) or an NNRTI. NNRTIs have been in clinical use since 1996 with the FDA approval of neviripine (NVP), followed soon after by delavirdine (DLV) in 1997, efavirenz (EFV) in 1998 and most recently etravirine (ETR) in 2008 (Figure 1.15). Unlike NRTIs, NNRTIs are administered in their active form and are highly specific to HIV-1 RT. Although there are only 4 NNRTIs currently approved for use, the class is in general highly diverse with over 50 families of molecules. Despite the immense diversity in structure NNRTIs traditionally have been found to act through a common mechanism. As mentioned previously NNRTIs inhibit RT by binding to an inducible hydrophobic pocket approximately 10Å from the polymerase active site. NNRTI binding acts to inhibit

DNA polymerization non-competitively relative to dNTP substrates by effecting the positioning of the polymerase active site. This mechanism was first proposed based on structural data from co-crystals of unliganded HIV-1 RT complexed with primer/templae and dNTPs, or with bound NNRTIs (reviewed in [228]), and is supported by kinetic data [229]. Further, inhibition of HIV-1 replication by NNRTIs is not limited to suppression of DNA polymerization. NNRTIs have been shown to interfere with the orientation of RT causing it to adopt an RNase H competent rather than polymerase competent mode [109], which has implications in mechanisms of drug resistance discussed in the following section.

1.4.3.1 First Generation NNRTIs and Cross-Resistance

Due to their common mechanism of action NNRTIs are particularly affected by cross resistance with the development of resistance to any single member of this class generally rendering all other members of the class unsuitable for treatment. The most prevalent mutations found in patients failing NNRTI therapy are K103N and Y181C. NVP and DLV both rely heavily on stacking interactions with aromatic residues Y181 and Y188 for binding, readily explaining the resistance conferred to these inhibitors by substitutions at these positions. EFV does not rely on these same stacking interactions and as such Y181C does not confer high-level resistance to EFV. EFV most commonly selects for K103N, which is proposed to block entrance into the NNRTI binding site by introducing a H-bond between asparagine at position 103 and the tyrosine at postion 188, creating an energy barrier to NNRTI binding [230]. Though most NNRTI resistance associated mutations (of which there are over 40) including K103N and Y181C are within the NNRTI binding pocket, mutations away

from this site including the connection domain mutation N348I have been shown to cause resistance to NNRTIs [231]. Connection domain mutations are associated with resistance to both AZT and NVP but not EFV or ETR. Resistance to NVP through N348I is related to NVP's enhancement of RNase H activity, with N348I overcoming this effect [232].

1.4.3.2 Next generation NNRTIs

In efforts to overcome problems with NNRTI cross resistance a number of different molecular families of next generation NNRTIs have been developed by screening compounds against WT, single and double mutant NNRTI resistance HIV-1 strains. These include but are not limited to the di-aryl-pyrimidine (DAPY) compounds (ETR and Ripilivirine or TMC278) developed by researchers at the Janssen Research Foundation and Tibotec, the triazole NNRTIs developed by Andrea Biosciences (eg. RDEA806), the 3-phosphoindoles developed by Index Pharmaceuticals (eg. IDX899) and the pyrazole family developed by Pfizer (eg. Lerivirine or UK-453061). Next generation NNRTIs are characterized by increased flexibility, allowing them to maintain activity in the context of existing NNRTI resistance (Reviewed in [233]). The next generations NNRTIs listed here share comparable, favorable *in vitro* resistance profiles. Crystal structures are available for the DAPY compounds ETR and TMC278, revealing that both inhibitors exhibit similar flexibility in adapting to resistance mutations while TMC278 is able to extend deeper into the NNRT binding pocket making contacts with the conserved reside W229 [234; 235]. Similarly crystal structures of RDEA806 show the compound extending

deep into the NNRTI binding pocket, making contacts with W229, Y181 and Y188 [236].

While these next generation NNRTIs continue to act via the same common binding site their ability to accommodate and adapt to the presence of drug resistance conferring mutations is an important advance in the fight against cross-resistance. Still, the development of compounds, which inhibit RT through completely distinct and separate mechanisms of action continues to be important and would provide the most effective protection against the development of cross-resistance. Novel NNRTIs have recently been developed which bind to a site distinct from the traditional NNRTI binding site. These compounds and their novel mechanism of action are discussed in the following section.

1.4.3.3 Novel NNRTIs (NcRTIs) that Bind Away from the NNRTI Binding Pocket

As discussed earlier a new class of NNRTIs has recently been identified that inhibit RT through unique mechanisms of action. Unlike traditional NNRTIs these compounds inhibit RT through a competitive mechanism and are as such referred to as NcRTIs. Of the two families of molecules so far identified of this class, the INDOPYs and the DAVPs, the former has been shown to bind at the polymerase actives site and as such has been discussed in the context of polymerase active site binding inhibitors. Unlike the INDOPYs, which are not affected by NNRTI resistance conferring mutations, the DAVPs are characterized by a unique resistance profile [237]. The most active DAVP developed, DAVP-1 is not significantly affected by NNRTI resistance mutations L100I or V179D, however, it is severely affected by K103N and

Y181C. Further, DAVP-1 differs from INDOPY-1 in its ability to readily bind unliganded RT in addition to binary complexes, while INDOPY-1 appears to only bind the latter [237]. Crystal structures of DAVP-1 in complex with RT confirm a unique binding site distinct from the NNRTI binding site [238]. DAVP-1 is seen to bind in a hinge region at the interface between the p66 thumb and p66 palm subdomains near the polymerase active site. The authors note that binding of DAVP-1 in this region likely causes misplacement of the primer, preventing stable closed complex formation on dNTP binding, resulting in a lack of nucleotide incorporation. The residues in contact with DAVP-1 are heavily conserved with only one, M184, observed to mutate as a result of antiviral drug pressure, in the case of M184V/I discrimination to 3TC [129]. While the highly conserved nature of the DAVP-1 binding site is promising in the context of resistance, susceptibility of DAVP-1 to K103N and Y181C is a concern. This resistance profile indicates that DAVP-1 must gain access to its highly conserved binding site using structural elements in common with the traditional NNRTI binding site.

1.4.4 Summary of RT inhibitors

We have seen that among inhibitors of RT that act at the polymerase active site the translocational equilibrium plays an important role in drug action and resistance. The nature of NRTIs affects the translocational equilibrium that in turn either protects or exposes chain terminators to resistance via the excision reaction. In the case of the non-obligate chain terminator EFdA inhibition is accomplished through a block to translocation preventing subsequent incorporation. Additionally studies with PFA and INDOPY-1 have provided important proof of principle that

small molecule inhibitors of RT can selectively target pre- and post-translocation complexes. In the context of delayed chain termination the enzyme is repelled from the active site and unable to engage the primer or establish a normal translocational equilibrium. In the context of inhibitors that bind outside of the polymerase active site, namely the NNRTIs, the use of a common binding site presents problems with cross-resistance. While next generation NNRTIs represent a major advance in this regard, with maintained activity in the context of traditional NNRTI resistance conferring mutations, a unique binding site would be an exciting development. The characterization of the NcRTI DAVP-1 demonstrates the potential for novel inhibitors that bind at novel sites, however susceptibility to existing NNRTI mutations likely limits the usefulness of this particular option. Together these examples demonstrate the variety of mechanisms through which RT polymerization may be inhibited.

1.5 Objectives

At the onset of this work the development of site-specific footprinting techniques created the opportunity for the study of the translocational equilibrium of RT. My first objective was investigating potential molecular determinants of this equilibrium. Mutant enzymes were generated by site-directed mutagenesis, allowing me to probe the contributions of interactions between specific amino acid residues in the fingers subdomain and the template overhang. I determined by site-specific footprinting that these mutations, namely F61A and A62V, had opposing effects on the translocational equilibrium. Through binding assays and IC50 determinations, I characterized the

effects of these mutations on the activity of PFA. This initial study is presented in the following chapter of this thesis.

Following my work on fingers domain mutations F61A and A62V my next objective was to characterize the role of the substrate of RT, the nucleic acid, on the translocational equilibrium. This was performed by site-specific footprinting of a large number of consecutive primers with follow up analysis using pre-steady state kinetics with defined sequences. The results of this study are presented in chapter three of this thesis.

Finally, I had the opportunity to characterize a novel drug resistance mutation Q151L. My objective in this work was to determine the mechanism of resistance of Q151L to the investigational NtRTI GS-9148 as well as to determine the mechanism of hypersusceptibility of Q151L to the related NtRTI tenofovir. This was achieved primarily by pre-steady state kinetic analysis in addition to molecular modeling and Structure Activity Relationship experiments. The results of this study are presented in chapter four of this thesis.

Figure 1.1. **Life Cycle of HIV** adapted from [239].

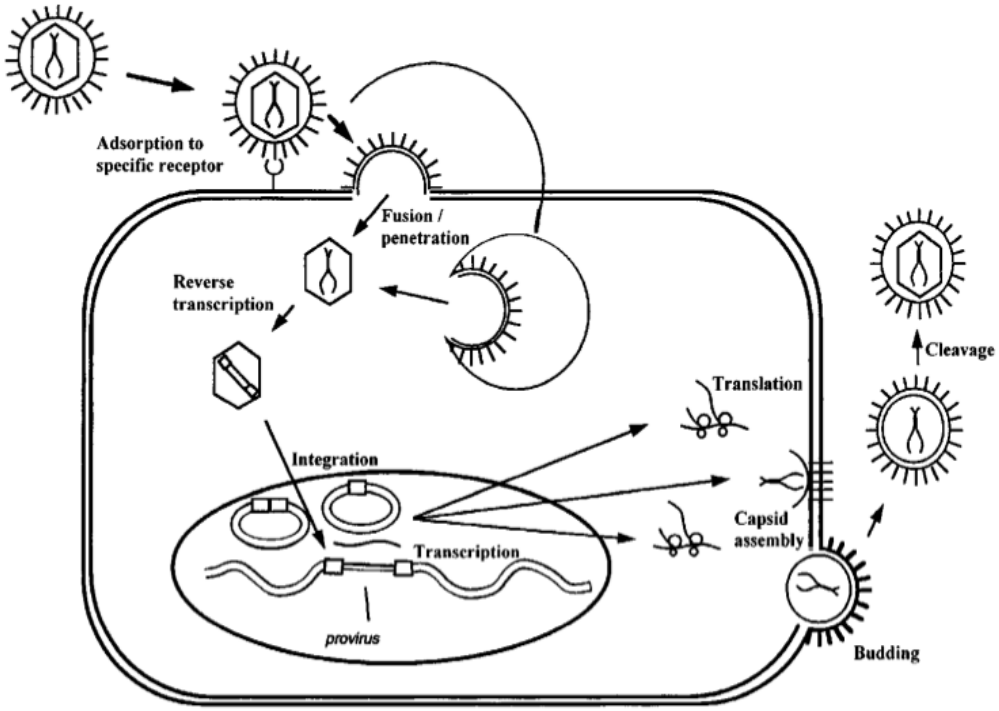

Figure 1. 1

Figure 1.2 **Expression of the HIV-1 genome** adapted from [91]. Schematic view of the linear proviral genome, with coding sequences of the HIV genes depicted as open rectangles.

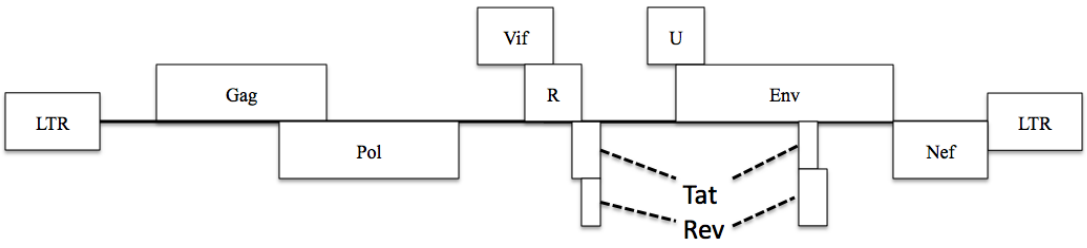

Figure 1. 2

Figure 1.3 **Structure of HIV-1 Reverse Transcriptase.** The polymerase domain of RT in the p66 domain is shown as fingers (yellow), palm (light blue) and thumb (green) subdomains linked to the RNase H domain (brown) via connection domain (purple) with p51 shown in grey (figure generated in PBD viewer from 1RTD).

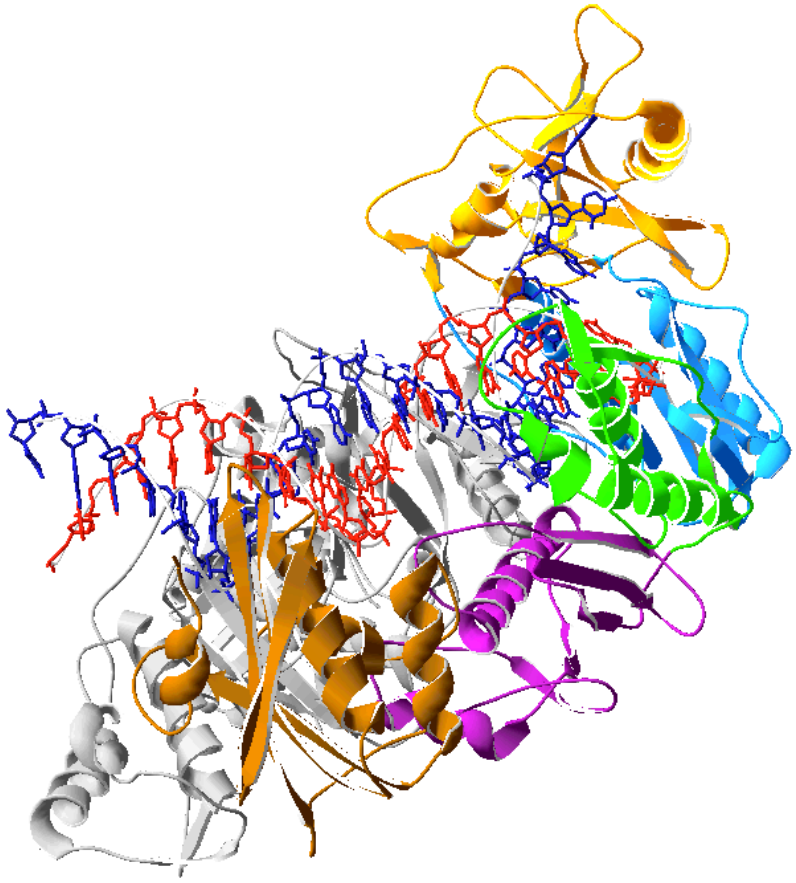

Figure 1. 3

Figure 1.4 **Reverse Transcription by HIV-1 RT**, adapted from [92]

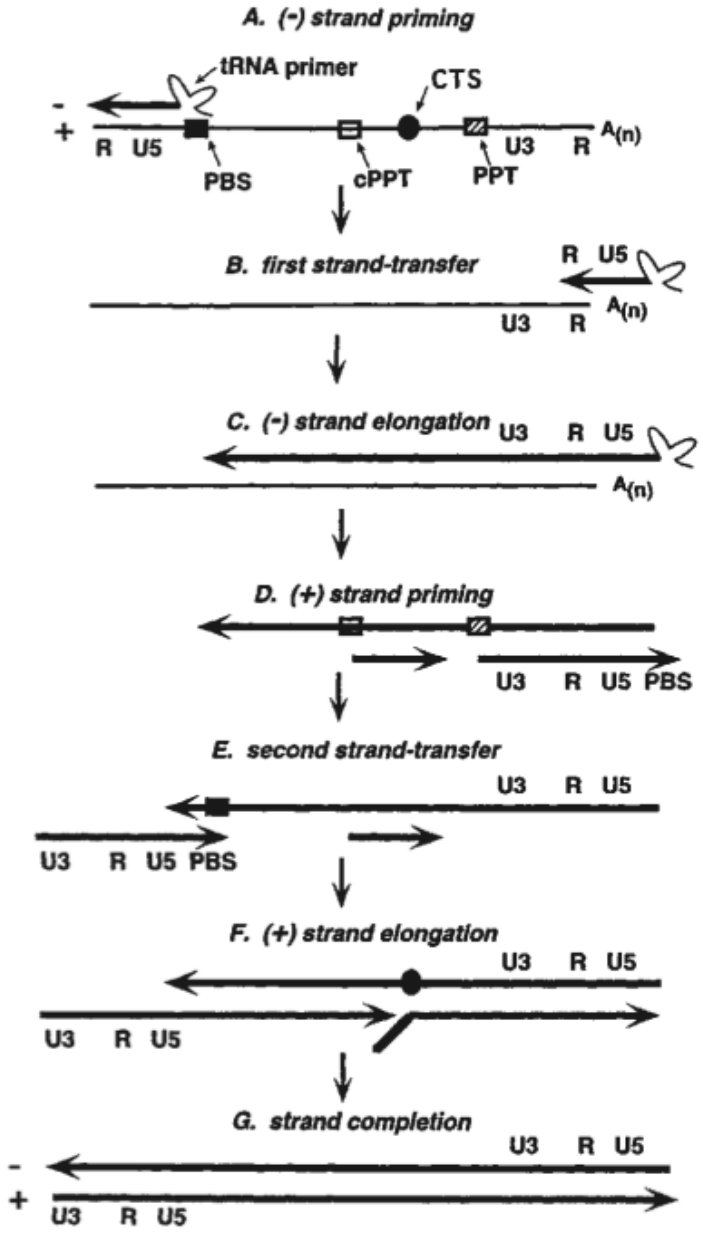

Figure 1. 4

Figure 1.5 **Site-Specific Footprinting and the Translocational equilibrium in HIV-1 RT.** Schematic representation of the relative positioning of the RT in both pre- and post-translocation conformations, the polymerase active site of RT is represented as a rectangle divided into priming (P) and nucleotide binding (N) sites. The positioning of RT on its nucleic acid substrate can be monitored with site-specific footprinting techniques. Template cleavage is mediated through C280 or the RNase H active site with the use of KOONO or Fe^{2+} respectively. Positions of template cleavage are indicated for both pre- and post-translocation conformations and each hydroxyl radical source. In the pre- and post-translocation conformations the nucleotide-binding site (N-site) is occupied by the 3' primer terminus and accessible for binding, respectively.

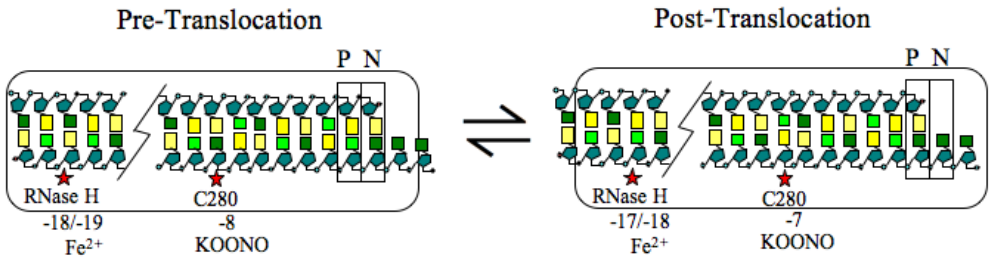

Figure 1. 5

Figure 1.6 **Structures of the Clinically Available NRTIs.**

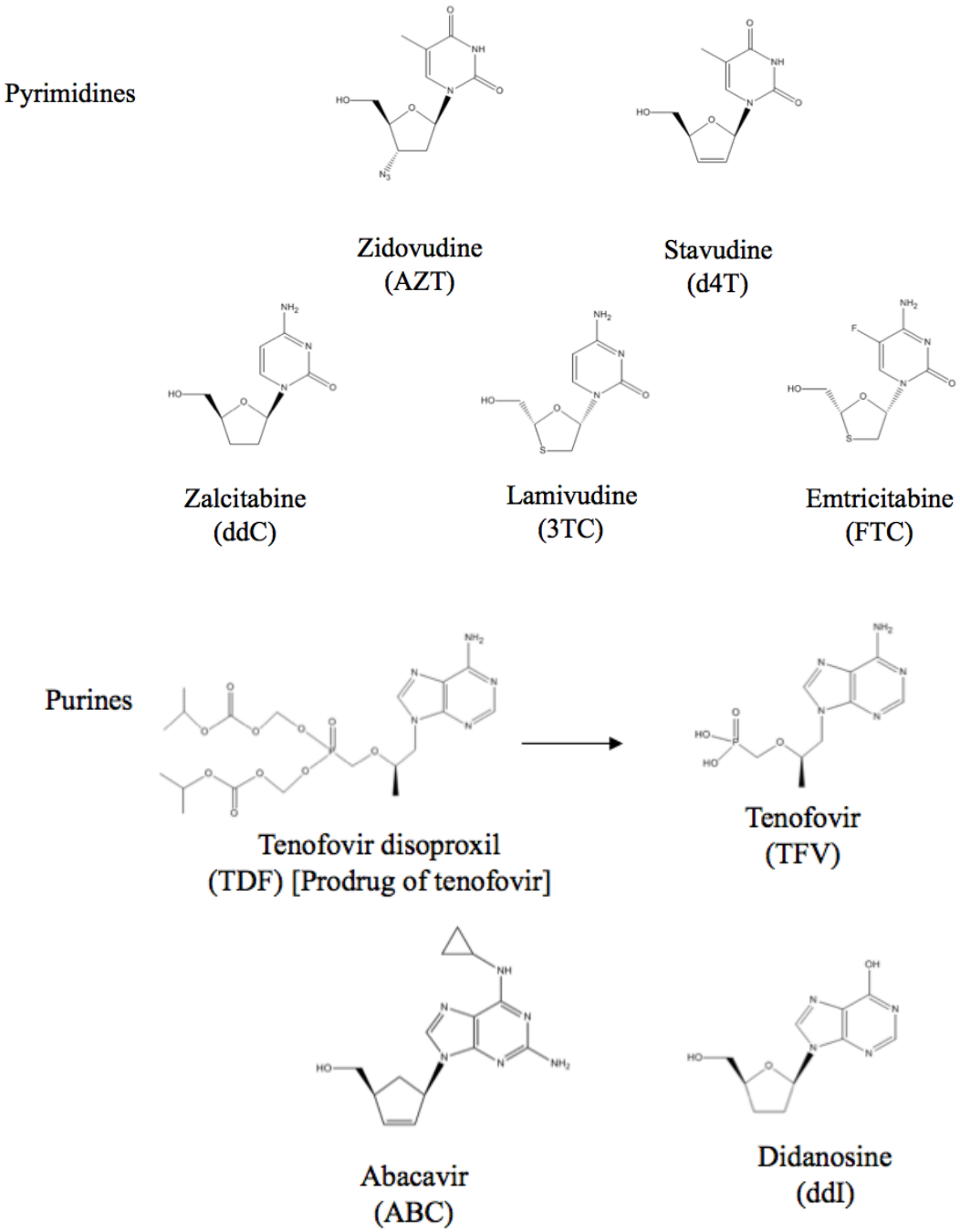

Figure 1. 6

Figure 1.7 **Excision and Dead End Complex (DEC) Formation.** Excision of an incorporated chain terminator (red) from the 3' primer terminus may only occur in the pre-translocation conformation (left). ATP or PPi are shown as acceptor substrates, liberating the incorporated chain-terminator from this conformation in the form of either a nucleotide triphosphate or dinucleotide tetraphosphate, respectively. DEC formation occurs when a free nucleotide binds to a post-translocation chain-terminated RT:DNA complex (right). The formation of a stable DEC prevents both the excision reaction as well as nucleotide incorporation.

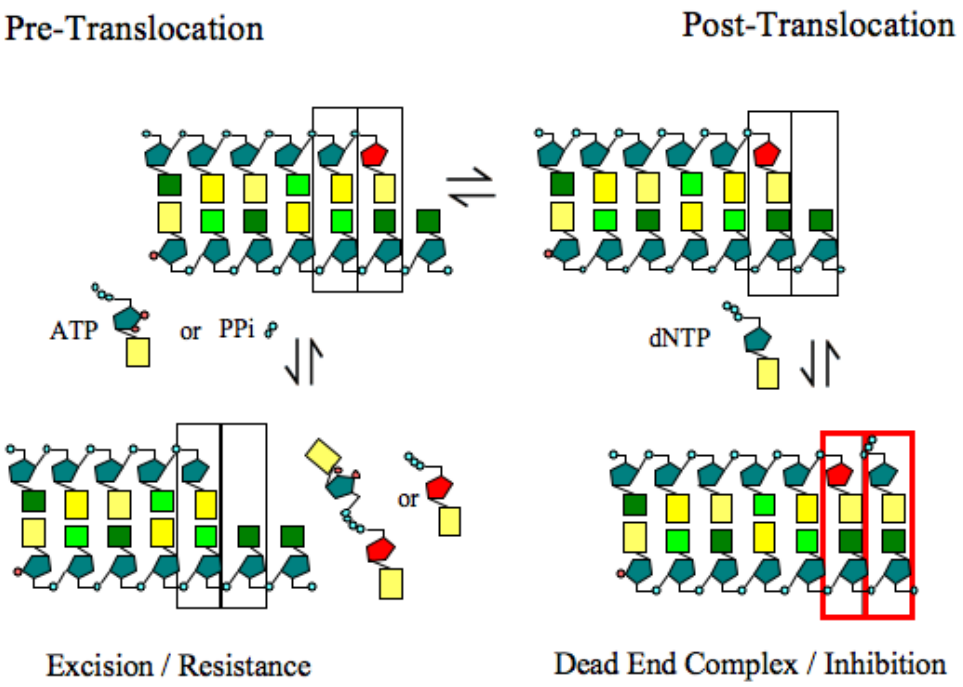

Figure 1. 7

Figure 1.8 **Structure of EFdA.**

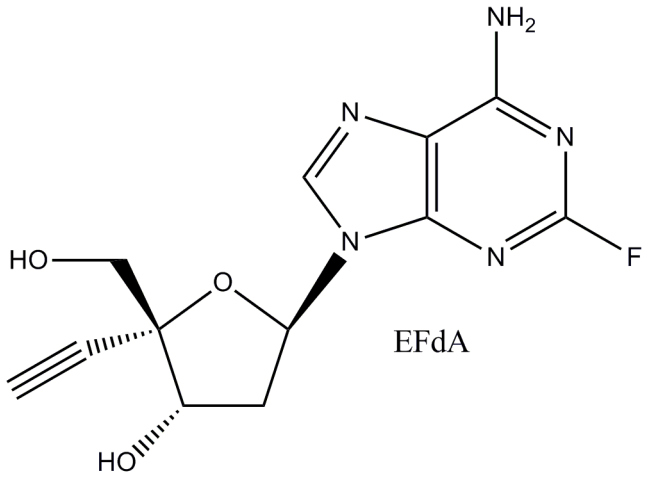

Figure 1. 8

Figure 1.9 **Non-obligate Chain Termination Mechanism of EFdA.** The polymerase active site of RT is represented as a rectangle divided into priming (P) and nucleotide binding (N) sites. EFd4 inhibits RT polymerization through a translocation deficiency mechanism. Binding of the incorporated inhibitor to a pocket in RT comprised of Ala-114, Tyr-115, Phe-160, Met-184 and the aliphatic chain of Asp-185 (grey circle) prevents translocation and the subsequent binding of the next nucleotide.

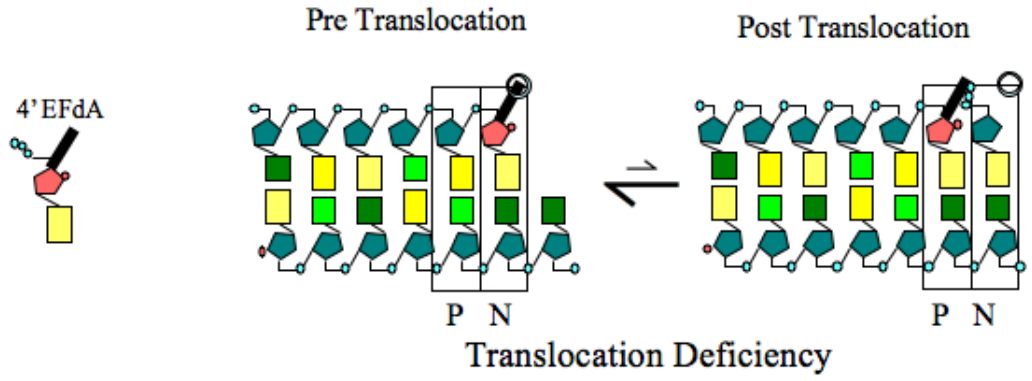

Figure 1. 9

Figure 1.10 **Structure of Entecavir**

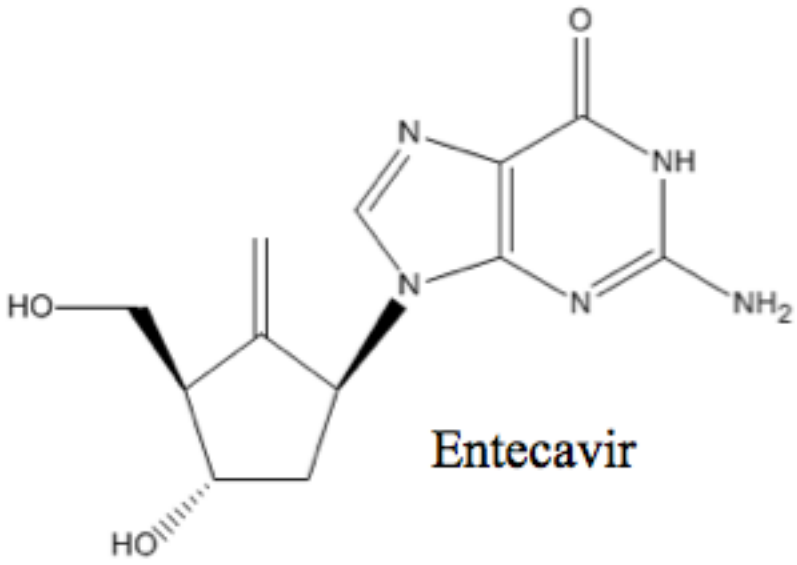

Figure 1. 10

Figure 1.11 **Mechanisms of Inhibition of Entecavir.** The polymerase active site of RT is represented as a rectangle divided into priming (P) and nucleotide binding (N) sites. Entecavir inhibits RT polymerization through both (a) delayed chain termination and (b) base pair confounding mechanisms. In the first mechanism RT performs three rounds of nucleotide incorporation following the incorporation of Entecavir at which point inhibition is achieved by a repulsion of the enzyme from the polymerase competent conformation, such that the 3' primer terminus is not located in the active site. Base pair confounding occurs when the inhibitor is present in the template strand.

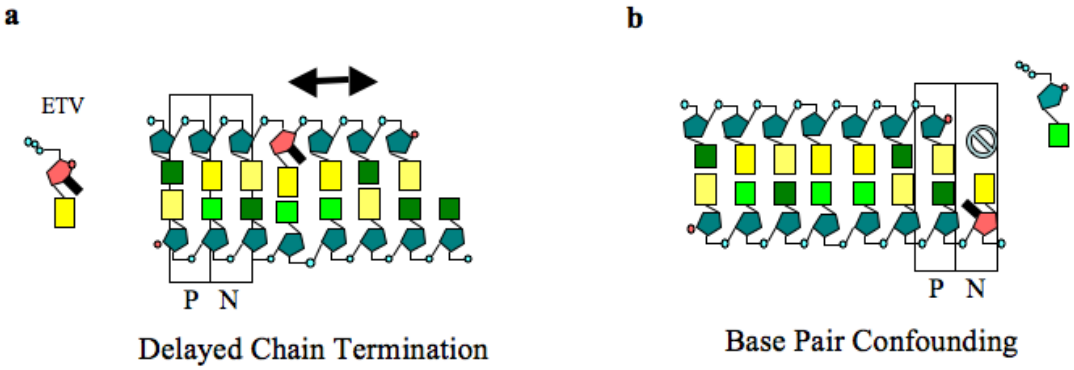

Figure 1. 11

Figure 1.12 **Structure of Foscarnet (PFA)**

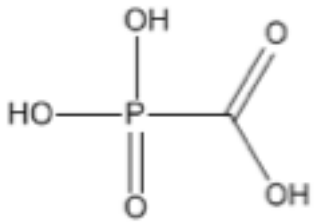

PFA

Figure 1. 12

Figure 1.13 **Translocation Specific Inhibition of RT.** (a) PFA and (b) INDOPY-1 inhibit RT polymerization by selectively binding to pre- and post-translocation conformations, respectively. The polymerase active site of RT is represented as a rectangle divided into priming (P) and nucleotide binding (N) sites. The binding of the inhibitors to their respective conformation results in the formation of a stable closed complex (red rectangle) analogous to the DEC formed by nucleotide binding to a chain-terminated RT:DNA complexes.

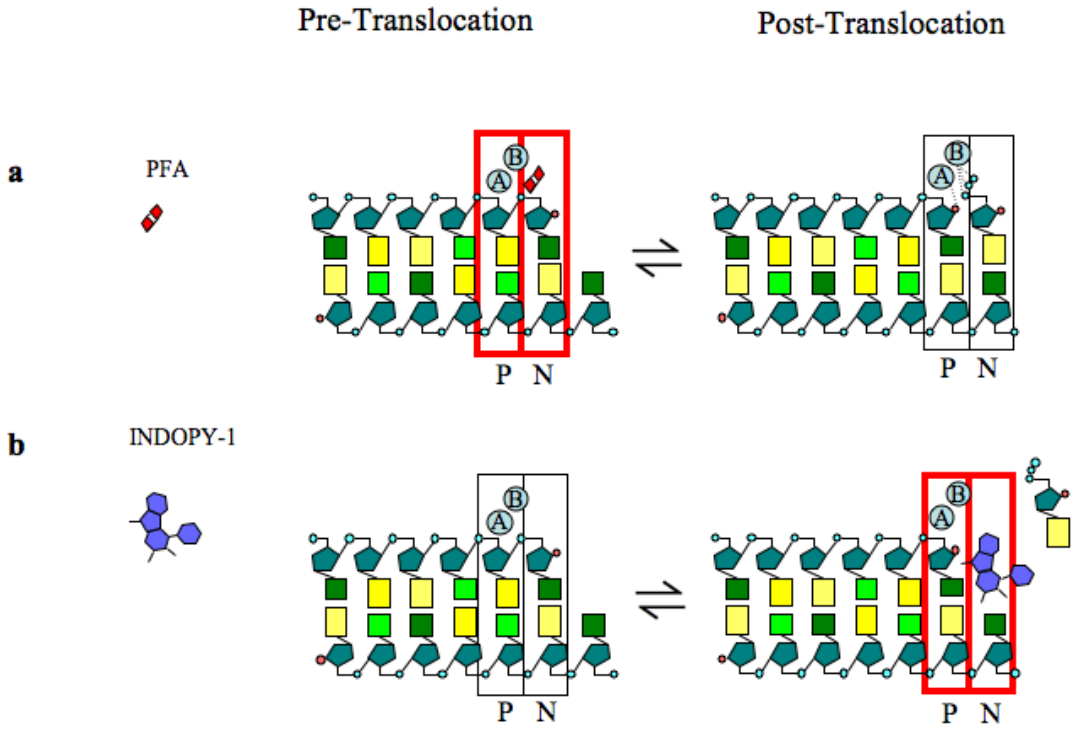

Figure 1. 13

Figure 1.14 **Structure of INDOPY-1.**

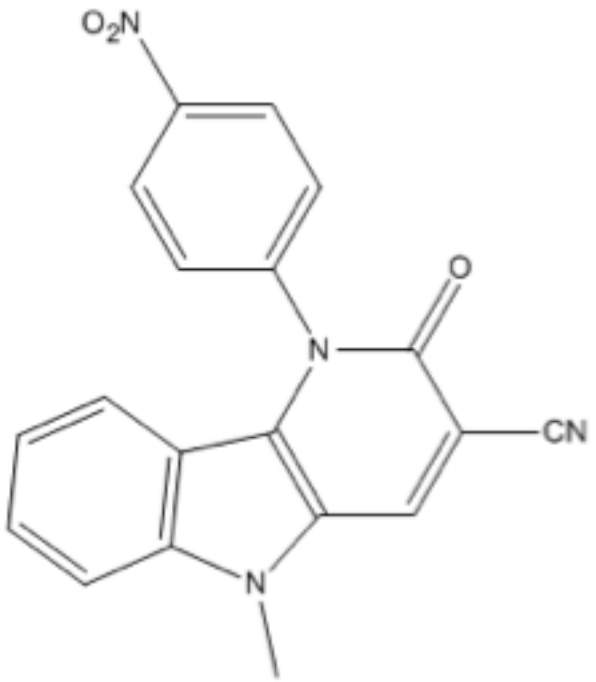

INDOPY-1

Figure 1. 14

Figure 1.15 **Structures of Clinically Available NNRTIs.**

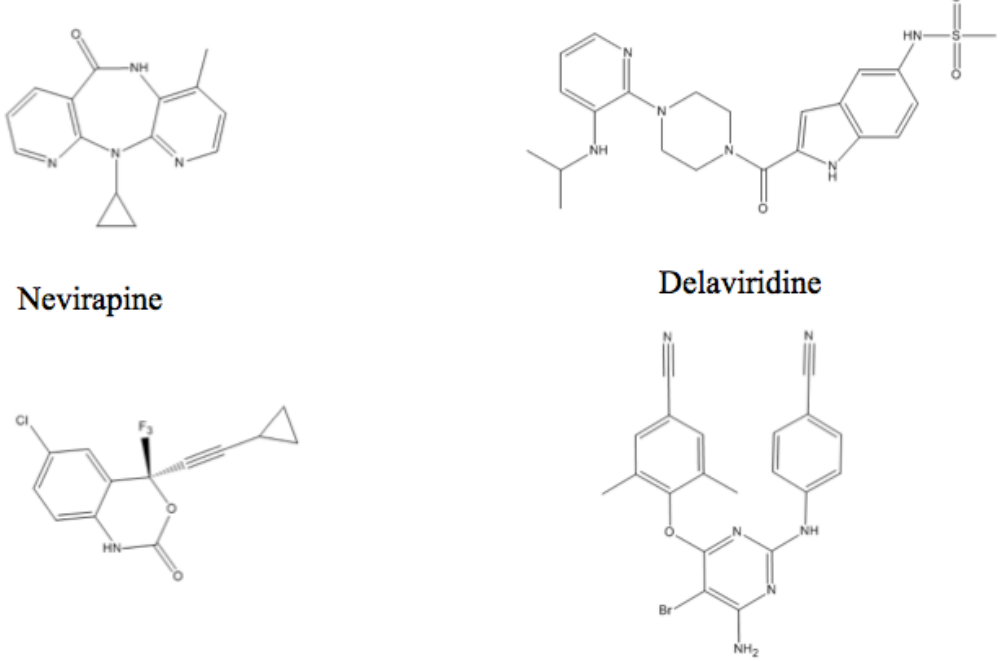

Figure 1. 15

Chapter 2

Effects of Mutations F61A and A62V in the Fingers Subdomain of HIV-1 Reverse Transcriptase on the Translocational equilibrium.

This chapter was adapted from an article authored by Brian Scarth[1], Suzanne McCormick[1] and Matthias Götte[1,2] that appeared in the ***Journal of Molecular Biology*** 2011 Jan 14;405(2):349-60

[1]Department of Microbiology & Immunology, McGill University, Montreal, QC, Canada, H3A 2B4

[2]Department of Biochemistry, McGill University, Montréal, QC H3A 1A3, Canada.

2.1 Abstract

Changes of the translocation status of HIV-1 Reverse Transcriptase (RT) can affect susceptibility to antiretroviral drugs. The pyrophosphate analogue phosphonoformic acid (PFA) binds specifically to and traps the pre-translocated complex of HIV-1 RT, while nucleotide-competing RT inhibitors (NcRTIs) trap the post-translocated conformation. Here we attempted to assess the potential role of residues in the fingers subdomain as determinants of polymerase translocation. The fingers can exist in open and closed conformations; however, the relationship between such conformational changes and the translocation status of HIV-1 RT remains elusive. We focused on substitution F61A, and the neighboring A62V that is frequently associated with drug resistance-conferring mutations. The proximity of these residues to the nucleic acid substrate suggested a possible role in translocation for these amino acid changes. We employed site-specific footprinting, binding assays, and DNA-synthesis inhibition experiments to study F61A and A62V, alone and against a background of known drug resistance mutations. We demonstrate that F61A causes a strong bias to the post-translocation state, while A62V shows a subtle bias toward pre-translocation regardless of the mutational background. Increases in the population of pre-translocated complexes were accompanied by increases in PFA activity, while F61A is literally resistant to PFA. Our data shed light on equilibria between pre- and post-translocated complexes with the fingers subdomain in its open or closed conformations. We propose that a binary, pre-translocated complex in a closed conformation is stabilized with A62V and destabilized with F61A.

2.2 Introduction

Due to its central role in viral replication, the reverse transcriptase (RT) of the human immunodeficiency virus type 1 (HIV-1) remains a major target for drug discovery and development efforts. The approved nucleoside and non-nucleoside analogue RT inhibitors (NRTIs and NNRTIs, respectively) act through different mechanisms of action. NRTIs act as chain terminators and compete with natural nucleoside triphosphate (dNTP) pools for incorporation, while NNRTIs act as allosteric non-competitive inhibitors of RT [99; 100]. Other classes of RT inhibitors that are currently not approved for clinical use can interfere with the function of the RT enzyme in a manner that markedly differs from the established mechanism of action described for NRTIs and NNRTIs. The recently discovered nucleotide-competing RT inhibitors (NcRTIs) are not incorporated into the growing chain, but inhibit DNA synthesis by competing with natural dNTPs at the active site despite their notable dissimilarity in structure [103; 227]. Despite these differences in comparison to dNTPs and NRTIs, the binding site for NcRTIs seems to overlap with the nucleotide binding site (N-site).

Site-specific footprinting experiments revealed that HIV-1 RT can shuttle between two adjacent positions on its primer/template substrate [125; 240]. The two conformations constitute the translocational equilibrium. Ligands such as dNTPs, NRTIs, and NcRTIs can trap the post-translocated complex that provides free access to the N-site [227]. In contrast, the pyrophosphate (PPi) analogue foscarnet (phosphonoformic acid, PFA) was shown to trap the pre-translocated complex [104]. In

this conformation, the 3'end of the primer occupies the N-site, which prevents binding of dNTPs, NRTIs, and NcRTIs in competitive fashion.

The requirement of a pre-translocated complex for PFA activity fits with the relationship between PFA resistance and susceptibility to the NRTI 3'-azido-3'deoxythymidine (zidovudine or AZT) [200; 218; 219; 241]. RT overcomes AZT inhibition through excision of the incorporated monophosphate with a pyrophosphate (PPi) donor such as ATP[102; 242]. This reaction requires the pre-translocated conformation [123; 125; 126; 176]. The translocation state of RT plays therefore an important role in susceptibility to PFA [104], NRTIs [123; 179]; [126], and NcRTIs [103; 227]. The determinants of translocation most likely exist at the interface between the nucleic acid substrate and the enzyme [115]; however, conformational changes upon nucleotide binding may also affect the translocation status of polymerases [107]. Nucleotide binding is associated with a closure of the fingers subdomain in HIV-1 RT [107], which traps the enzyme in its post-translocation state. Formation of a new phosphodiester bond defines the pre-translocated complex for the next round of nucleotide incorporation. Translocation of HIV-1 RT may only take place in the open conformation following or concomitantly with the release of PPi. The enzyme can then freely move between pre- and post-translocated states [104; 125; 126; 180] until the next nucleotide traps again the post-translocated complex.

Here we asked whether changes in the fingers subdomain that affect the open and closed conformations of the complex may in turn affect the translocation status of HIV-1 RT. F61 appears to interact with the template overhang and stabilizes the ternary complex with the nucleotide substrate [107; 123; 179; 243]. Several studies have

shown that the F61A mutation compromises nucleotide binding [222; 223; 224; 225; 227; 244]. The adjacent residue A62 may likewise affect the stability of the ternary complex. This mutation was identified in mutational patterns associated with NRTI multi-drug resistance, including the 69ss insertion complex [192; 196; 198] and the Q151M cluster [154; 245]. Of note, the former complex confers resistance to NRTIs through increases in excision [192; 193; 196; 198; 246], while the latter discriminates against the inhibitor [156; 247]. We have generated F61A- and A62V-containing mutant enzymes and show that F61A strongly influences the translocation status of HIV-1 RT, creating a strong bias towards post-translocation, while A62V creates a bias towards pre-translocation. Binding experiments show destabilization of ternary complexes by F61A, while A62V appears to improve complex formation. Together, our data suggest a possible relationship between the translocational equilibrium and conformational changes in the fingers subdomain.

2.3 Materials and Methods

Enzymes and nucleic acids

Heterodimeric reverse transcriptase p66/p51 was expressed and purified as previously described [248]. Mutant enzymes were generated through site directed mutagenesis using the Stratagene Quick-change kit according to the manufacturer's protocol. Oligo-deoxynucleotides used in this study were chemically synthesized and purchased from Invitrogen Life Technologies. The following sequence was used as a template:

PPT57:

CGTTGGGAGTGAATTAGCCCTTCCAGTCCCCCCTTTTCTTTTAAAAAAGTG

GCTAAGA

The following sequences were used as primers:

PPT17: TTAAAAGAAAAGGGGGG

PPT18: TTAAAAGAAAAGGGGGGA

PPT19: TTAAAAGAAAAGGGGGGAC

PPT20: TTAAAAGAAAAGGGGGGACT

PPT+16: GGGGACTGGAAGGGCTAATT

Deoxynucleotides were purchased from Fermentas Life Sciences. Phosphonoformic acid was purchased from Sigma Aldrich Chemicals.

All concentrations reported for assay conditions are final concentration after mixing.

DNA synthesis

50 nM of the 5'-^{32}P-labelled PPT17 primer was heat annealed with 125 nM PPT57. The DNA/DNA hybrid was incubated with 250 nM HIV-1 RT in a buffer containing 50 mM Tris-HCl pH 7.8, 50 mM NaCl and 6 mM $MgCl_2$, with 10 µM of each of the four dNTPs in the presence or absence of 10 µM PFA all in a final reaction volume of 20 µl. The reaction was carried out at 37°C with 1.8 µl aliquots removed at indicated times and added to 8.2 µl of formamide with traces of bromophenol blue and xylene cyanol to stop the reaction. Aliquots were then boiled and loaded directly on a 12% denaturing polyacrylamide gel followed by phosphorimaging to visualise extension products.

Site-specific footprinting

Performed as previously described[125], briefly: KOONO was prepared by stirring 10 ml of 1.2 M KNO_2 with 1.4 ml of 30% H_2O_2 on ice. 10 ml of 1.4 M HCl was added to the stirring solution and immediately quenched with 10 ml of 2 M KOH. Aliquots were stored at -80°C. In preparation of the footprinting reaction, the 5' P^{32} labelled template was heat annealed with the primer. The DNA/DNA hybrid (125 nM) was incubated with 750 nM RT in a buffer containing sodium cacodylate pH 7 (120 mM), NaCl (20 mM), DTT (0.5 mM) and $MgCl_2$ (6 mM) in a final volume of 20 µl. Reactions were incubated at 37°C for 10 minutes followed by the addition of 1.5 µl of KOONO (100 mM).

Gel mobility shift assays

Binary complex formation was assessed by enzyme titration as previously described under the following conditions[249]: RT (7.8-1000 nM) was titrated with 50 nM of 5'-^{32}P-labelled primer/template in a buffer containing 50mM Tris-HCl pH 7.8, 50 mM

NaCl and 6 mM $MgCl_2$ in a final volume of 20 µl. Samples were loaded in 50% sucrose on non-denaturing 6% polyacrilamide gels. The results were quantified as a fraction of shifted primer/template for each concentration of RT used. Apparent K_d^{DNA} for binary complex formation was estimated by fitting the quantified results to the quadratic equation:

$$[RT/PT] = 0.5(K_d^{DNA} + [PT] + [RT]) - (0.25(K_d^{DNA} + [PT] + [RT])^2 - [PT]*[RT]^{1/2}$$

where [RT/PT] is the concentration of binary complex observed, [PT] is the concentration of primer/template [RT] represents the concentration of RT and K_d^{DNA} is the determined as the concentration of RT required for 50% of total binary complex formation[100].

To test for stable ternary complex formaiont 50 nM of 5'-^{32}P-labelled primer/template was incubated with 250 nM RT in the same buffer conditions as above. Different concentrations of PFA or dCTP were added prior to the addition of heparin (1µg/µl). The complexes were incubated for 60 minutes at room temperature. Samples were then loaded in 50% sucrose on non-denaturing 6% polyacrylamide gels. The results were quantified as the fraction of shifted primer/template for each concentration of ligand used. Apparent K_d was estimated by fitting the quantified results to a hyperbola for one site binding ($Y=B_{maz}*X(K_d+X)$) where Y is the percent of substrate shifted, X is the concentration of ligand (PFA or dNTP), B_{max} is the maximum value amount of primer/template shifted and K_d is determined as the concentration of substrate (PFA or dCTP) to produce 50% of maximum shift as previously described [180]. For experiments with dCTP binding, purified chain

terminated primers were prepared as previously described to prevent incorporation of dCTP during binding experiments [181].

IC_{50} determinations

The inhibitory effect of PFA on DNA synthesis of WT or mutant HIV-1 RT was assessed through a filter-based assay. In a 10 µl reaction, 900 ng of heteropolymeric activated calf thymus DNA (Sigma Aldrich Chemicals) was incubated for 30 minutes at room temperature with 900 ng of HIV-1 RT (WT or mutant) in a buffer containing 50 mM Tris-HCl (pH 7.8) and 50 mM NaCl. 1 µl of [3H]dTTP, 10 mM dNTP mix and a gradient of PFA or PPi. The reaction was started by the addition of 6 mM $MgCl_2$. The samples were incubated for 1 hour at 37ºC and the reaction was quenched by the addition of 250 µl of 10% trichloroacetic acid. Samples were then filtered and scintillation analysis was used to measure the amount of incorporated [3H]dTTP.

IC_{50} values were obtained through analysis with the Prism program using the formula for one site competition [$Y=Bottom + (Top-Bottom)/(1+10^{(X-logIC50)})$] where Y is the amount of product formed, X is the concentration of inhibitor (PFA or PPi), Top and Bottom are maximum and minimum amounts of product formation and IC50 is determined as the amount of inhibitor required to elicit 50% inhibition.

2.4 Results

The aim of this study was to assess the role of fingers mutations F61A and A62V in HIV-1 RT as possible molecular determinants for polymerase translocation. We performed site-specific footprinting experiments to characterize the effects of these amino acid substitutions on the translocation status of the RT-primer/template complex and its function. In this context, we focused on nucleotide binding and binding of the PPi analogue PFA that require formation of a post-translocated and pre-translocated complex, respectively.

Effects of fingers substitutions on the translocation status of HIV-1 RT - We have previously shown that treatment of RT-DNA/DNA complexes with the chemical nuclease potassium peroxynitrite (KOONO) cleaves the template hyper-reactively at positions -7 or -8[125]. These cuts, referred to as the site-specific footprint of the complex, are indicative of post- and pre-translocated complexes, respectively. Cuts at both positions indicate a mixture of the two populations. Given that the particular sequence context of the nucleic acid substrate as well as the mutational context of RT can affect the ratio of the populations, we studied the footprints of mutant enzymes F61A, A62V and the double mutant F61A/A62V with different primer/templates. We utilized four substrates that show a broad spectrum of cleavage patterns with WT RT. The sequences, referred to as PPT17, PPT18, PPT19, and PPT20, are derived from the polypurine tract (PPT) of HIV-1. The number refers to the length of the primers that were gradually truncated at their 3'-end. With WT RT PPT17 shows a bias to the

post-translocated conformation, while PPT20 shows a strong bias to the pre-translocated conformation and PPT18 and PPT19 show mixtures of the two extremes with WT RT (Figure 2.1, first panel). The A62V mutation does not significantly affect the cleavage patterns (Figure 2.1, second panel). In contrast, F61A and F61A/A62V containing RT induce a strong bias to the post-translocated conformation. Complexes that existed predominantly in the pre-translocated state (PPT20), or as mixtures (PPT19 and PPT18), are shifted to the post-translocated state (Figure 2.1, third and fourth panel).

To further assess a potential role of A62V in HIV-1 RT translocation, we studied the effect of this mutation against a background of various NRTI-resistance conferring mutations in our footprinting experiments (Figure 2.2). The panel of mutants was monitored with PPT18 that shows a mixture of the two conformations with WT HIV-1 RT; with the hypothesis being that near isoenergetic complexes may be more susceptible to perturbations of the translocational equilibrium. The results are presented as percentage of complexes that exist in the pre-translocation state over the entire population of complexes. Independently of the specific mutational background A62V shows increases in the population of pre-translocated complexes (Figure 2.2 b). The A62V mutant and the TAMs-containing enzyme, respectively, show subtle but reproducible and statistically significant increases in this population when compared with WT RT by unpaired t-test ($p < 0.0001$). The addition of A62V against a background of TAMs caused further increases ($p < 0.0001$). Similar effects are observed when the A62V mutation is added to enzyme constructs containing the 69ss insertion ($p < 0.0001$) and the Q151M cluster ($p = 0.0015$), respectively. The

complete Q151M cluster (A62V/V75I/F77L/Q151M/F116Y) shows greater increases in the pre-translocated population as compared to the A62V/Q151M mutant ($p < 0.0001$), which shows that the other mutations at positions 75, 77, and 116 can also affect the translocational equilibrium perhaps in concert with A62V. Moreover, a subtle shift away from a predominant post-translocated population of complexes is even seen when comparing the F61A/A62V double mutant to the heavily biased F61A ($p = 0.004$).

Inhibition of DNA synthesis by PFA – We next asked whether such changes in the translocational equilibrium might translate into differences in enzymatic function. We have previously shown that complexes with primer/template sequences that are biased towards pre-translocation represent hot-spots for PFA mediated inhibition of DNA synthesis[104]. In contrast, primer/templates that show a bias towards post-translocation are less sensitive or even resistant to the inhibitor. Thus, the subtle bias toward pre-translocation associated with A62V, if significant, may translate into increased inhibitory effects of PFA, while F61A could provide a certain degree of resistance to the inhibitor. To test this hypothesis, we monitored DNA synthesis over multiple nucleotide incorporation events in the absence (Figure 2.3 a), and in the presence of a fixed concentration of PFA (Figure 2.3 b). The time course does not reveal any significant differences in DNA synthesis when WT RT was compared with the A62V mutant. In contrast, the F61A mutant is severely compromised in this regard. A significant fraction of the primer remains unextended. Interestingly, the

F61A/A62V double mutant can partially rescue the deficits in DNA synthesis introduced by F61A.

The addition of PFA resulted in three major pausing sites that eventually disappear over time. The inhibitory effects are slightly enhanced with the A62V mutant with earlier pausing sites persisting longer. In contrast, F61A shows marked reductions in pausing and time-dependent formation of the full-length product, which is not seen with WT RT or the A62V mutant under these conditions. These data demonstrate severe reductions in inhibitory potency. The F61A/A62V double mutant shows a similar phenotype. Formation of the full-length product is even more pronounced as a result of increases in primer usage as compared to F61A. Thus, the two mutants appear to exert opposing effects on DNA synthesis in the absence and in the presence of PFA.

To translate these findings into quantitative terms, we measured half maximal inhibitory concentrations (IC_{50}) of PFA and PPi on heteropolymeric DNA substrates. We included the panel of enzymes with resistance conferring mutations in this analysis, and found that enzymes containing A62V tended to lower the IC_{50} value for PFA (Figure 2.3 c). For instance, for WT RT, A62V, TAMs, and TAMs/A62V we measured IC_{50} values of 416 nM, 292 nM, 482 nM, and 203 nM, respectively. All enzymes showed IC_{50}s between 250 and 615 μM for PPi, except for mutants F61A and F61A/A62V, whose IC_{50} were above 1 mM (more than 3 times higher than for the WT enzyme) (data not shown). Although the differences in RT translocation and PFA sensitivity are subtle, these differences are significant with respect to the experimental errors in these assays. The effect on IC_{50} values is much more

pronounced with the F61A mutant enzyme. Both F61A and the F61A/A62V double mutant show > 10-fold increases in IC_{50} values for PFA when compared with WT RT.

Translocation Independent effects of A62V on PFA binding – Despite a good correlation between our footprints and IC_{50} measurements that link a bias to the pre-translocated conformation to increases in inhibitory effects, changes in inhibition of DNA synthesis may also be assigned to differences in affinity to PFA. To address this problem, we determined the stability of ternary complexes with a substrate that shows a strong bias towards pre-translocation, eliminating the effect of A62V seen at near isoenergetic positions. The position chosen, PPT+16, is equally biased toward pre-translocation for all enzymes tested (Figure 2.4 b) with the exception of F61A and F61A/A62V (F61A/A62V data not shown), which were not biased toward pre-translocation for any position tested. At this position the F61A containing enzymes displayed weak cuts with no bias. PFA forms a stable ternary complex with WT HIV-1 RT with this sequence[104]. Such complexes resist challenge with an enzyme trap such as heparin, while binary complexes in the absence of a ligand are unstable under these conditions. To control for possible differences in binary complex formation in the absence of trap, we determined the equilibrium dissociation constant (K_d^{DNA}), as previously described[249]. For the mutants A62V, F61A and F61A/A62V the K_d^{DNA} was seen to be similar to WT with values of 77.8 ± 11 nM, 66.0 ± 9 nM, 93.3 ± 17 nM and 107 ± 18 nM for WT, A62V, F61A and F61A/A62V respectively under our conditions (Figure 2.4 c and d).

With WT RT and the A62V mutant, increasing concentrations of PFA or dNTP (dCTP in our assay) correlate with an increase in ternary complex formation (Fig. 5). We measured equilibrium dissociation constants (K_d^{PFA}) of 4.6 μM and 1.9 μM for WT RT and A62V, respectively with PFA. A62V was seen to have a similar increase in affinity toward dCTP relative to WT with K_d^{dCTP} values determined to be 15.2 μM and 5.8 μM with WT and A62V, respectively. In contrast, a stable ternary complex is not formed with the F61A mutant. The F61A/A62V double mutant shows a mixed phenotype in that ternary complexes become visible at high concentrations of PFA or dNTP. These findings support the notion that A62V can at least in part counteract the effects of F61A, although the effect mediated through the F61A substitution is dominant.

We included the panel of resistant mutant enzymes in this analysis to assess the impact of A62V against different mutational patterns, and determined KdPFA values for PFA binding (Table 1). Similar to the difference between WT and A62V, decreases in KdPFA values of approximately 50% were also seen when comparing TAMs with TAMs/A62V, M41L/69SS/T215Y with M41L/A62V/69SS/T215Y, and Q151M with A62V/Q151M or the entire Q151M cluster. Together these findings point to 1.5- to 3-fold increases in PFA affinity associated with the A62V substitution. The specific mutational context may cause such variations; however, the trend toward increased inhibitor binding in the presence of A62V is evident.

2.5 Discussion

The translocational equilibrium of HIV-1 RT can be influenced by several parameters, including the particular sequence of the primer/template [125]. Specific amino acids that contact the nucleic acid substrate may individually or as a group contribute to the movement of RT [115]. In this study, we focused on positions 61 and 62 of the flexible β3-β4 loop in the fingers subdomain that are located in close proximity to the template 5'-overhang [107; 115; 123; 250]. Our site-specific footprinting experiments demonstrate that the F61A mutation causes a strong bias toward post-translocation, while the A62V mutation causes a subtle bias toward pre-translocation. Such shifts in the translocation status of HIV-1 RT correlate with opposing functional consequences. F61A shows substantial reductions in sensitivity and affinity to the pyrophosphate analogue PFA that traps the pre-translocated complex. Conversely, A62V increases binding of PFA and, in turn, inhibition, although these effects are less pronounced then those seen with F61A. The results were essentially reversed when the two mutations were studied in the context of NcRTIs that trap the RT-primer/template complex in the post-translocation state [227]. In this context, F61A shows increased sensitivity to NcRTIs [227], while A62V has been associated with resistance to these compounds [227; 251]. The combined findings suggest that both mutations F61A and A62V can influence the translocational equilibrium of HIV-1 RT in complementary fashion.

Although the F61A-associated complex exists predominantly post-translocation, several studies have shown that this mutation displays diminished binding of the natural nucleotide substrate [222; 223; 225; 227]. These data point to altered

interaction between the incoming nucleotide and the fingers subdomain. However, the F61A-mediated diminution in binding of PFA can be explained by a reduced population of the pre-translocated complex and/or altered contacts with the inhibitor.

Crystallographic snapshots that represent various stages during DNA synthesis may help to distinguish between these possibilities. While structures of ternary complexes of HIV-1 RT with nucleic acid substrate and PFA are not available, binary complexes comprised of HIV-1 RT and a DNA:DNA substrate have been solved for both pre- and post-translocation conformations [123; 250]. Superimposing the pre- and post-translocation structures shows the β3-β4 loop is in its open conformation with no significant changes in this region (Figure 2.6 a)[123; 250]. Thus, structural perturbations introduced by F61A will likely affect both pre- and post-translocated binary complexes to the same extent. Complexes with the fingers in its closed conformation have been crystallized solely in the post-translocation state with a bound nucleotide substrate [107; 250]. In this complex, F61 anchors the template via stacking interaction with the base moiety at position n+2 (Figure 2.6 b) [250]. The lack of this stacking interaction in the context of F61A provides a plausible explanation for decreases in the stability of the complex with an incoming nucleotide [222; 223; 224; 225; 227].

Although a closed binary complex has yet to be captured and structurally characterized, such a complex will likely exist immediately following bond formation. The ultimate phosphodiester bond of the primer may here serve as the structural equivalent of the α-phosphate of an incoming nucleotide in the post-translocated ternary complex. The side chain of R72 is able to provide crucial

contacts in both cases [198]. Our data show that increasing concentrations of PFA traps the closed pre-translocated complex in the context of wild type HIV-1 RT. In contrast, F61A is unable to form a stable complex with PFA. The F61A mutation will likely decrease the stability of both the closed ternary complex and a closed binary complex (in the absence of PFA) due to the lack of stacking interaction with the nucleic acid. The ability of F61A to perform nucleotide incorporation, albeit with reduced efficiency, indicates that formation of a closed complex is not completely eliminated. However, our data show that ternary complexes with either the nucleotide substrate or PFA are not stable in the presence of trap. The consequences for PFA binding and inhibition are more pronounced, because the inhibitor can dissociate from the complex, while nucleotide incorporation may only require transient formation of a closed complex at the moment of bond formation.

We have previously proposed a Brownian Ratchet model for RT translocation in which the enzyme moves freely between pre- and post-translocation states in the open conformations [125]. Thermal energy in the form of Brownian motion is sufficient the drive the movement relative to the nucleic acid substrate [104; 109; 240; 252]. Our observation that F61A is biased toward post-translocation suggests that this is the preferred conformation of the translocational equilibrium of open complexes. However, certain primer/template sequences may shift the overall equilibrium towards the closed, pre-translocated conformation that we can observe in our footprinting experiments with WT RT and the A62V mutant.

The A62V mutation appears to increase this effect to a certain degree. Increases in the population of closed complexes in the pre-translocated state help to

explain increases in affinity and sensitivity to PFA. These findings are consistent with previous data showing increased rates of ATP-mediated excision of AZT-MP with mutant enzymes containing A62V [198]. The authors suggested that the mutation affects the positioning of R72 in close proximity of the α and β phosphates of the bound nucleotide. We propose that A62V can cause analogous structural alterations that involve the precise positioning of R72 in the closed binary complex in its pre-translocated conformation. This helps to explain why A62V can at least in part compensate for the deficits introduced by F61A, although it is evident that the loss of stacking interaction with the template overhang is dominant.

Taken together, our data point to the existence of a closed binary complex in the pre-translocation state. The nucleotide binding site is occluded in this conformation; however, the direct link to the translocational equilibrium provides access to the post-translocation conformation that permits nucleotide binding, and, in turn, continuation of DNA synthesis. The formation of a stable, closed pre-translocated complex depends crucially on the sequence. Hence, this model may provide an explanation for the sequence-dependent differences with respect to both nucleotide incorporation and excision [125; 189]. One would predict that sequences that promote formation of this complex decrease efficiency of nucleotide incorporation and increase efficiency of excision. Detailed kinetic studies with appropriately defined primer/templates are required to address this question.

Acknowledgments: We would like to thank Dr. Egor Tchesnokov for inspiring discussion. This study was supported by the Canadian Institutes for Health Research (CIHR). MG is recipient of a national career award from the CIHR.

2.6 Figures and Tables

Figure 2.1. **KOONO experiments at consecutive primer-template positions.** WT A62V F61A and F61A/A62V containing RT were incubated with four double stranded DNA substrates with consecutive primer terminus positions. These binary complexes were treated with KOONO, producing cleavage fragments at positions -8 or -7 on the template strand corresponding to a pre- or post-translocation conformation respectively. Due to the relative positioning of the 3' end of the primer, -8/-7 cuts move along the template for each primer. Fragments are labelled on the gel for PPT17 (left side) and PPT20 (right side), fragments from PPT19 and PPT18 are staggered between these two extremes. A schematic indicates the distance from the nucleotide-binding site of RT to the position of KOONO cleavage on the template (bold) for pre- and post-translocated complexes for each substrate. 5'-^{32}P labelled template cleavage fragments are resolved on a 12% polyacrylamide gel at single nucleotide resolution.

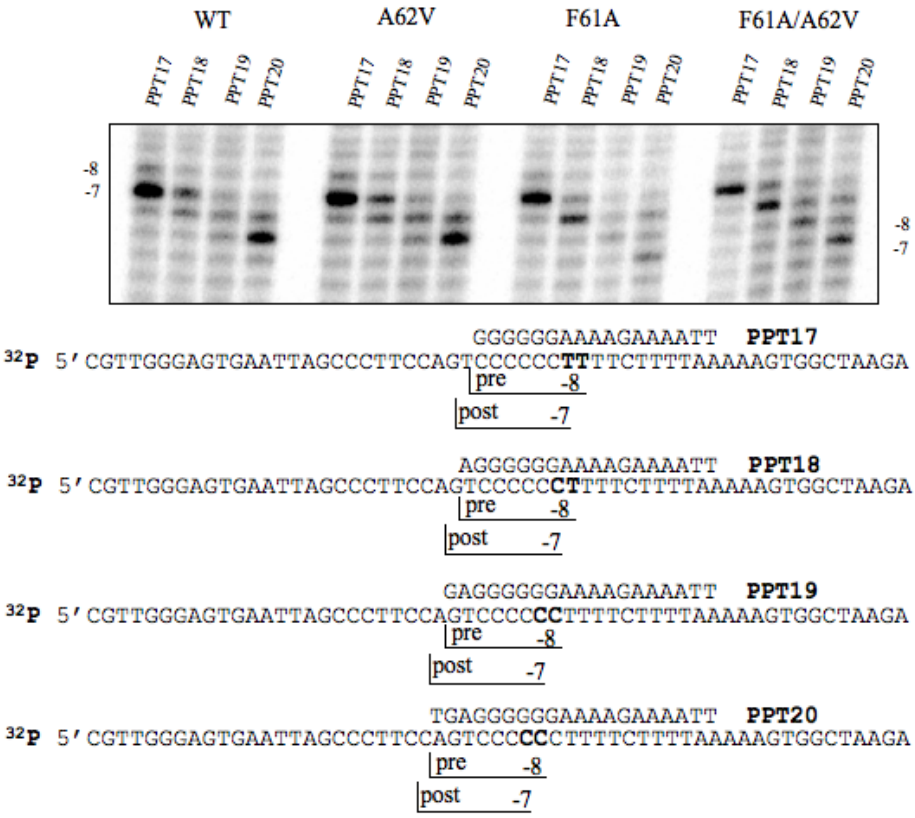
WT
A62V
F61A
F61A/A62V
PPT17
PPT18
PPT19
PPT20
-8
-7
GGGGGGAAAAGAAAATT PPT17
32P 5′CGTTGGGAGTGAATTAGCCCTTCCAGTCCCCCCTTTTCTTTTAAAAAGTGGCTAAGA
pre -8
post -7
AGGGGGGAAAAGAAAATT PPT18
32P 5′CGTTGGGAGTGAATTAGCCCTTCCAGTCCCCCCTTTTCTTTTAAAAAGTGGCTAAGA
pre -8
post -7
GAGGGGGGAAAAGAAAATT PPT19
32P 5′CGTTGGGAGTGAATTAGCCCTTCCAGTCCCCCCTTTTCTTTTAAAAAGTGGCTAAGA
pre -8
post -7
TGAGGGGGGAAAAGAAAATT PPT20
32P 5′CGTTGGGAGTGAATTAGCCCTTCCAGTCCCCCCTTTTCTTTTAAAAAGTGGCTAAGA
pre -8
post -7

Figure 2. 1

Figure 2.2. **KOONO experiments using a mixed-translocation primer-template system.** Binary stalled complexes were monitored for translocational equilibrium with PPT18 to assess changes to the equilibrium at a position of mixed-translocation. (a) The primer and template used indicating the size of expected (-8) pre and (-7) post translocation cuts on the 5'-^{32}P labelled template. (b) Cleavage fragments obtained from enzymes with and without the A62V mutation. (c) Analysis of the proportion of pre-translocation fragments for WT, F61A, F61A/A62V, A62V, TAMs (M41L/ D67N/T215Y/L210W), TAMs/A62V, 69ss/M41L/T215Y, M41L/A62V/69ss/T215Y, Q151M, A62V/Q151M and Q151M cluster (A62V/V75I/F77L/F116Y/Q151M) from multiple experiments.

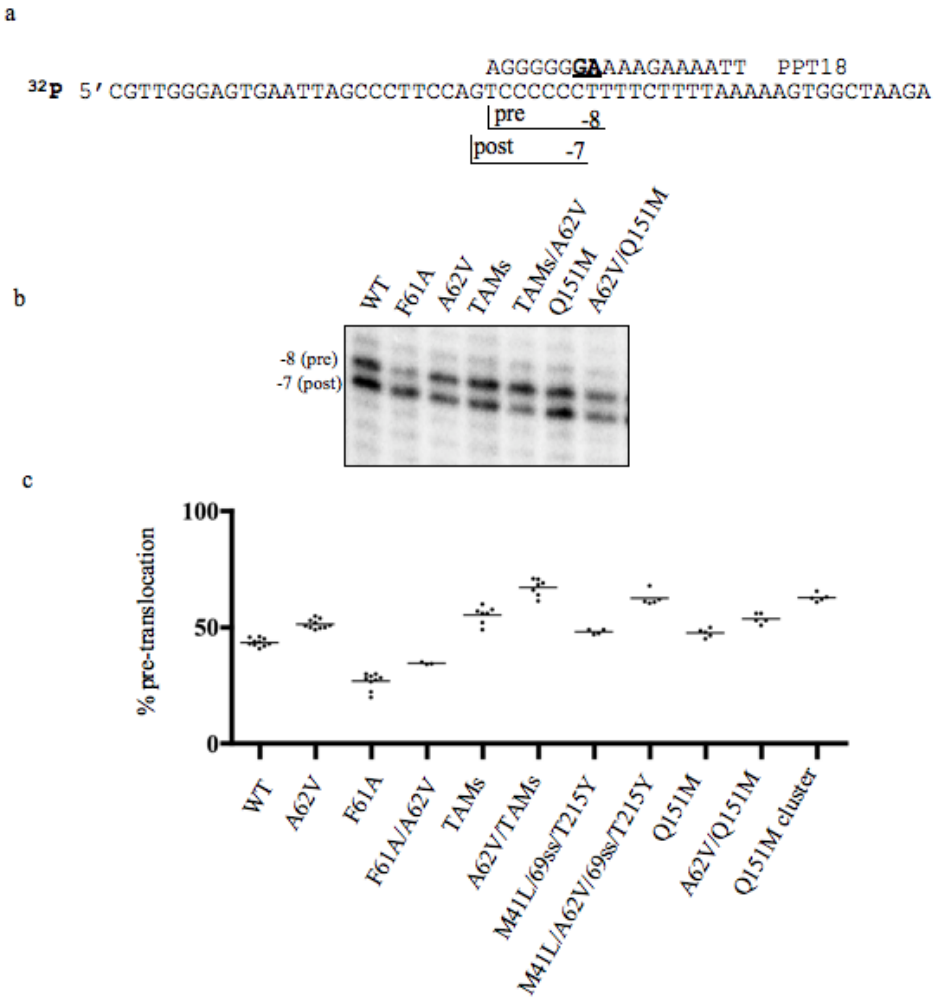
a
AGGGGGGAAAAGAAAATT PPT18
32P 5′CGTTGGGAGTGAATTAGCCCTTCCAGTCCCCCCTTTTCTTTTAAAAAGTGGCTAAGA
pre -8
post -7
b
WT
F61A
A62V
TAMs
TAMs/A62V
Q151M
A62V/Q151M
-8 (pre)
-7 (post)
c
% pre-translocation
100
50
0
WT
A62V
F61A
F61A/A62V
TAMs
A62V/TAMs
M41L/69ss/T215Y
M41L/A62V/69ss/T215Y
Q151M
A62V/Q151M
Q151M cluster

Figure 2. 2

Figure 2.3. **Sensitivity to Inhibition of DNA synthesis by PFA.** WT and mutant RTs (A62V, F61A and F61A/A62V) were monitored for DNA synthesis inhibition by PFA. 250 nM RT was incubated with 50 nM primer-template at 37ºC with 10 μM dNTPs in the absence (a) and presence (b) of 10 μM PFA over a time course of 10 minutes. Results shown are from a single representative experiment rearranged for presentation. *indicates pausing sites of PFA inhibition. (c) IC_{50} values for PFA were determined using a filter based assay with a heteropolymeric DNA template for WT, A62V, F61A, F61A/A62V, TAMs (M41L/ D67N/T215Y/L210W) TAMs/A62V, 69ss/M41L/T215Y, M41L/A62V/69ss/T215Y, Q151M, A62V/Q151M and the Q151M cluster (A62V/V75I/F77L/F116Y/Q151M).

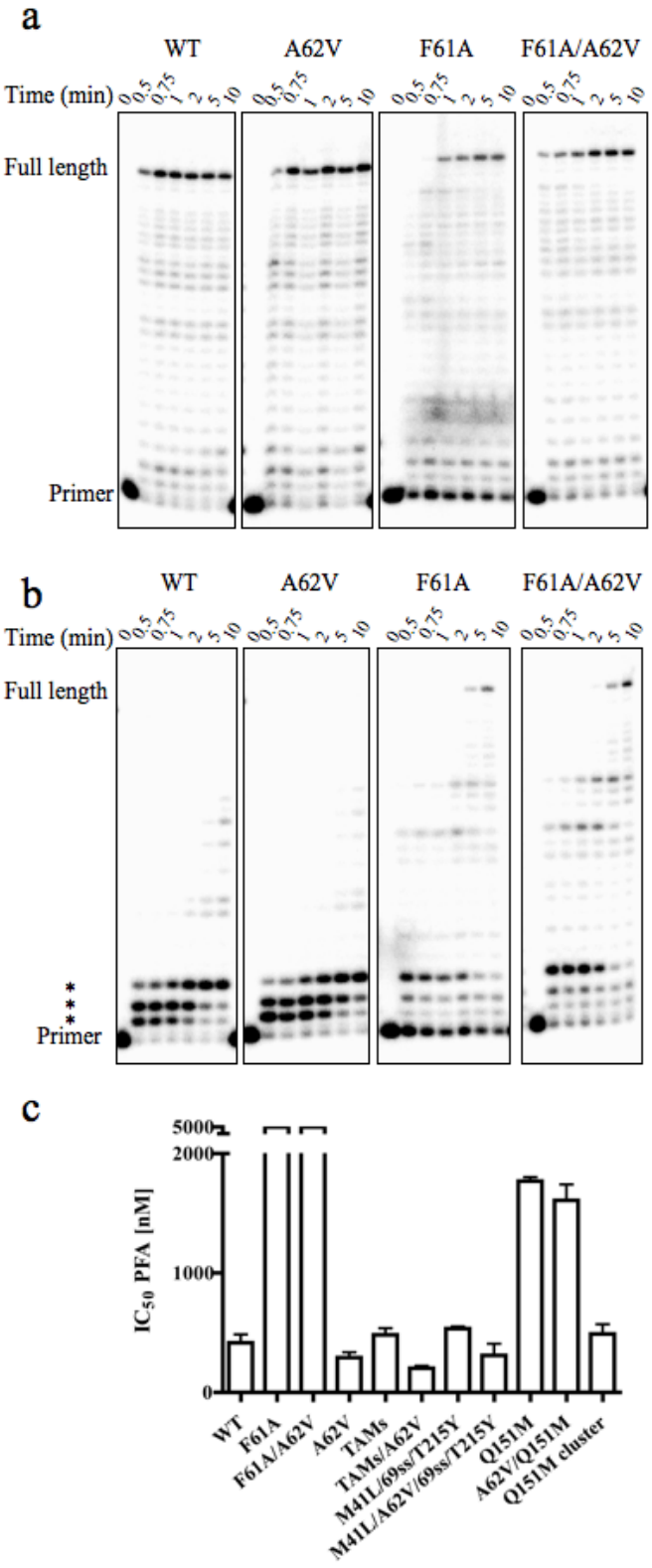
a
WT
A62V
F61A
F61A/A62V
Time (min)
0.5
0.75
1
2
5
10
Full length
Primer
b
WT
A62V
F61A
F61A/A62V
Time (min)
Full length
Primer
c
5000
2000
1000
0
IC50 PFA [nM]
WT
F61A
F61A/A62V
A62V
TAMs
TAMs/A62V
M41L/69ss/T215Y
M41L/A62V/69ss/T215Y
Q151M
A62V/Q151M
Q151M cluster

Figure 2. 3

Figure 2.4. **Binary complex formation with WT and mutant RTs using a pre-translocation system**. (a) Primer template sequence used indicating the size of expected (-8) pre and (-7) post translocation cuts on the 5'-^{32}P labelled template. (b) Cleavage fragments obtained for WT, F61A, A62V, TAMs (M41L/ D67N/T215Y/L210W), TAMs/A62V, 69ss/M41L/T215Y, M41L/A62V/69ss/T215Y, Q151M, A62V/Q151M and Q151M cluster (A62V/V75I/F77L/F116Y/Q151M). (c) Reactions containing 50 nM 5'-^{32}P labelled primer/template were incubated with increasing concentrations of WT (shown) and mutant RT and resolved on a 6% non-denaturing gel to separate unbound substrate from formed binary complexes. (d) Results of binary complex formation experiments with WT, A62V, F61A and F61A/A62V were fit to a quadratic equation to determine the K_d^{DNA} in terms of the amount of enzyme required to form a binary complex with 50% of the substrate.

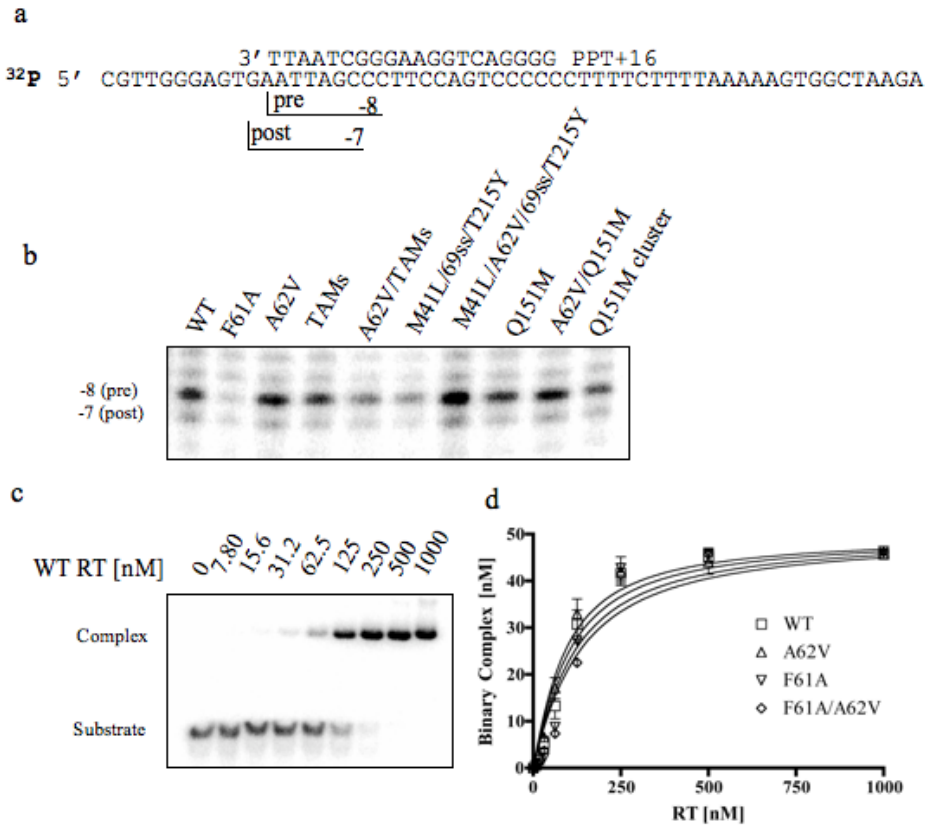
a
3′ TTAATCGGGAAGGTCAGGGG PPT+16
32P 5′ CGTTGGGAGTGAATTAGCCCTTCCAGTCCCCCCTTTTCTTTTAAAAAGTGGCTAAGA
pre -8
post -7
b
WT
F61A
A62V
TAMs
A62V/TAMs
M41L/69ss/T215Y
M41L/A62V/69ss/T215Y
Q151M
A62V/Q151M
Q151M cluster
-8 (pre)
-7 (post)
c
WT RT [nM]
0
7.80
15.6
31.2
62.5
125
250
500
1000
Complex
Substrate
d
Binary Complex [nM]
RT [nM]
WT
A62V
F61A
F61A/A62V

Figure 2. 4

Figure 2.5. **Ternary complex formation with PFA and dCTP using a pre-translocation system.** WT and mutant RT were monitored for ternary complex formation with PFA and dCTP. 250 nM RT was incubated with 50 nM μM 5'-^{32}P labelled primer/template and a range of concentrations of PFA (up to 125 μM) and dCTP (up to 200 or 2000 μM where indicated). Complex formation was challenged for 60 minutes with 1 μg/μl of Heparin trap, which was sufficient to prevent all complex formation when added prior to enzyme (Hep (+) control). Samples were resolved on a 6% non-denaturing gel with maximum complex formation seen in absence of Heparin (Hep (-) control) and increasing complex formation with increasing concentration of PFA or dCTP. Primers were chain terminated with ddTTP to prevent incorporation during dCTP binding experiments as per materials and methods.

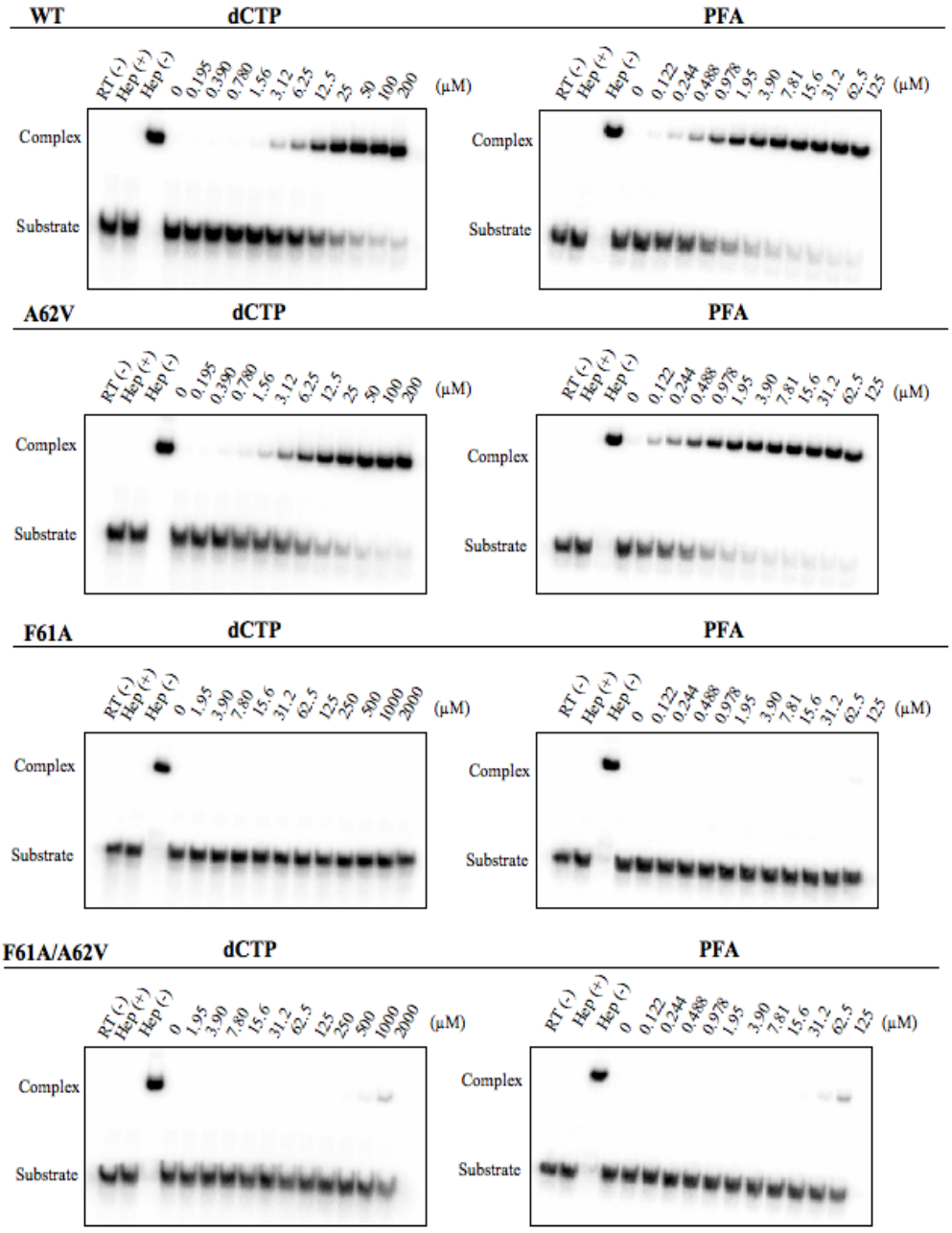
WT
dCTP
PFA
RT (-)
Hep (+)
Hep (-)
0 0.195 0.390 0.780 1.56 3.12 6.25 12.5 25 50 100 200 (μM)
0 0.122 0.244 0.488 0.978 1.95 3.90 7.81 15.6 31.2 62.5 125 (μM)
Complex
Substrate
A62V
dCTP
PFA
0 0.195 0.390 0.780 1.56 3.12 6.25 12.5 25 50 100 200 (μM)
0 0.122 0.244 0.488 0.978 1.95 3.90 7.81 15.6 31.2 62.5 125 (μM)
F61A
dCTP
PFA
0 1.95 3.90 7.80 15.6 31.2 62.5 125 250 500 1000 2000 (μM)
0 0.122 0.244 0.488 0.978 1.95 3.90 7.81 15.6 31.2 62.5 125 (μM)
F61A/A62V
dCTP
PFA
0 1.95 3.90 7.80 15.6 31.2 62.5 125 250 500 1000 2000 (μM)
0 0.122 0.244 0.488 0.978 1.95 3.90 7.81 15.6 31.2 62.5 125 (μM)

Figure 2. 5

Figure 2.6**. The position and orientations of F61 in binary and ternary crystal structures relative to the template overhang.** (a) Superposition of two binary post-translocation open complexes (1N5Y-blue and 1T03-yellow), and a binary pre-translocation open complex (1N6Q - green) shows no change in position or orientation of F61, regardless of translocation status. (b) Residues and nucleotides (yellow) within 4Å of F61 (red) in a post-translocation ternary complex (1T05). (c) The relative difference between the orientation of F61 in (b) and (d) the pre-translocation binary complex (1T03) with residues and nucleotides (aqua) within 4Å of F61 (purple) indicated. A stacking interaction between F61 and the template overhang is only seen in the post-translocation ternary complex (b and c).

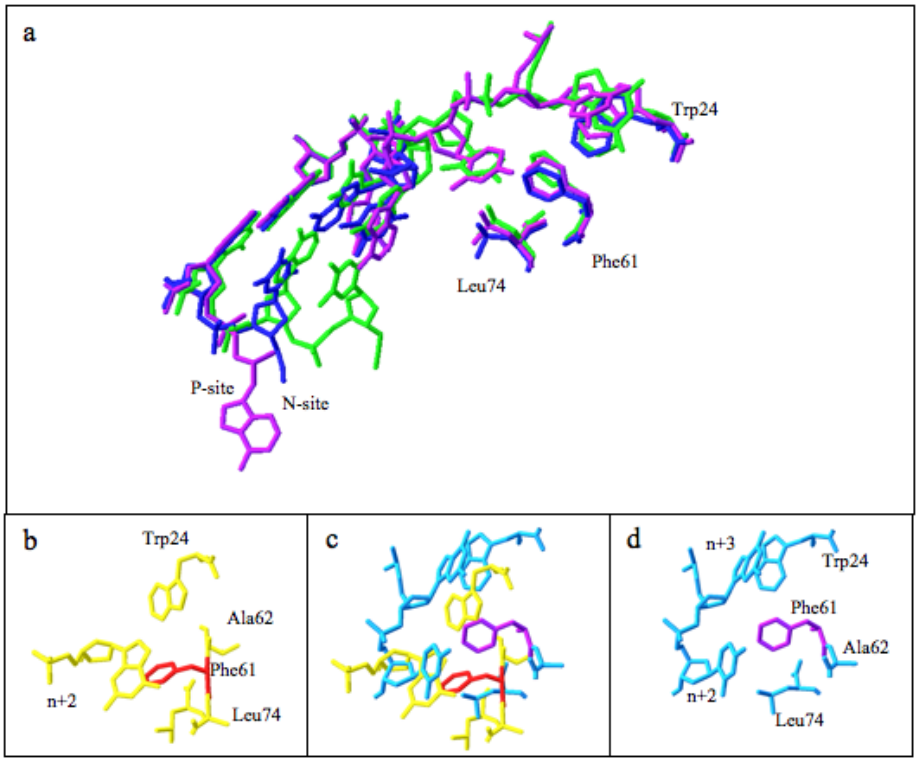

Figure 2. 6

Table 2.1 **Band-shift experiments with a pre-translocation primer-template system**

Enzyme	K_d^{PFA} (uM)[a]	Fold change/WT
WT	4.6±0.6	/
F61A	n.d.	n.d.
F61A/A62V	n.d.	n.d.
A62V	1.9±0.2	0.41
TAMs[b]	3.7±0.4	0.80
TAMs[b]/A62V	2.3±0.3	0.50
M41L/69ss/T215Y	8.4±1.6	1.8
M41L/A62V/69ss/T215Y	2.3±0.4	0.50
Q151M	7.4±0.9	1.6
A62V/Q151M	3.3±0.6	0.72
Q151M cluster[c]	2.1±0.3	0.46

[a] Values determined from bandshift experiments using PPT+16 (Pre-translocation system) and represent a minimum of 3 replicates ± standard deviation.
[b] TAMs (M41L/D67N/L210W/T215Y)
[c] Q151M cluster (A62V/V75I/F77L/F116Y/Q151M)
n.d. not determined

Table 2. 1

Chapter 3

Impact of the Translocational equilibrium of HIV-1 Reverse Transcriptase on Nucleotide Incorporation and Excision

This chapter is adapted from a manuscript authored by Brian Scarth[1] and Matthias Götte[1,2], which is currently in preparation for submission to the ***Journal of Molecular Biology***

[1]Department of Microbiology & Immunology, McGill University, Montreal, QC, Canada, H3A 2B4

[2]Department of Biochemistry, McGill University, Montréal, QC H3A 1A3, Canada.

3.1 Preface

Characterization of fingers subdomain mutants F61A and A62V as determinants of the translocational equilibrium revealed a possible link between the translocational equilibrium and conformational changes in the fingers. Our observation that the lack of stacking interactions between F61A and the template overhang results in sequence-independent strong post-translocation bias, led us to predict that the post-translocation conformation was a default state. We proposed that the pre-translocation state makes use of the stacking interaction in a closed binary complex, under certain sequence contexts. To test this hypothesis, in the following study, we have determined the contribution of the nucleic acid sequence to the translocational equilibrium over a large number of sequences, using site-specific footprinting. We observe that the post-translocation conformation is indeed the common state of the enzyme for the majority of sequenes. Defined sequences were then used to assess the impact of translocation bias on both nucleotide incorporation and excision using single turn-over pre-steady state kinetics.

3.2 Abstract

The translocation of HIV-1 reverse transcriptase (RT) is a critical step in the incorporation of nucleotides by this viral polymerase. The translocation status of RT has important consequences for drug susceptibility and mechanisms of drug resistance. We have assessed the role of the nucleic acid sequence, a determinant of the translocational equilibrium, as it relates to kinetic parameters of nucleotide incorporation and excision. Using site-specific footprinting techniques with consecutive primers we determined the translocational equilibrium to be heavily biased toward post-translocation in the majority of sequence contexts. Using pre-steady state kinetics we show that a post-translocation bias leads to 14-143 fold increases in efficiency of nucleotide incorporation as compared to pre-translocation bias. Differences are manifested in both the binding affinity (K_D) and catalytic rate (k_{pol}) and possible mechanisms are discussed. Pre-translocation sequences are observed for a minority of sequences tested. The 3' primer terminus is seen to be an important determinant of strong pre-translocation bias with a requirement of thymidine at this position observed for sequences tested. In pyrophosphorolysis experiments we observe improved catalytic rate (k_{pyro}) and binding affinity for PPi (K_D^{PPi}) with sequences with sufficient access to this conformation, in agreement with the requirement of this conformation for the excision reaction. Consequences to mechanisms of excision based drug resistance are discussed.

3.3 Introduction

The reverse transcriptase (RT) of human immunodeficiency virus type-1 (HIV-1) is critically required for viral replication and thus serves as a major target for drug development and discovery efforts. The two classes of clinically approved inhibitors of RT, the nucleoside analogue RT inhibitors (NRTIs) and the non-nucleoside RT inhibitors (NNRTIs) act through distinct mechanisms of action. NRTIs mimic and compete with the natural dNTP substrates for incorporation into the extended primer and act as chain terminators through the lack of a 3' OH group [51]. NNRTIs inhibit the catalytic step of the polymerase reaction allosterically through binding to an induced hydrophobic pocket approximately 10 Å from the polymerase active site [51]. Additional inhibitors of RT polymerase activity, nucleoside-competing RT inhibitors (NcRTIs), have recently been described which, despite structural dissimilarity to the natural dNTP substrate, compete for binding with dNTPs at the active site [103; 226; 253]. NcRTIs were seen to bind to a site that overlapped with the nucleotide-binding site (N-site). Unlike dNTPs, the binding of NcRTIs to an accessible N-site is not directed by the nature of the templated nucleotide at position n+1, instead the presence of a pyrimidine (especially thymidine) at the 3' primer terminus was seen to promote NcRTI binding [226].

Site-specific footprinting revealed that RT can shuttle between two adjacent positions on its primer/template representing the translocational equilibrium [125]. Pre-

and post-translocation conformations are defined by the position of the 3' primer terminus in the active site [240]. Ligands such as dNTPs, NRTIs and NcRTIs selectively bind to, and trap, RT:DNA/DNA complexes in the post-translocation conformation where the N-site is available for binding [125; 226]. These ligands do not bind to the pre-translocation conformation as the 3' primer terminus occludes the n-site in this conformation. The pyrophosphate analogue foscarnet, or phosphonoformic acid (PFA) was shown to selectively bind to the pre-translocation conformation [104].

The translocational equilibrium of RT is studied due to its importance in the mechanisms of action for the mentioned inhibitors, as well as roles in drug resistance mechanisms [104; 126; 227]. Resistance to NRTIs can occur through the discrimination of NRTIs in favor of the natural substrate or through the increased excision of incorporated NRTIs [101; 176]. The excision reaction can only occur when the complex is found in the pre-translocation conformation with the incorporated NRTI at the 3' primer terminus located in the N-site [123; 179]. Mutations that confer resistance to PFA have been shown to decrease susceptibility to the NRTI AZT through decreased excision [200; 218; 219]. The mutation E89K confers resistance to PFA by decreasing access to the pre-translocation conformation, which would negatively affect both the activity of PFA and the excision reaction [104].

The translocational equilibrium is determined by several factors including the temperature, chemical nature of the 3' primer terminus, mutational context of the enzyme, and the sequence of the nucleic acid substrate used [104; 125; 126; 188; 252]. The determinants of the translocational equilibrium most likely exist at the interface between the enzyme and its nucleic acid substrate [115]; however, conformational

changes upon nucleotide binding may also affect the translocational equilibrium of polymerases [107; 188; 254]. We have recently described a possible relationship between the closure of the fingers subdomain and the pre-translocation conformation [188]. We observed the loss of stacking interactions between the fingers subdomain and the template overhang in the context of the F61A mutation selectively diminished the stability of the pre-translocation conformation. This was also associated with decreased polymerase activity and strong resistance to PFA. The closure of the fingers following nucleotide binding allows for the proper positioning of the nucleotide for bond formation [107]. Immediately following bond formation the newly formed 3' primer terminus is located in the N-site, defining the pre-translocation conformation. PPi release may occur either prior to or concomitant with the opening of the fingers, with the fingers domain possibly existing in an equilibrium between open and closed conformations among pre-translocation complexes [188]. Crystallographic studies have described binary pre-translocation conformations with the fingers subdomain in both open and closed conformations [123; 141; 250]. Establishment of the translocational equilibrium occurs through the rapid shuttling between pre- and post-translocation conformations only with the fingers in the open conformation [252].

In the present study we investigated the relative distribution of the translocational equilibrium in different nucleic acid sequence contexts and determined the effect of bias towards both pre- and post-translocation conformations on nucleotide incorporation and excision. We employed site-specific footprinting using consecutive primers on a variety of templates and pre-steady state kinetics at

defined positions to address these questions. We determined the translocational equilibrium of RT to be strongly biased toward the post-translocation conformation in the majority of sequence contexts tested. A nucleic acid consensus sequence capable of predicting the translocational equilibrium remains elusive, however, the presence of a thymidine at the 3' primer terminus is seen to be required for a strong pre-translocation bias. Strong pre-translocation bias is seen to be associated with decreased efficiency of incorporation at defined positions, for the incorporation of each of the four natural substrates. Decreased incorporation in this context is mediated primarily through decreased catalytic rate with decreased binding also observed for all substrates except dCTP. The efficiency of the excision reaction is affected by translocation bias in complementary fashion to the incorporation reaction with higher efficiency of excision observed in the context of pre-translocation bias.

3.4 Materials and Methods

Enzymes and nucleic acids

Heterodimeric reverse transcriptase p66/p51 was expressed and purified as previously described [248]. Oligodeoxynucleotides used in this study were chemically synthesized and purchased from Invitrogen Life Technologies (Carlsblad, CA).

The following templates and primers were used for initial screening of consecutive primers in site-specific footprinting assays:

PPT57

5’

CGTTGGGAGTGAATTAGCCCTTCCAGTCCCCCCTTTTCTTTTAAAAAGTGG

CTAAGA

Primers designed for screening were 20 nt in length beginning with the complementary region such that the 5’ end of the primer is opposite the 3’ end of the template (PPTxx01 TCTTAGCCACTTTTTAAAAG) with each subsequent primer shifted one nucleotide along the template. Primers used in this study for screening with the PPT57 template were as follows:

PPTxx06 GCCACTTTTTAAAAGAAAAG

PPTxx07 CCACTTTTTAAAAGAAAAGG

PPTxx08 CACTTTTTAAAAGAAAAGGG

PPTxx09 ACTTTTTAAAAGAAAAGGGG

PPTxx10 CTTTTTAAAAGAAAAGGGGG

PPTxx11 TTTTTAAAAGAAAAGGGGGG

PPTxx12 TTTTAAAAGAAAAGGGGGGA

PPTxx13 TTTAAAAGAAAAGGGGGGAC

PPTxx14 TTAAAAGAAAAGGGGGGACT

PPTxx15 TAAAAGAAAAGGGGGGACTG

PPTxx16 AAAAGAAAAGGGGGGACTGG

PPTxx17 AAAGAAAAGGGGGGACTGGA

PPTxx18 AAGAAAAGGGGGGACTGGAA

PPTxx19 AGAAAAGGGGGGACTGGAAG

PPTxx20 GAAAAGGGGGGACTGGAAGG

PPTxx21 AAAAGGGGGGACTGGAAGGG

PPTxx22 AAAGGGGGGACTGGAAGGGC

PPTxx23 AAGGGGGGACTGGAAGGGCT

PPTxx24 AGGGGGGACTGGAAGGGCTA

PPTxx25 GGGGGGACTGGAAGGGCTAA

PPTxx26 GGGGGACTGGAAGGGCTAAT

PPTxx27 GGGGACTGGAAGGGCTAATT

PPTxx28 GGGACTGGAAGGGCTAATTC

PPTxx29 GGACTGGAAGGGCTAATTCA

A similar system was designed for screening of template PBS50 (5' AAATCTCTAGCAGTGGCGCCCGAACAGGGACCTGAAAGCGAAAGGGAAA C) with the following primers:

PBSxx1 GTTTCCCTTTCGCTTTCAGG

PBSxx2 TTTCCCTTTCGCTTTCAGGT

PBSxx3 TTCCCTTTCGCTTTCAGGTC

PBSxx4 TCCCTTTCGCTTTCAGGTCC

PBSxx5 CCCTTTCGCTTTCAGGTCCC

PBSxx6 CCTTTCGCTTTCAGGTCCCT

PBSxx7 CTTTCGCTTTCAGGTCCCTG

PBSxx8 TTTCGCTTTCAGGTCCCTGT

PBSxx9 TTCGCTTTCAGGTCCCTGTT

PBSxx10 TCGCTTTCAGGTCCCTGTTC

PBSxx11 CGCTTTCAGGTCCCTGTTCG

PBSxx12 GCTTTCAGGTCCCTGTTCGG

PBSxx13 CTTTCAGGTCCCTGTTCGGG

PBSxx14 TTTCAGGTCCCTGTTCGGGC

PBSxx15 TTCAGGTCCCTGTTCGGGCG

PBSxx16 TCAGGTCCCTGTTCGGGCGC

PBSxx17 CAGGTCCCTGTTCGGGCGCC

PBSxx18 AGGTCCCTGTTCGGGCGCCA

PBSxx19 GGTCCCTGTTCGGGCGCCAC

PBSxx20 GTCCCTGTTCGGGCGCCACT

PBSxx21 TCCCTGTTCGGGCGCCACTG

PBSxx22 CCCTGTTCGGGCGCCACTGC

PBSxx23 CCTGTTCGGGCGCCACTGCT

PBSxx24 CTGTTCGGGCGCCACTGCTA

PBSxx25 TGTTCGGGCGCCACTGCTAG

PBSxx26 GTTCGGGCGCCACTGCTAGA

PBSxx27 TTCGGGCGCCACTGCTAGAG

PBSxx28 TCGGGCGCCACTGCTAGAGA

PBSxx29 CGGGCGCCACTGCTAGAGAT

PBSxx30 GGGCGCCACTGCTAGAGATT

Finally, two overlapping templates were designed (42A 5' TTAGTAGGTACATAACTATCTATTGATACAGACCTAAAACAA and 42B 5' TCTAGGATGTATGTTTAGTAGGTACATAACTATCTATTGATA) for screening with the following primers:

ScPr2xx01 TTGTTTTAGGTCTGTATCAA

ScPr2xx02 TGTTTTAGGTCTGTATCAAT

ScPr2xx03 GTTTTAGGTCTGTATCAATA

ScPr2xx04 TTTTAGGTCTGTATCAATAG

ScPr2xx05 TTTAGGTCTGTATCAATAGA

ScPr2xx06 TTAGGTCTGTATCAATAGAT

ScPr2xx07 TAGGTCTGTATCAATAGATA

ScPr2xx08 AGGTCTGTATCAATAGATAG

ScPr2xx09 GGTCTGTATCAATAGATAGT

ScPr2xx10 GTCTGTATCAATAGATAGTT

ScPr2xx11 TCTGTATCAATAGATAGTTA

ScPr2xx12 CTGTATCAATAGATAGTTAT

ScPr2xx13 TGTATCAATAGATAGTTATG

ScPr2xx14 GTATCAATAGATAGTTATGT

ScPr2xx15 TATCAATAGATAGTTATGTA

ScPr2xx16 ATCAATAGATAGTTATGTAC

ScPr2xx17 TCAATAGATAGTTATGTACC

ScPr2xx18 CAATAGATAGTTATGTACCT

ScPr2xx19 AATAGATAGTTATGTACCTA

ScPr2xx20 ATAGATAGTTATGTACCTAC

ScPr2xx21 TAGATAGTTATGTACCTACT

ScPr2xx22 AGATAGTTATGTACCTACTA

ScPr2xx23 GATAGTTATGTACCTACTAA

ScPr2xx24 ATAGTTATGTACCTACTAAA

ScPr2xx25 TAGTTATGTACCTACTAAAC

ScPr2xx26 AGTTATGTACCTACTAAACA

ScPr2xx27 GTTATGTACCTACTAAACAT

ScPr2xx28 TTATGTACCTACTAAACATA

ScPr2xx29 TATGTACCTACTAAACATAC

ScPr2xx30 ATGTACCTACTAAACATACA

ScPr2xx31 TGTACCTACTAAACATACAT

ScPr2xx32 GTACCTACTAAACATACATC

ScPr2xx33 TACCTACTAAACATACATCC

ScPr2xx34 ACCTACTAAACATACATCCT

ScPr2xx35 CCTACTAAACATACATCCTA

ScPr2xx36 CTACTAAACATACATCCTAG

All concentrations reported for assay conditions are final concentration after mixing unless otherwise stated.

Site-specific footprinting

Performed as previously described [125], briefly: KOONO was prepared by stirring 10 ml of 1.2 M KNO_2 with 1.4 ml of 30% H_2O_2 on ice. 10 ml of 1.4 M HCl was added to the stirring solution and immediately quenched with 10 ml of 2 M KOH. Aliquots were stored at -80°C. In preparation of the footprinting reaction, the 5' P^{32} labelled templates were heat annealed with corresponding primers, with individual hybrids prepared for each consecutive primer on each template. The DNA/DNA hybrid (125 nM) was incubated with 750 nM RT in a buffer containing sodium cacodylate pH 7 (120 mM), NaCl (20 mM), DTT (0.5 mM) and $MgCl_2$ (6 mM) in a final volume of 20 µl. Reactions were incubated at 37°C for 10 minutes followed by the addition of 1.5 µl of KOONO (100 mM). Reactions were precipitated with a 5-fold excess of isopropanol containing 0.3 M NH4Ac and 0.1 µg *E.Coli* tRNA at 4°C for 30 min then washed with 80% ethanol at 4°C for 10 min prior to resuspension in 10 µl of formamide buffer containing trace amounts of xylene cynol and bromophenol blue. Samples were resolved on 12% denaturing polyacrilamide gels and visualized by phosphorimaging.

Validation of potential consensus sequence for pre-translocation bias

A java script was written that allowed for the sampling and alignment of random sequences from within the sequence contexts examined in this study. This was performed in order to validate a potential consensus sequence observed in the context of pre-translocation bias during site-specific footprinting of consecutive primers. Random sets of five sequences were assessed for 80% or greater consensus for presence of pyrimidine or purine at each position. Alignment of 1000 sets of sequences determined that consensus at 7 or more positions, as observed for pre-translocation bias, would occur with random sequences over 50% of the time. This script is available online at http://cglmedia.com/Consensus%20Sequence/index.html?rowcount=5&run_iterations=1000.

Single turn-over pre-steady state kinetics

Performed as previously described [112]. 100 nM of 5' labelled primer was heat annealed with 200 nM of corresponding template, as indicated. The DNA/DNA hybrid was incubated with 500 nM HIV-1 RT in a buffer containing 50 mM Tris-HCl pH 7.8, 50 mM NaCl, and 6 mM $MgCl_2$. Substrate was prepared in the same buffer as the RT-P/T and the reaction was started and stopped by computer control using a Kintek RFQ-3 Quench Flow (Austin, TX). Equal volumes of RT-P/T and substrate were mixed in this manner for times ranging from 0.025 s to 2.0 s and stopped by the addition of excess 0.5 M EDTA. Substrate concentrations ranged from 780 nM to 200 μM for each of dATP, dTTP, dCTP and dGTP. Samples were diluted in formamide buffer containing trace amounts of bromophenol blue and xylene cynol and heat

denatured at 95°C for 5 minutes. Samples were resolved and visualized as above. Incorporation was quantified using ImageQuant (GE Healthcare) as (product/total)*100 nM and results were plotted in Prism 4.0 using the non-linear regression for one-phase exponential association to the equation [product]=A*(1-exp(-k_{obs}*t)) where t is time, A is amplitude of product formed and k_{obs} is the observed rate at a given concentration of substrate. Rates obtained from each concentration of substrate were replotted against the concentration of substrate using the non-linear regression for Michealis Menten with the equation $k_{obs}=k_{pol}$ *[substrate]/(K_d+[substrate]) which allows for the determination of the kinetic constants k_{pol} and K_d for the chemical reaction of nucleotide incorporation.

PPi mediated excision of chain-terminated primers

Indicated primers were chain terminated with ddTTP or ddATP and gel purified as previously described [181]. These chain-terminated primers were then heat annealed to 2-fold excess of corresponding templates and 50 nM of the resulting hybrid was incubated with 250 nM RT in buffer containing 50 mM Tris-HCl pH 7.8, 50 mM NaCl, and 0.2 mM EDTA. Depending on the sequence context different nucleotides were included in rescue mixes as follows: For primer/templates PPTxx26^{ddTTP}/PPT57 and PPTxx27^{ddTTP}/PPT57 a mix was used containing 1 μM of dTTP, 1 μM dCTP, and 10 μM ddATP. For reactions with primer/template PPTxx18^{ddATP}/PPT57 a mix containing 1 μM dATP, 1 μM dGTP and 10 μM ddCTP was used. For reactions with primer/template PPTxx27^{ddATP}/PPT57(27T) a mix containg 1 μM dATP, 1 μM dCTP and 10 μM ddTTP was used. For all sequence contexts the rescue mix also included

3.9 – 500 μM inorganic PPi. Reactions were initiated with the addition of 6 mM $MgCl_2$ with samples taken from 30 s to 20 min and resolved and visualized as above. 100% extension of unchain-terminated primers was observed for all sequence contexts under these reaction conditions, thus eliminating differences in incorporation. Correction for minimal (<10%) extension of chain-terminated primers in the absence of PPi indicated that any extension products under experimental conditions represented products of the excision reaction. Results were analyzed as above. A range of [PPi]s were assessed, allowing for determination of k_{pyro} and $K_{d\text{-}PPi}$ using the equation $k_{obs}=K_{pyro}*[PPi]/(K_{d\text{-}PPi}+X)$ as used for the forward reaction.

3.5 Results

Site-specific footprinting of consecutive primers

We have previously shown that treatment of RT:DNA/DNA complexes results in site specific cleavage of the template at the -7 and -8 positions [125]. These cleavage products represent RT:DNA/DNA complexes in the post- and pre-translocation conformation respectively. The ratio of pre- and post-translocation complexes captured by this technique represents the translocational equilibrium of the enzyme. The nucleic acid sequence context used is one factor that can significantly affect this equilibrium [125; 188]. Four templates were designed with corresponding primers of 20 nucleotides in length at each consecutive position for an unbiased assessment of the translocational equilibrium in a large number of sequence contexts. The templates chosen were derived from the polypurine tract (PPT57), primer binding site (PBS50) and a portion of the RT coding region of the pol gene (42A and 42B) from the HIV-1 genome. As each primer is a single position closer to the labeled 5' end of the template, the relative size of -7 and -8 cleavage products decrease by one nucleotide for each subsequent primer (Figure 3.1). For example, when both pre- and post-translocation cuts are present the -8 (pre-translocation) cut of a given primer will be the same size as the -7 (post-translocation) cut of the primer preceeding it (ending one nucleotide closer to the 3' end of the template). If all of the primers tested were perfectly balanced between pre- and post-translocation there would be two cuts present in each lane, staggered relative to the lane preceding and following.

Both pre- and post-translocation cuts were observed with the PPT derived template PPT57 for three of the primers tested (Figure 3.1, lanes marked +). A single cut is observed for the majority of sequences tested, which corresponds to the post-translocation conformation (-7 relative to the primer terminus). A single cut corresponding to the pre-translocation conformation (-8 relative to the primer terminus) was observed for two of the primers tested with this template (Figure 3.1, lanes marked *). Similar results were obtained with the PBS derived template (Figure 3.2) and both other templates used (not shown), with the majority of sequences tested displaying a single cut corresponding to the post-translocation conformation. In addition to the expected cleavage products corresponding to the pre- and post-translocation conformations, cleavage products beyond this typical register were observed in some cases. In particular, strong cleavage products were observed with the PPT57 template with primers PPTxx09 and PPTxx10 corresponding to conformations such that position n+2 and n+1, respectively, of the template overhang reside in the N-site of RT (Figure 3.1, lanes marked with overhead line).

Additionally, the use of partially overlapping templates 42A and 42B resulted in the observation of a "template-end effect", where primers near the 5' end of template 42A display increased pre-translocation cleavage or a complete loss of post-translocation cleavage products, as observed with primers ScPrxx23 and ScPrxx24 respectively (Figure 3.3, first panel). When the same primers were tested in the presence of a template overhang, by use of template 42B, these same primers both primarily display the post-translocation cleavage product typical of all sequences tested (Figure 3.3, second panel).

Effect of the translocational equilibrium on the incorporation of nucleotides

As the post-translocation conformation is required for nucleotide binding and incorporation [107], we sought to determine the impact of translocation bias on the incorporation of nucleotides. Sequences were selected from the PPT derived template, PPT57, such that the incorporation of each of the four natural nucleotides could be monitored in the context of both pre- and post-translocation bias. The heavily biased pre-translocation primers from the PPT57 template, PPTxx14 and PPTxx27, were used for the incorporation of dGTP and dCTP, respectively. Modified templates were designed with changes to the n+1 position such that the PPTxx14 primer could be used for the incorporation of dATP and dTTP. These modified templates resulted in no change to the translocational equilibrium as confirmed by site-specific footprinting (not shown). Primers PPTxx21, PPTxx20, and PPTxx11 were used to study the incorporation of dCTP, dGTP and dATP in the context of a post-translocation bias, respectively. A modified template with changes to the n+1 position relative to PPTxx11 was designed to study the incorporation of dTTP, again this change to the template at the n+1 position did not effect the translocational equilibrium as confirmed by site-specific footprinting.

Single-turnover pre-steady state kinetic analysis of these sequences was performed to determine the rate of incorporation, k_{pol}, and binding constant, K_d, for each position (Table 3.1). As expected, for all sequences tested, the efficiency of incorporation (k_{pol}/K_d) was greater in the context of a post-translocation bias than in the context of a pre-translocation bias. The change in efficiency varied from 14-143

fold depending on the nucleotide, with dCTP and dTTP displaying the smallest and greatest difference between pre- and post-translocation, respectively. Although the efficiencies varied within the pre- and post-translocation groups, depending on the nucleotide, the lowest efficiency of incorporation observed in the context of a post-translocation bias (dCTP at 1.4 $\mu M^{-1}s^{-1}$), was still 3-fold higher than the most efficient incorporation observed in the context of a pre-translocation bias (dATP at 0.48 $\mu M^{-1}s^{-1}$). Unexpectedly, the lower efficiency in the context of a pre-translocation bias was mediated primarily through reduced rates of incorporation while reduced binding was observed to a lesser extent for each substrate except dCTP (Table 3.1).

Impact of the 3' primer terminus on the translocational equilibrium

Of all sequences tested, the heavily biased pre-translocation and mixed-translocation sequences were observed primarily at primers ending in thymidine. Of the eighty-nine distinct primers that were monitored five were determined to exist heavily biased toward pre-translocation, defined as greater than 70% pre-translocation (5.6%). Each of these five primers contained a thymidine at the 3' terminus, representing 20% of the primers used containing thymine at that position. Sequences that exist as a mixture of pre- and post-translocation were more equally represented with respect to the nature of the 3' primer terminus. Of the seven such positions observed, adenosine, guanidine or cytidine are represented each twice with the remaining primer containing thymine at the 3' primer terminus.

Manual alignment of the five heavily biased pre-translocation sequences revealed common sequence elements that may represent a consensus sequence for the

strong pre-translocation bias (Figure 3.4). A java script was written that allowed random sampling of all sequence contexts tested to assess the significance of the observed consensus. Sampling of 1000 sets revealed that a consensus sequence of similar complexity (seven common elements with 80% or higher consensus) would be found in a sample of five sequences over 50% of the time, indicating that the putative consensus sequence determined from this study could be attributable to random chance (see materials and methods). In the absence of a more robust consensus sequence we focused on the presence of thymidine at the 3' primer terminus as a possible requirement for a strong pre-translocation bias.

Heavily biased pre-translocation sequences and their corresponding templates were modified such that the thymidine at the 3'primer terminus was replaced with adenosine (Figure 3.5). For the sequences tested the presence of thymidine was seen to be required for a strong pre-translocation bias. The replacement of thymidine with adenosine resulted in either a complete loss of the pre-translocation cut or a change from heavily biased to mixed pre-/post-translocation with primers PPTxx14 and PPTxx27 respectively (Figure 3.5, second and fourth panels). A mixed pre-/post-translocation position containing cytidine at the 3' primer terminus was similarly modified with no change to the translocational equilibrium observed when adenosine was present (not shown).

Effect of the translocational equilibrium on the rescue of chain terminated primers

To study the effect of access to the pre-translocation conformation on the excision of chain terminated primers, sequences were selected such that the excision

of the same nucleotide could be compared in the context of either a pre- or post-translocation bias. Primers PPTxx27 and PPTx26 were selected for the excision of ddTTP for pre- and post-translocation, respectively. Purified chain-terminated primers were generated for each position. There was no change observed in the translocational equilibrium for chain-terminated primers relative to the natural nucleotide, as confirmed by site-specific footprinting (not shown). These purified chain-terminated primers were used in single-turn over rescue assays with varying concentrations of PPi to determine both the rate of pyrophosphorolysis (k_{pyro}) and the K_d of PPi (Table 3.2). The efficiency of the excision reaction (k_{pyro}/K_d) was 8-fold greater in the context of a pre-translocation bias ($PPTxx27^{ddTTP}$) as compared to the post-translocation sequence ($PPTxx26^{ddTTP}$).

Similar experiments with ddATP were performed with $PPTxx18^{ddATP}$ serving as the post-translocation substrate. As no heavily biased sequence was available with a 3' primer terminus adenosine, the modified $PPTxx27^{ddATP}$, which displays a mixed pre-/post-translocational equilibrium, was used. Again, no change in the translocational equilibrium was observed in the presence of chain-terminated primers relative to natural nucleotide. For excision of ddATP the difference in efficiency of the excision reaction between the post-translocation sequence ($PPTxx18^{ddATP}$) and the mixed-translocation sequence ($PPTxx27^{ddATP}$) was 10-fold (Table 3.2).

3.6 Discussion

The aim of this study was to determine the effect of the sequence context on the translocational equilibrium of HIV-1 RT and to translate the effects of either pre- or post-translocation bias on the incorporation and excision of nucleotides. The sequence context has previously been shown to affect the translocational equilibrium, with access to the pre-translocation conformation shown to effect the excision of NRTIs including AZT and tenofovir [125; 126]. The relative distribution of the translocational equilibrium over a large number of sequences, and, the effects of translocation bias on individual kinetic parameters of nucleotide incorporation and excision, however, have not previously been studied. We utilized site-specific footprinting and pre-stready state single-turnover kinetic tools to explore these effects.

Nature of the Translocational Equilibrium in Different Nucleic Acid Sequence Contexts

Previous studies demonstrate that RT:DNA/DNA complexes can exist either heavily biased to pre-translocation, post-translocation or as a mixture of the two [125; 188]. The small number of sequences characterized, however, could not address the question of which of these conditions, if any, was common and which was rare. The pyrophosphate analogue PFA, which was shown to selectively bind the pre-translocation conformation, was used to identify 'hot spots' of inhibition at sites with a pre-translocation bias [104]. The relatively small number of sites detected in these assays suggested that the pre-translocation bias was rare. Similar experiments with

the post-translocation specific, nucleotide competing RT inhibitor (NcRTI) Indopy-1, also reveal a small number of sites of inhibition [226; 227]. These results cannot fully represent the distribution of pre- and post-translocation bias across different nucleic acid sequence contexts, however, as other factors affect the activity of the inhibitors used. For example, Indopy-1 preferentially binds to sites containing thymidine at the 3' primer terminus, in addition to requiring access to the post-translocation conformation [226]. Monitoring the translocational equilibrium of a large number of consecutive sequences allowed us to address the question without introducing any bias related to the activity of PFA or Indopy-1. We have determined by site-specific footprinting that for WT RT the translocational equilibrium is biased to post-translocation over the majority of sequences for all templates tested.

In the Brownian ratchet mechanism of translocation proposed for RT an equilibrium is reached between pre- and post-translocation conformations following each round of nucleotide incorporation [240]. In the context of our results, a post-translocation bias can be considered the standard condition with some sequences perturbed from this state due to interactions between the enzyme and its nucleic acid substrate. A post-translocation bias is favorable for the incorporation of nucleotides and serves the function of RT as a DNA polymerase. Which interactions are responsible for disturbing the post-translocation bias? Changes to any interaction between RT and its nucleic acid substrate could theoretically affect the translocational equilibrium, however, in the absence of a significant consensus sequence we are limited in our ability to specify which interactions may be more important than others. We have previously shown through site directed mutagenesis

that the loss of a stacking interaction between nucleotides of the template overhang and F61 of the fingers subdomain results in a strong bias towards post-translocation, regardless of the sequence context [188]. In the present study, a 'template end' effect was seen in which the absence of the template overhang resulted in the enzyme adopting conformations allowing contact between the enzyme and the template overhang to be maintained. In addition to F61, W24 can also be seen in crystal structures to stack with nucleotides of the template overhang [107]. These stacking interactions are observed for F61 only when the fingers subdomain is in the closed conformation as seen in ternary complexes [107] and a recently published pre-translocation binary complex [141]. Unfortunately, analysis of the sequences identified in the present study do not explain which nucleotide or combination of nucleotides, with respect to the nature of the nucleobase, are necessary in the template in order to achieve these favorable, sequence dependent interactions with the template overhang.

Impact of Translocation Bias on the Incorporation of Nucleotides

Nucleotide incorporation by RT requires access to the n-site for binding of the templated nucleotide followed by a conformational change resulting in bond formation [107; 112]. We have employed single-turnover pre-steady state kinetics to monitor the effect of pre- and post-translocation biases of the translocational equilibrium on kinetic parameters of incorporation. Diminished binding to the n-site is manifested in increased K_d values, as observed in the context of a pre-translocation bias for each nucleotide studied except dCTP. Reduced binding can be readily explained by decreased access to the n-site as these RT:DNA/DNA complexes exist primarily with the 3' primer terminus occupying this position. Access to the n-site

under these conditions is not completely blocked however, as individual complexes freely oscillate between the two conformations.

Once a nucleotide is bound, the ability to undergo productive conformational change and bond formation is manifested in the catalytic rate k_{pol}. Unexpectedly, the majority of the difference in catalytic efficiency (k_{pol}/K_d) observed between complexes with either pre- or post-translocation biases was the result of decreased rates of incorporation rather than diminished binding. Published rates of nucleotide incorporation by RT vary widely, depending on the sequence used, ranging from 0.0088-0.96 s^{-1} [100; 255; 256] to 83-183 s^{-1} [257; 258; 259]. In the present study we report differences of ~10-20 fold in k_{pol} values between pre- and post-translocation sequences, with faster rates observed in the context of post-translocation bias. Ignatov *et al* have observed differential dissociation kinetics between random sequences and defined positions near the central termination sequence, which they attribute to differential partitioning between pre- and post-translocation complexes [114]. Mathematical modeling was used to assign 2-3 fold higher rates of dissociation to post-translocation complexes. Our experiments, however, were carried out under single-turn over conditions with excess enzyme and differences in dissociation between pre- and post-translocation complexes should not influence our results. As the most obvious difference between two systems with either a pre- or post-translocation bias is access to the n-site, these differences in the rate were not immediately explained. Crystal structures are available for both pre- and post-translocation conformations [123; 141; 250] however, these are not the complexes to be compared in this instance. Incorporation only occurs in the post-translocation

conformation, and differences observed are likely due to differences between two distinct post-translocation conformations. Further, these crystal structures are generated by cross-linking of the enzyme to the primer/template, and therefore, they do not represent differences in translocation bias attributable to the sequence.

Two models can be invoked to explain the differences observed between pre- and post-translocation bias (Figure 3.6). In the first model, sequences biased to either pre- or post-translocation differ in the orientation of the primer terminus in the different post-translocation conformations for each sequence (Figure 3.6 a). The effects of these differences would manifest in changes in the catalytic rate of incorporation. In the second model, sequences biased to either pre- or post-translocation differ only in their residency time at either pre- or post-translocation conformation. In this model rates of incorporation are influenced by the rate of conversion from pre- to post-translocation, which would occur before binding and incorporation (Figure 3.6 b).

Support of the first model can be found in the observation that thymidine at the 3' primer terminus is necessary for a strong pre-translocation bias in some sequence contexts. This indicates that changes within the active site directly influence this equilibrium, and may therefore affect the chemistry at the active site. Unlike differences in the catalytic rate caused by drug resistance conferring mutations, such as Q151M or K65R, that can be traced to single amino acids within the active site [156; 260], the translocational equilibrium may be affected by contacts both within or distant from the active site [125; 188]. Further, contacts between F61 of the fingers subdomain and the template overhang have been shown to both strongly affect the translocational

equilibrium and serve as important anchor required for stable closed complex formation [188]. A closed pre-translocation binary complex has recently been solved [141]. The partitioning of pre-translocation binary complexes between open and closed conformation would support the second model proposed here for differences in rates of nucleotide incorporation. The contribution of a more stable, closed pre-translocation binary complex would be supported by the lower dissociation rates of pre-translocation complexes determined by Ignatov *et al* [114]. Conversion from the closed to open form would be necessary before translocation could occur, effectively limiting the number of complexes available for incorporation. The eventual conversion from closed to open pre-translocation complexes followed by the kinetically invisible translocation to the post-translocation conformation would be manifest as slower rates of incorporation. The two models proposed here are not mutually exclusive and contributions from both models may be responsible for the observations reported here. Further studies of the differential stability of sequences biased to pre- and post-translocation conformations are required to validate the second model. Crystallographic studies using defined sequences, without cross-linking, may reveal the differences at the active site predicted by the first model.

Impact of translocation bias on excision of nucleotides

The excision reaction can only occur in the pre-translocation conformation such that the scissile bond between the 3' primer terminus and the penultimate nucleotide is properly positioned in the active site for transfer of the 3' nucleotide to an acceptor substrate such as ATP or PPi [187]. We employed single-turnover pre-steady state

kinetics to determine kinetic parameters of the excision reaction and found, as expected, that increased access to the pre-translocation conformation was correlated with increased efficiency of PPi-mediated excision. Although ATP is most likely the biologically relevant acceptor substrate in the context of TAMs and other mutations that increase excision [187], we employed PPi in our study for practical purposes. First, as the present study only concerns the role of the translocational equilibrium in the context of WT RT, the use of the more efficient substrate PPi was favorable, as excision activity with ATP is low for WT RT [178]. Secondly, as our study included the excision of ddATP, ATP may have interfered with our results as the high concentrations required for excision have been seen to lead to incorporation of ATP [126].

The present results are in agreement with previous studies in which improved access to the pre-translocation conformation was associated with increased excision activity [125; 126]. In a recent report V75I, a drug resistance conferring mutation associated with d4T, slightly increased the proportion of pre-translocation complexes while decreasing the rate of excision [150]. The effect on translocation was small, however, and V75I is thought to interfere with the binding of PPi, overriding any translocation-dependent benefits to excision. These studies each examined excision at a single concentration of ATP or PPi and therefore do not address changes in binding of the acceptor substrate related to translocation. Here we have determined the impact translocation bias on kinetic parameters including the rate of pyrophosphorolysis (k_{pyro}) and the binding affinity for PPi (K_d^{PPi}). Results with sequences biased toward post-translocation are similar to those observed by Ray *et al* [178]. Excision efficiency is

increased for removal of both ddTTP and ddATP in the presence of pre-translocation or mixed translocation bias, respectively. These differences are manifested in both 4-6 fold increases in rate and ~2-fold increases in binding affinity. Interestingly, although the mixed translocation sequence used for ddATP was not as strongly biased to pre-translocation as that used for ddTTP, we observed near identical kinetics. This suggests that there is a threshold of sufficient access to the pre-translocation conformation after which additional access does not improve efficiency.

Though the changes observed are relatively small compared to the up to 360-fold changes in overall efficiency reported for sequence dependent differences in excision by Meyer *et al* [189], they are consistent with changes in activity previously reported related to the translocational equilibrium [125]. The large sequence dependent effect observed by Meyer *et al* may be related to the use of highly excision competent resistant forms of RT enhancing small differences observed here with WT. Our present results are somewhat inconsistent with their finding that thymidine analogues are less sensitive to changes in the sequence context than other nucleotides. We see near equal differences in excision efficiency related to differences in translocational equilibrium regardless of the substrate used (ddTTP vs ddATP). This suggests that the differences observed by Meyer *et al* may not have been limited to differences in the translocational equilibrium.

Consistent with Meyer *et al*, we have shown previously, however, that AZT is particularly insensitive to sequence dependent changes in dead-end complex formation; the binding of the next nucleotide to a chain-terminated RT:DNA/DNA complex [190]. This effect of AZT could be attributed to steric conflict with the 3' azido

group and incoming dNTPs [181]. Observations that the nature of the nucleobase and not the 3'azido group of AZT is responsible for conferring resistance by TAMs, however, stress the importance of the base in addition to modification of the sugar [181]. The present finding that thymidine is more likely to be found at the 3' primer terminus in the context of an excision competent mixed or pre-translocation bias adds further evidence that thymidine and thymidine analogues are more often efficient substrates for the excision reaction *in vivo*. Further study of thymidine analogues with modifications to the base are required to address the specific contribution of the structure and functional groups of this substrate to both the translocational equilibrium and the excision reaction.

3.7 Figures and Tables

Figure 3.2 **KOONO experiments at consecutive primer-template positions using a PPT derived template.** WT RT was incubated with double stranded DNA substrates with consecutive primer terminus positions. These binary complexes were treated with KOONO, producing cleavage fragments at positions -8 or -7 on the template strand corresponding to a pre- or post-translocation conformation, respectively. Due to the relative positioning of the 3' end of the primer, -8/-7 cuts are shifted on the template for each primer. (a) A schematic indicates the distance from the nucleotide-binding site of RT to the position of KOONO cleavage on the template for pre- and post-translocated complexes for representative primers PPTxx06 and PPTxx07 and the relative positions of the primers used. (b) 5'-^{32}P labelled template cleavage fragments are resolved on a 12% polyacrilamide gel at single nucleotide resolution, -8 or -7 fragments are labelled for the outermost lanes. Lanes are labelled with the abbreviated numerical suffix for the primer used (eg. PPTxx06 is 06). Sequences that exist heavily biased to pre-translocation or as mixtures of pre- and post-translocation are annotated (*) and (+) respectively above the primer label on the gel. Sequences where a significant proportion of cleavage fragments are seen outside of the expected -7 or -8 positions are annotated with an overhead line above the primer label on the gel.

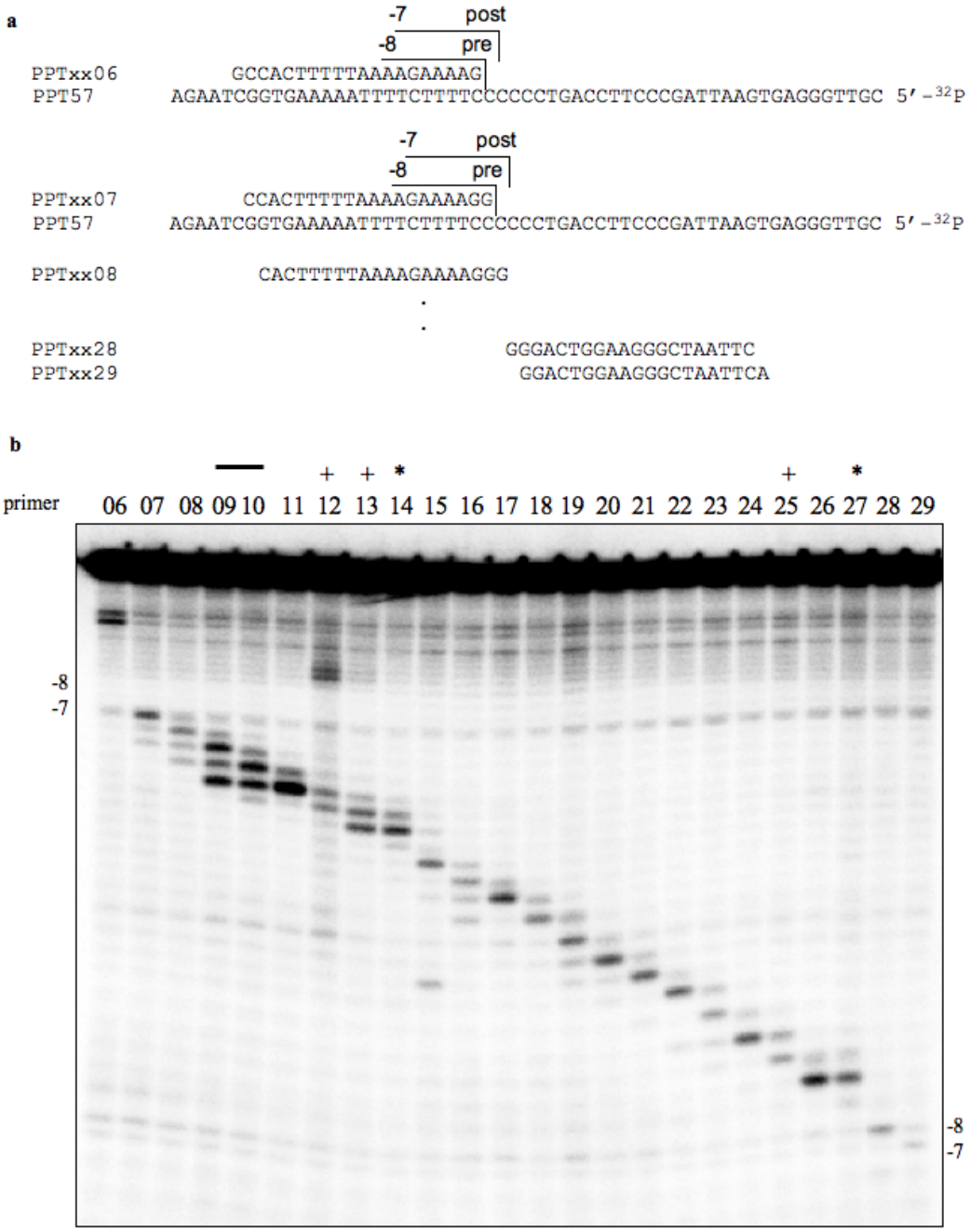
a
-7
post
-8
pre
PPTxx06 GCCACTTTTTAAAAGAAAAG
PPT57 AGAATCGGTGAAAAATTTTCTTTTCCCCCCTGACCTTCCCGATTAAGTGAGGGTTGC 5′-32P
-7
post
-8
pre
PPTxx07 CCACTTTTTAAAAGAAAAGG
PPT57 AGAATCGGTGAAAAATTTTCTTTTCCCCCCTGACCTTCCCGATTAAGTGAGGGTTGC 5′-32P
PPTxx08 CACTTTTTAAAAGAAAAGGG
PPTxx28 GGGACTGGAAGGGCTAATTC
PPTxx29 GGACTGGAAGGGCTAATTCA
b
primer
06 07 08 09 10 11 12 13 14 15 16 17 18 19 20 21 22 23 24 25 26 27 28 29
-8
-7
-8
-7

Figure 3. 1

Figure 3.2 **KOONO experiments at consecutive primer-template positions using a PBS derived template.** WT RT was incubated with double stranded DNA substrates with consecutive primer terminus positions. These binary complexes were treated with KOONO, producing cleavage fragments at positions -8 or -7 on the template strand corresponding to a pre- or post-translocation conformation respectively. Due to the relative positioning of the 3' end of the primer, -8/-7 cuts shift on the template for each primer. (a) A schematic indicates the distance from the nucleotide-binding site of RT to the position of KOONO cleavage on the template for pre- and post-translocated complexes for representative primers PBSxx01 and PBSxx02 and the relative positions of the primers used. (b) 5'-^{32}P labelled template cleavage fragments are resolved on a 12% polyacrylamide gel at single nucleotide resolution, -8 and -7 fragments are labelled for the outermost lanes. Lanes are labelled with the abbreviated numerical suffix for the primer used (eg. PBSxx01 is 01). Sequences that exist heavily biased to pre-translocation or as mixtures of pre- and post-translocation are annotated (*) and (+) respectively above the primer label on the gel. Sequences where a significant proportion of cleavage fragments are seen outside of the expected -7 or -8 positions are annotated with an overhead line above the primer label on the gel.

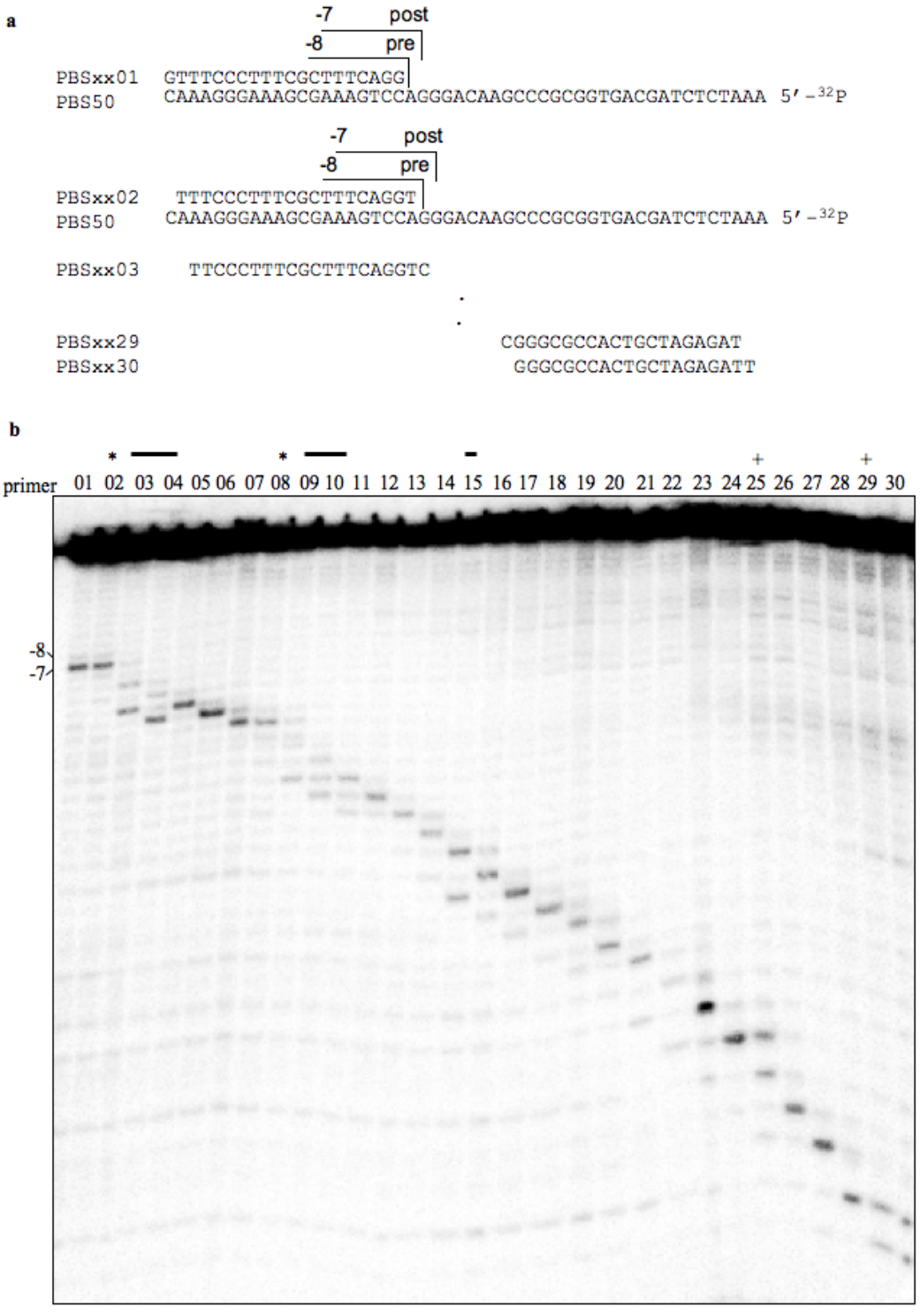
a
-7
post
-8
pre
PBSxx01 GTTTCCCTTTCGCTTTCAGG
PBS50 CAAAGGGAAAGCGAAAGTCCAGGGACAAGCCCGCGGTGACGATCTCTAAA 5′-32P
-7
post
-8
pre
PBSxx02 TTTCCCTTTCGCTTTCAGGT
PBS50 CAAAGGGAAAGCGAAAGTCCAGGGACAAGCCCGCGGTGACGATCTCTAAA 5′-32P
PBSxx03 TTCCCTTTCGCTTTCAGGTC
PBSxx29 CGGGCGCCACTGCTAGAGAT
PBSxx30 GGGCGCCACTGCTAGAGATT
b
primer 01 02 03 04 05 06 07 08 09 10 11 12 13 14 15 16 17 18 19 20 21 22 23 24 25 26 27 28 29 30
-8
-7

Figure 3. 2

Figure 3.3 **KOONO footprinting of overlapping templates reveals a "template end" effect on RT position.** WT RT was incubated with double stranded DNA substrates with consecutive primer terminus positions. These binary complexes were treated with KOONO, producing cleavage fragments at positions -8 or -7 on the template strand corresponding to a pre- or post-translocation conformation respectively. (a) a schematic indicating the relative position of identical primers on overlapping templates used to probe the affect of primers near the template end (42A) or in the presence of a template overhang (42B). Positions of -8 and -7 cuts are indicated schematically for primer ScPr19 (a) and on the gels for the outermost primers ScPr19 and ScPr22 (b). Lanes are labelled with the abbreviated numerical suffix of the primer used (eg. ScPr19 is 19). Cleavage fragments are resolved on 12% polyacrilamide gels at single nucleotide resolution.

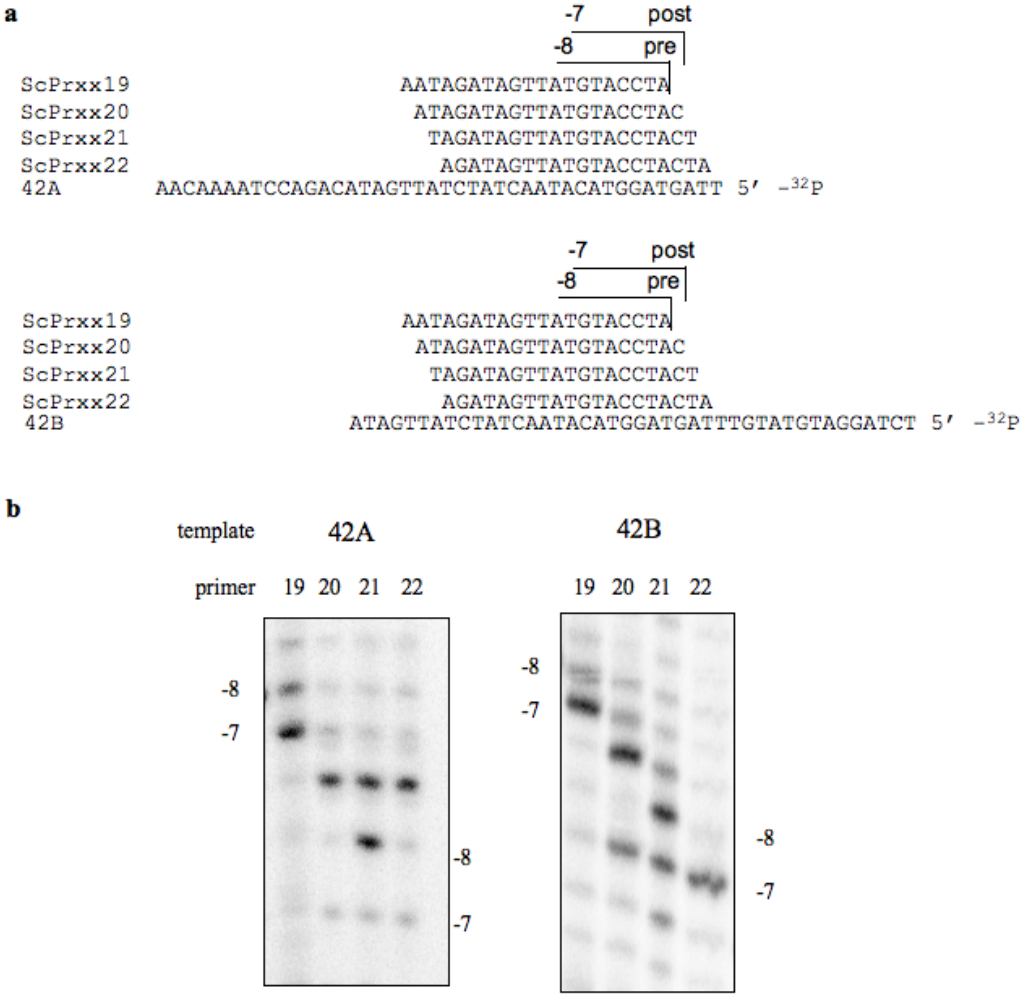
a
-7
post
-8
pre
ScPrxx19
ScPrxx20
ScPrxx21
ScPrxx22
42A
AATAGATAGTTATGTACCTA
ATAGATAGTTATGTACCTAC
TAGATAGTTATGTACCTACT
AGATAGTTATGTACCTACTA
AACAAAATCCAGACATAGTTATCTATCAATACATGGATGATT 5′ -32P
-7
post
-8
pre
ScPrxx19
ScPrxx20
ScPrxx21
ScPrxx22
42B
AATAGATAGTTATGTACCTA
ATAGATAGTTATGTACCTAC
TAGATAGTTATGTACCTACT
AGATAGTTATGTACCTACTA
ATAGTTATCTATCAATACATGGATGATTTGTATGTAGGATCT 5′ -32P
b
template
42A
42B
primer
19 20 21 22
19 20 21 22
-8
-7
-8
-7
-8
-7
-8
-7

Figure 3. 3

Figure 3.4 **Alignment of heavily biased pre-translocation sequences.** (a) Sequences of primer/templates identified as heavily biased for pre-translocation in KOONO experiments. (b) Manual alignment of template sequences centered over position n-1 relative to the 3' end of the primer. Positions with 80% or greater consensus are indicated in green and red for conserved purine or pyrimidine residues, respectively.

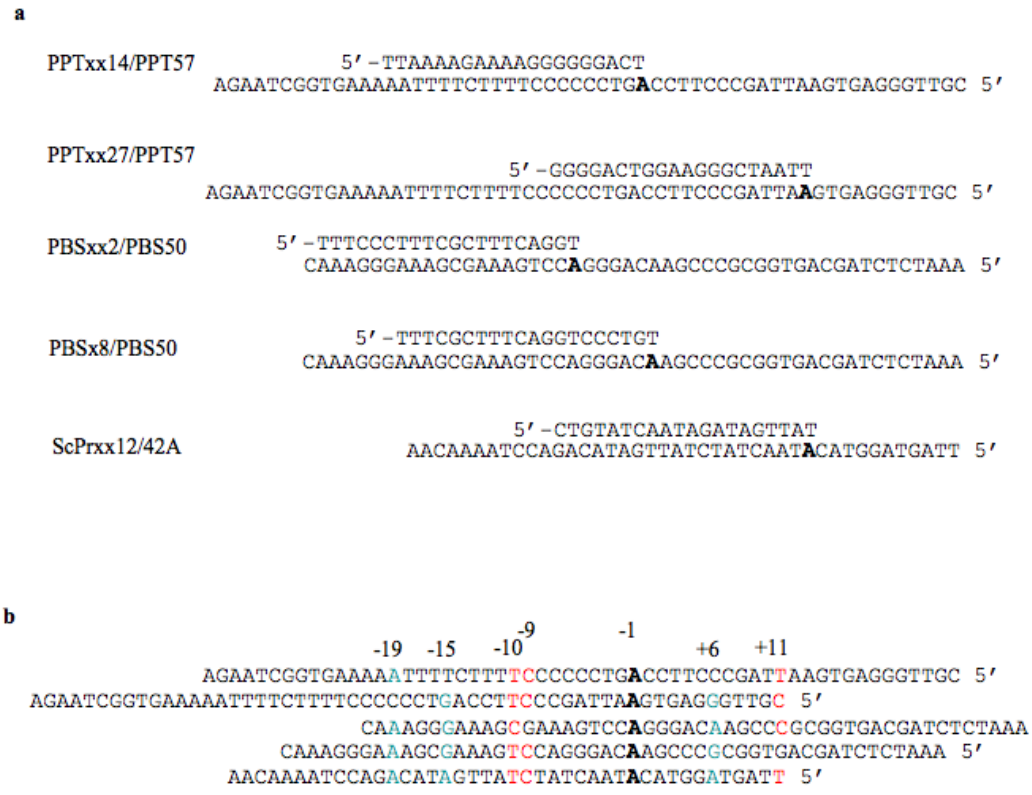

Figure 3. 4

Figure 3.5 **Requirement of a 3' thymidine for pre-translocation bias.** WT RT was incubated with double stranded DNA substrates with consecutive primer terminus positions. These binary complexes were treated with KOONO, producing cleavage fragments at positions -8 or -7 on the template strand corresponding to a pre- or post-translocation conformation respectively. (a) Primers were selected to include positions of heavy pre-translocation bias (primers PPTxx14 and PPTxx27, both on template PPT57). Modified templates PPT57(14T) and PPT57(27T) (modifications in bold) were used to monitor the change from thymidine to adenosine at the 3' primer terminus. (b) -8 and -7 cleavage fragments are labelled for the outermost lanes of the gels and lanes are labelled with the abbreviated numerical suffix of the primer used (eg. PPTxx12 is 12). The presence of adenosine at the 3' primer terminus results in the loss of the pre-translocation, -8 cut (14A, second panel) or a shift from pre-translocation bias to a mixture of pre- and post-translocation (27A, fourth panel) depending on the sequence tested. Cleavage fragments are resolved on 12% polyacrilamide gels at single nucleotide resolution.

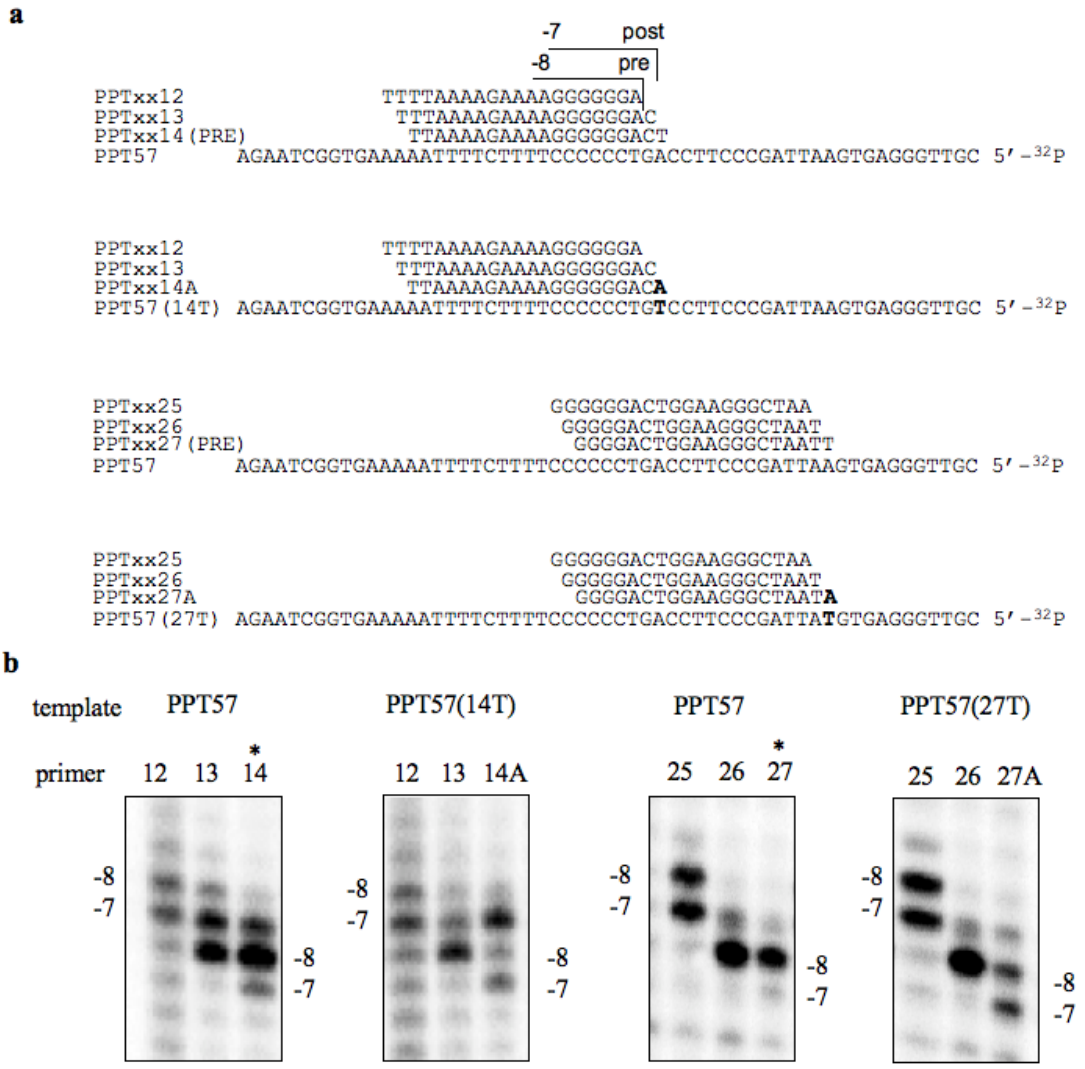
a
-7
post
-8
pre
PPTxx12 TTTTAAAAGAAAAGGGGGGA
PPTxx13 TTTAAAAGAAAAGGGGGGAC
PPTxx14(PRE) TTAAAAGAAAAGGGGGGACT
PPT57 AGAATCGGTGAAAAATTTTCTTTTCCCCCCTGACCTTCCCGATTAAGTGAGGGTTGC 5′-32P
PPTxx12 TTTTAAAAGAAAAGGGGGGA
PPTxx13 TTTAAAAGAAAAGGGGGGAC
PPTxx14A TTAAAAGAAAAGGGGGGACA
PPT57(14T) AGAATCGGTGAAAAATTTTCTTTTCCCCCCTGTCCTTCCCGATTAAGTGAGGGTTGC 5′-32P
PPTxx25 GGGGGGACTGGAAGGGCTAA
PPTxx26 GGGGGACTGGAAGGGCTAAT
PPTxx27(PRE) GGGGACTGGAAGGGCTAATT
PPT57 AGAATCGGTGAAAAATTTTCTTTTCCCCCCTGACCTTCCCGATTAAGTGAGGGTTGC 5′-32P
PPTxx25 GGGGGGACTGGAAGGGCTAA
PPTxx26 GGGGGACTGGAAGGGCTAAT
PPTxx27A GGGGACTGGAAGGGCTAATA
PPT57(27T) AGAATCGGTGAAAAATTTTCTTTTCCCCCCTGACCTTCCCGATTATGTGAGGGTTGC 5′-32P
b
template
PPT57
PPT57(14T)
PPT57
PPT57(27T)
primer
12 13 14*
12 13 14A
25 26 27*
25 26 27A
-8
-7

Figure 3. 5

Figure 3.6 **Models for the effect of translocation bias on catalytic rate of nucleotide incorporation.** Schematic representations of nucleotide incorporation including the contribution of the translocational equilibrium in the absence (a) and presence (b) of a closed binary pre-translocation complex. The rate of conversion between open pre- and post-translocation conformations (k_{pre} and k_{post}) is rapid and is not proposed to contribute to the catalytic rate (k_{pol}). (a) In the first model the orientation of bound nucleotide at the active site in the context of post translocation bias (shown in red) differs from that of the equivalent complex in the context of pre-translocation bias, leading to an increased rate of conversion (k_{pol}) of the ternary complex (RT_{post}:DNAn:dNTP) to the post-incorporation complex, having undergone conformational change (RT'_{post}:DNA_{n+1}). (b) In this alternate model, pre-translocation binary complexes, in the context of pre-translocation bias, are removed from the reaction (shown in red) by a conformational change (k_{close}) and the conversion to the open form (k_{open}) is significantly slow enough to affect the observed rate of catalysis (k_{pol}) further down the reaction pathway.

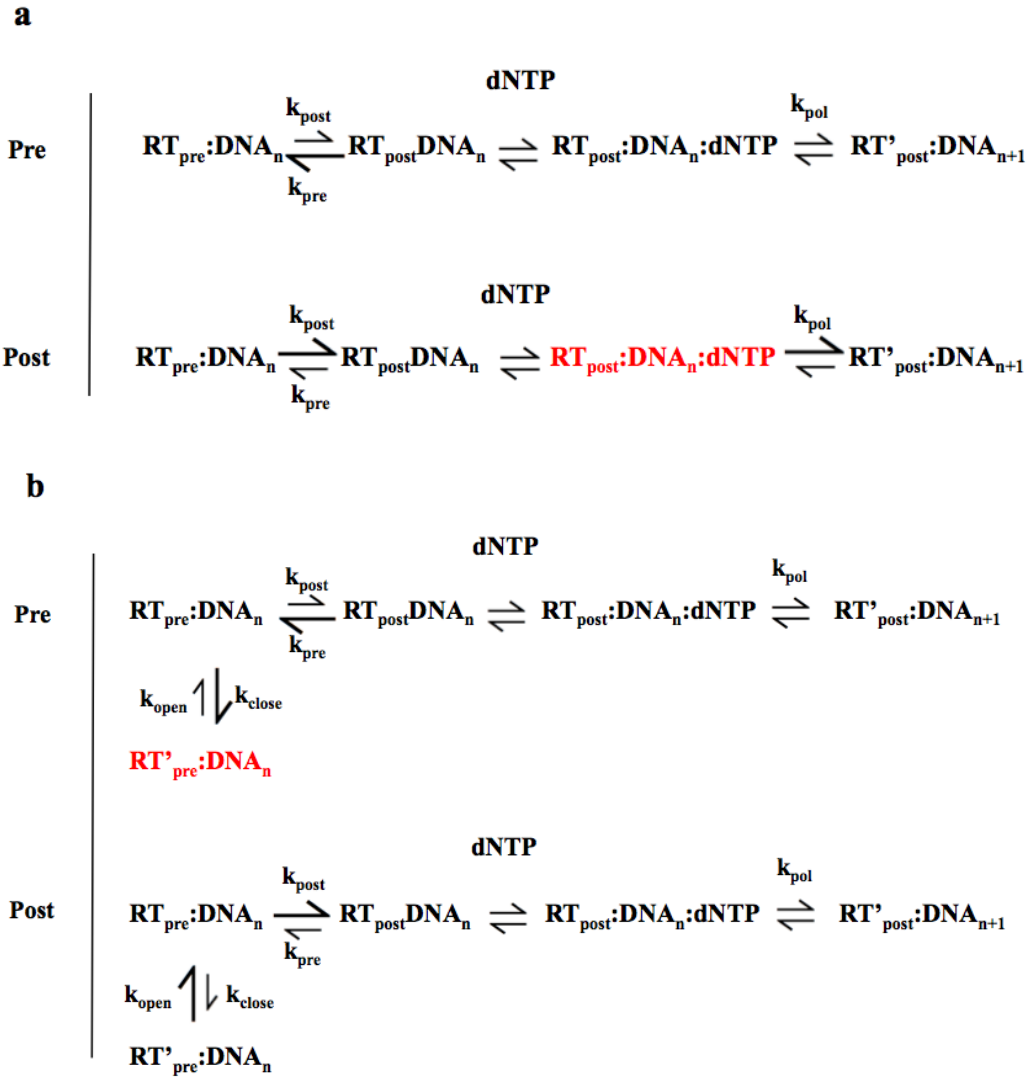
a
Pre
dNTP
k_{post}
k_{pre}
k_{pol}
$RT_{pre}:DNA_n \rightleftharpoons RT_{post}DNA_n \rightleftharpoons RT_{post}:DNA_n:dNTP \rightleftharpoons RT'_{post}:DNA_{n+1}$
Post
dNTP
k_{post}
k_{pre}
k_{pol}
$RT_{pre}:DNA_n \rightleftharpoons RT_{post}DNA_n \rightleftharpoons RT_{post}:DNA_n:dNTP \rightleftharpoons RT'_{post}:DNA_{n+1}$
b
Pre
dNTP
k_{post}
k_{pre}
k_{pol}
$RT_{pre}:DNA_n \rightleftharpoons RT_{post}DNA_n \rightleftharpoons RT_{post}:DNA_n:dNTP \rightleftharpoons RT'_{post}:DNA_{n+1}$
k_{open}
k_{close}
$RT'_{pre}:DNA_n$
Post
dNTP
k_{post}
k_{pre}
k_{pol}
$RT_{pre}:DNA_n \rightleftharpoons RT_{post}DNA_n \rightleftharpoons RT_{post}:DNA_n:dNTP \rightleftharpoons RT'_{post}:DNA_{n+1}$
k_{open}
k_{close}
$RT'_{pre}:DNA_n$

Figure 3. 6

Table 3.1 **Pre-steady state kinetics of nucleotide incorporation in the context of pre- and post-translocation bias**

Nucleotide	Primer/ Template	PRE/ POST	k_{pol} (s^{-1})[a]	K_d (μM)[a]	Efficiency k_{pol}/K_d ($\mu M^{-1}s^{-1}$)	Efficiency POST/PRE
dATP	PPTxx14/ PPT57(15T)	PRE	8.2 ± 0.7	17.2 ± 4.0	0.48	54
	PPTxx11/ PPT57	POST	110 ± 2.8	4.2 ± 0.37	26	
dTTP	PPTxx14/ PPT57(15A)	PRE	1.8 ± 0.079	26.0 ± 3.4	0.069	143
	PPTxx11/ PPT57(12A)	POST	33.7 ± 1.1	3.4 ± 0.5	9.9	
dCTP	PPTxx27/ PPT57	PRE	1.3 ± 0.03	12.6 ± 1.2	0.10	14
	PPTxx21/ PPT57	POST	25.9 ± 1.1	18.6 ± 2.3	1.4	
dGTP	PPTxx14/ PPT57	PRE	5.1 ± 0.3	19.1 ± 4.0	0.27	35
	PPTxx20/ PPT57	POST	63.7 ± 2.0	6.69 ± 0.7	9.5	

[a] Errors reported represent the deviation of points from the curve fit generate by GraphPad Prism (Version 5.0)

Table 3. 1

Table 3.2 **PPi mediated excision of ddTTP and ddATP in the context of pre- and post-translocation bias**

Primer/ Template	PRE/ POST	k_{pyro} (min^{-1})[a]	K_d (μM)[a]	Efficiency k_{pyro}/K_d ($\mu M^{-1}min^{-1}$)	Efficiency PRE/POST
PPTxx27^{ddTTP}/ PPT57	PRE	2.3 ± 0.17	96.5 ± 20	0.024	8.3
PPTxx26^{ddTTP}/ PPT57	POST	0.67 ± 0.047	230 ± 34	0.0029	
PPTxx27^{ddATP}/ PPT57	MIX	3.0 ± 0.38	116 ± 39	0.025	10
PPTxx17^{ddATP}/ PPT57(27T)	POST	0.47 ± 0.0066	238 ± 7.2	0.0020	

[a] errors presented represent deviation from the replot generated in Graphpad Prism (Version 5.0)

Table 3. 2

Chapter 4

Mechanism of resistance to GS-9148 by the Q151L mutation in HIV-1 Reverse Transcriptase

This chapter was adapted from an article authored by Brian J Scarth[1], Kirsten L White[2], James M. Chen[2], Eric B. Lansdon[2], S. Swaminathan[2], Michael D. Miller[2], and Matthias Götte[1, 3] that is currently in the final stages of review for publication in the journal ***Antimicrobial Agents and Chemotherapy***

[1]Department of Microbiology & Immunology, McGill University, Montreal, QC, Canada, H3A 2B4

[2]Gilead Sciences, Inc, 333 Lakeside Drive, Foster City, California, 94404, USA

[3]Department of Biochemistry, McGill University, Montréal, QC H3A 1A3, Canada.

4.1 Preface

During my studies of the translocational equilibrium of RT I had the opportunity to characterize the novel nucleotide analogue RT inhibitor (NtRTI) GS-9148 in the context of a novel drug resistance mutation Q151L. Prior to my involvement with this work, Q151L had been seen to be highly and selectively resistant to GS-9148, while displaying hypersusceptibility to the related NtRTI tenofovir in cell culture [261]. Using pre-steady state kinetics and structure activity relationship experiments, I determined the mechanism of resistance of Q151L to GS-9148 to be increased discrimination. Hypersusceptibility of Q151L to tenofovir was determined to be related to a decreased rate of excision of the inhibitor relative to WT. Though these results were not seen to be related to changes in the translocational equilibrium, they are included here as a they relate to my work with mechanisms of drug susceptibility and resistance by RT.

4.2 Abstract

GS-9148 is an investigational, phosphonate nucleotide analogue inhibitor of reverse transcriptase (RT; NtRTI) of human immunodeficiency virus type 1 (HIV-1). This compound is an adenosine derivative with a 2',3'-dihydrofuran ring structure that contains a 2'-fluoro group. The resistance profile of GS-9148 is unique in that the inhibitor can select for the very rare Q151L mutation in HIV-1 RT as a pathway to resistance. Q151L is not stably selected by any of the approved nucleoside or nucleotide analogues; however, it may be a transient intermediate that leads to the related Q151M mutation, which confers resistance to multiple compounds that belong to this class of RT inhibitors. Here, we employed pre-steady state kinetics to study the impact of Q151L on substrate and inhibitor binding, and the catalytic rate of incorporation. Most importantly, we found that Q151L is unable to incorporate GS-9148 under single turnover conditions. Interference experiments showed that the presence of GS-9148-diphosphate, i.e. the active form of the inhibitor, does not reduce the efficiency of incorporation for the natural counterpart. We therefore conclude that Q151L severely compromises binding of GS-9148-diphosphate to RT. This effect is highly specific, since we also demonstrate that another NtRTI, tenofovir, is incorporated with similar selectivity as seen with wild-type RT. Incorporation assays with other related compounds and models based on the RT/DNA/GS-9148-diphosphate crystal structure suggest that the 2'-fluoro group of GS-9148 may cause steric hindrance with the side chain of Q151L.

4.3 Introduction

The DNA polymerase activity of HIV-1 RT is targeted by nucleos(t)ide analogue RT inhibitors (N(t)RTIs) that represent the backbone of frequently used drug regimens. N(t)RTIs compete with natural dNTP pools for incorporation and cause chain-termination. There are currently seven approved NRTIs available for the treatment of HIV-1 infection [8]. The only approved NtRTI, i.e. tenofovir, is a phosphonate with an acyclic linker attached to the adenine base [8]. An investigational NtRTI, GS-9148, has recently been shown to be active against HIV-1 in cell culture and to possess a promising resistance profile in addition to a low nephrotoxic potential [185; 262]. GS-9148 is the intracellularly metabolized form of the orally bioavailable phosphonate GS-9131 [263] (Figure 4.1). GS-9148 undergoes two phosphorylations to become GS-9148-diphosphate (DP), which, like tenofovir-DP, is the active metabolite that is incorporated by HIV-1 RT. In contrast to tenofovir, GS-9148 is composed of a 2',3'-dihydrofuran that contains a 2'-fluoro group [264] (Figure 4.1).

In vitro selection experiments in cell culture revealed the emergence of two different resistance pathways. The compound selects either for Q151L with high-level resistance to GS-9148 [261], or for a combination of K70E, D123N, and T165I, that shows low-level resistance to GS-9148 [265]. Q151L is a potential intermediate in the development of the Q151M cluster that is associated with resistance to multiple NRTIs. However, the Q151L mutation is severely compromised in replication capacity, which helps to explain its low prevalence [157]. While Q151M shows low-level resistance to GS-9148, Q151L shows specific high-level resistance to this

compound in phenotypic susceptibility assays [265]. Interestingly, Q151L shows hypersusceptibilty to tenofovir in cell culture [261].

Resistance to N(t)RTIs is associated with two major biochemical mechanisms: certain mutations discriminate against the inhibitor at the level of binding and incorporation, while other mutations were shown to excise the incorporated inhibitor in the presence of ATP that can act as a pyrophosphate (PPi) donor [13]. To elucidate the underlying biochemical mechanisms of resistance for Q151L RT to GS-9148, we employed pre-steady state kinetics that revealed that Q151L severely compromises the binding of GS-9148-DP. Experiments with related compounds point to a possible steric hindrance associated with the 2'-fluoro group of the sugar moiety that was confirmed by modeling studies.

4.4 Materials and Methods

Enzymes and nucleic acids

Heterodimeric reverse transcriptase p66/p51 was expressed and purified as previously described [248]. Mutant enzymes were generated through site directed mutagenesis using the Stratagene Quick-change kit according to the manufacturer's protocol. Oligodeoxynucleotides used in this study were chemically synthesized and purchased from Invitrogen Life Technologies (Carlsblad, CA).

The following sequence was used as a template:

42D

5'GGATAAAGATTCAGTCTAGGATGTATGTTTAGTAGGTACATAACTATCT

ATTGATACAGACCTAAAACAA

The initial primer used in DNA synthesis inhibition assays was:

20D

5' TGTTTTAGGTCTGTATCAAT

For pre-steady state kinetic analysis and other experiments we examined incorporation at the +3 position using the appropriate primer:

20D+3:

5'TTGTT TTAGGTCTGTATCAATAG

Primers were 5' radio-labelled and gel purified as previously described [112]. Labelling was performed using polynucleotide kinase purchased from Fermentas Life Science (Burlington, ON CAN) and γ-^{32}P ATP purchased from PerkinElmer (Waltham, MA). Deoxynucleotides were purchased from Fermentas Life Science. 2'-modified

adenosine analogues were purchased from Trilink Biotechnologies (San Diego, CA). GS-9148-DP and PMPA-DP were provided by Gilead Sciences, Inc.

DNA-synthesis inhibition assay

50 nM of the 5' labeled 20D primer was heat annealed with 100 nM 42D template. The DNA/DNA hybrid was incubated with 250 nM HIV-1 RT in a buffer containing 50 mM Tris-HCl pH 7.8, 50 mM NaCl and 0.2 mM EDTA with 1 μM of each of the four dNTPs in the presence or absence of 10 μM of chain terminator (GS-9148-DP, tenofovir-DP or ddATP) as indicated. The mixture was incubated at 37°C and the reaction started by the addition of 6 mM $MgCl_2$. At 10 minutes the reaction was stopped by the addition of a 2-volume excess of formamide buffer containing trace amounts of bromophenol blue and xylene cynol and heat denatured at 95°C for 5 minutes. The products of DNA synthesis were resolved on 12% denaturing polyacrylamide gel by electrophoresis and visualized by PhosphorImaging.

Assessment of 2' modified adenosine analogues

Structure-activity Relationship (SAR) experiments were performed as the DNA synthesis inhibition assay using the 20D+3 primer and a time point of 10 s with 1 μM of dATP or 1 mM of araATP, 2'-azido-2'-dATP, or 2'-fluoro-2'-dATP as indicated. Samples were resolved and visualized as above. Incorporation of the 2'-modified adenosine analogues by each of the mutant enzymes was normalized to incorporation of dATP by that enzyme under reaction conditions.

Pre-steady state kinetics

Performed as previously described [112; 151; 266]. 100 nM of the 5' labelled 20D+3 primer was heat annealed with 200 nM 42D template. The DNA/DNA hybrid was incubated with 500 nM HIV-1 RT in a buffer containing 50 mM Tris-HCl pH 7.8, 50 mM NaCl, and 6 mM $MgCl_2$. Substrate was prepared in the same buffer as the RT-P/T and the reaction was started and stopped by computer control using a Kintek RFQ-3 Quench Flow (Austin, TX). Equal volumes of RT-P/T and substrate were mixed in this manner for times ranging from 0.015 s to 2.0 s and stopped by the addition of excess 0.5 M EDTA. Substrate concentrations ranged from 780 nM to 200 μM for dATP, GS-9148-DP, tenofovir-DP, and ddATP. Samples were diluted in formamide buffer containing trace amounts of bromophenol blue and xylene cynol and heat denatured at 95°C for 5 minutes. Samples were resolved and visualized as above. Incorporation was quantified using ImageQuant (GE Healthcare) as (product/total)*100 nM and results were plotted in Prism 4.0 using the non-linear regression for one-phase exponential association to the equation [product]=A*(1-exp(-k_{obs}*t)) where t is time, A is amplitude of product formed and k_{obs} is the observed rate at a given concentration of substrate. Rates obtained from each concentration of substrate were replotted against the concentration of substrate using the non-linear regression for Michealis Menten with the equation $k_{obs}=k_{pol}$ *[substrate]/(K_d+[substrate]) which allows for the determination of the kinetic constants k_{pol} and K_d for the chemical reaction of nucleotide incorporation as previously described [112; 151; 266].

ATP mediated excision of chain terminated primers

20D+3 primer was chain terminated with tenofovir-DP or GS-9148-DP and gel purified as previously described [181]. These chain terminated primers were then heat annealed to 2-fold excess of template 42D and 50 nM of the resulting hybrid was incubated with 250 nM RT (WT or mutants K65R or Q151L) in buffer containing 50 mM Tris-HCl pH 7.8, 50 mM NaCl, and 0.2 mM EDTA. A rescue mix containing 1 μM of dATP, 1 μM dTTP, and 10 μM ddGTP, and either 3.1-200 μM inorganic pyrophosphate or 3.2 mM of ATP as pyrophosphate donors for the excision reaction. ATP was treated with inorganic pyrophosphatase to eliminate contaminating PPi. Reactions were initiated with the addition of 6 mM $MgCl_2$ and samples were taken from 30 s to 20 min for PPi and 5 min to 90 min for ATP. Samples were resolved and visualized as above. 100% extension of unchain-terminated Primer+3 was observed for all mutants under these reaction conditions, thus eliminating differences in incorporation. Correction for minimal (<10%) extension of chain-terminated primer+3 in the absence of a PPi donor indicated that any extension products under experimental conditions represented products of the excision reaction. Results were analyzed as above, results with ATP were analyzed at a single concentration and fitted to a one-phase exponential with the equation $[product]=A*(1-\exp(-k_{obs}*X))$. For PPi a range of [PPi]s were assessed, allowing for determination of k_{pyro} and $K_{d\text{-}PPi}$ using the equation $k_{obs}=K_{pyro}*[PPi]/(K_{d\text{-}PPi}+X)$ as used for the forward reaction.

Molecular Modeling

Molecular modeling of Q151L and Q151M bound to GS-9148-DP was based on ternary crystal structures of WT HIV-1 RT bound to GS-9148-DP [267]. The X-ray model was converted into its corresponding minimized model using Sybyl Molecular Modeling Software, version 6.8, (Tripos Inc., St. Louis MO, USA). Mutants Q151L and Q151M were generated using methods previously described [197]. The modified side-chain conformations of the Q151M and Q151L were then minimized.

4.5 Results

Biochemical resistance profile of GS-9148-DP - Inhibition of DNA synthesis with the adenosine analogues GS-9148-DP, tenofovir-DP, and ddATP was evaluated with purified RT enzymes using a short DNA template (Figure 4.2). Full-length product formation was initially monitored at a single concentration of inhibitors with WT RT and enzymes containing mutations Q151L, Q151M, and K65R, respectively. K65R confers decreased susceptibility to both tenofovir and didanosine (ddI, i.e. the prodrug of ddATP), and was included in this study for comparative purposes.

The presence of 10 μM of each of the A-analogues studied in the context of WT RT resulted in significant decreases in full-length product formation and the accumulation of chain-terminated sites opposite the complementary thymidines. GS-9148-DP and tenofovir-DP showed similar levels of inhibition under these conditions, with subtle increases in early chain-termination with tenofovir-DP. The presence of ddATP showed the most efficient inhibitory effects that resulted in greater accumulation of chain-termination products at position n+1 and no observable full-length product. These results are consistent with the EC_{50} values of the three drugs [185].

In cell culture, K65R is associated with reduced susceptibility to tenofovir and ddI, but retains its susceptibility to GS-9148 [185]. Here we show, as expected, that the K65R mutation in HIV-1 RT decreases sensitivity to ddATP, now with visible full-length product formation. K65R appears least sensitive to tenofovir-DP with the

largest amount of full-length product. The mutant also displayed clear chain-termination in the presence of GS-9148-DP, although full-length product formation increased noticeably when compared with WT RT. However, it is conceivable that K65R may also diminish excision of GS-9148, as has been shown for AZT and tenofovir [136; 268], which would help to explain the lack of reduced susceptibility data obtained in cell culture [185]

The Q151L mutant RT shows the strongest resistance to inhibition by GS-9148-DP. Inhibition of DNA synthesis is essentially not seen under these conditions. This effect is highly specific, as the activity of tenofovir-DP and ddATP is almost identical to that of WT RT. It appears as if Q151L can cause even subtle increases in inhibition with tenofovir-DP, while subtle reductions in inhibition are seen with ddATP. These patterns differ from the established Q151M mutant. Although Q151M displays decreased susceptibility to GS-9148-DP, it is more subtle than for Q151L [261] formation of the full-length product remains reduced, and chain-termination is visible. This mutation also causes subtle reduction in inhibition with tenofovir-DP and ddATP.

Pre-steady-state kinetic analysis - We next employed pre-steady-state kinetics for single nucleotide incorporation events to translate our initial findings into quantitative terms. We measured the rate constant k_{pol} and the equilibrium binding constant K_d for the natural substrate dATP and each of the inhibitors, GS-9148-DP, tenofovir-DP, and ddATP against WT RT and mutant enzymes, respectively (Table 1). The overall

efficiency of incorporation is expressed as the ratio of k_{pol}/K_d. An enzyme's selectivity against a given inhibitor is defined as the ratio of [k_{pol}/K_d (natural nucleotide)]/[k_{pol}/K_d (nucleotide analogue)] and the level of resistance in these biochemical experiments is defined as the ratio of selectivity $_{Mutant}$ / selectivity $_{WT\ RT}$.

WT RT incorporated the substrates with efficiencies in the order dATP > ddATP > tenofovir-DP > GS-9148-DP, although the differences amongst the inhibitors are subtle. A selectivity of 16.5 against GS-9148-DP is primarily the result of a 10-fold increase in K_d with a minimal (<2-fold) decrease in k_{pol}. Thus, a diminution in substrate affinity appears to be the major factor that reduces efficiency of incorporation. In contrast, a selectivity of 5 against ddATP is the result of a pronounced decrease in k_{pol}, with no significant change in K_d relative to the natural substrate dATP. Thus, in this case, substrate binding does not appear to be affected, it is rather the rate-limiting step of the conformational closing of the thumb and fingers loop over the nucleotide binding site or the chemical step that is compromised. A selectivity of 10.8 against tenofovir-DP is a mixture of changes in both K_d and k_{pol} values, suggesting that substrate binding as well as the conformational change or chemical step are compromised.

K65R caused reductions in the efficiency of incorporation of each of the three inhibitors. Incorporation of the natural substrate is approximately 2-fold reduced. The strongest effect is seen with tenofovir-DP. Changes in kinetic parameters translate into 6.1-fold resistance to this inhibitor, which is in accordance with previous reports

of a k_{pol}-mediated effect for K65R with tenofovir [136; 138]. Resistance to GS-9148-DP is less pronounced (2.9-fold), and almost negligible with ddATP (1.2-fold).

Q151L showed approximately 10-fold reductions in efficiency of incorporation of the natural substrate dATP when compared with WT RT. We were unable to measure incorporation of GS-9148-DP at concentrations up to 200 μM, which is in agreement with the lack of inhibition of polymerization shown in Figure 4.2. The combined data suggest that Q151L literally prevents incorporation of this inhibitor under single turnover conditions. In contrast, efficiency of incorporation of tenofovir-DP is slightly increased. In an attempt to elucidate the underlying mechanism of this exclusion, we employed an incorporation interference experiment to assess whether GS-9148-DP can bind to the binary RT-primer/template complex. We looked for changes in kinetic parameters for dATP incorporation in the presence of a fixed concentration of 60 μM GS-9148-DP. If the analogue is able to compete with the natural substrate for binding, we would expect to see further increases in K_d values. However, incorporation of dATP was unaffected by the presence of GS-9148-DP. Knowing that any product formation observed would not be the incorporation of GS-9148-DP under these conditions, we conclude that binding of the inhibitor is severely compromised by the Q151L mutation. The related Q151M mutation showed only low-levels of resistance to the three inhibitors.

Modeling of GS-9148-DP binding to Q151L containing RT

The crystal structure of WT RT bound to a DNA/DNA primer template and incoming GS-9148-DP has recently been solved [267]. This structure was used as a scaffold to model the binding of GS-9148-DP to Q151L and Q151M containing RT (Figure 4.3). In the WT and Q151M models, GS-9148-DP fits within the NRTI binding pocket and lacks negative interactions with RT. In contrast, the model generated for Q151L shows the development of a negative steric interaction with the 2'-fluoro moiety of GS-9148-DP and the side chain of Q151L.

Structure-Activity Relationships (SAR) with 2'Modified Adenosine Analogues

To further investigate the potential role of the 2'-fluoro group in the diminished binding of GS-9148-DP to the Q151L mutant RT, we included additional related adenosine analogues in our inhibition studies (Figure 4.4A). The analogues used were araATP, 2'-azido-2'-dATP, and 2'-fluoro-2'-dATP. These compounds differ from GS-9148-DP in that they contain a standard phosphoester link rather than the phosphonate moiety that is present in GS-9148-DP and tenofovir-DP. Rigorous kinetic analysis such as pre-steady state kinetics was limited due to the poor overall incorporation of these substrates, which are actively incorporated only at high concentrations as described for ATP. An assessment at a single concentration of 1 mM and a single time point revealed structurally related trends across the panel of mutant RTs. Incorporation of 1 mM of the 2'-modified substrates was normalized against the incorporation of 1 μM of the natural substrate dATP for each enzyme. Under this type of analysis, araATP was mostly unaffected by the different mutants compared to WT with relative efficiencies in the order Q151M > WT > Q151L >

K65R. 2'-azido-2'-dATP was strongly disfavored for incorporation by all enzymes including WT RT. 2'-fluoro-2'-dATP was incorporated by WT at levels similar to araATP and was strongly disfavored by Q151L. The pattern is similar as seen with GS-9148-DP, which points to an important role of the 2'-fluoro-group in determining resistance in the context of Q151L.

Nucleotide excision by Q151L – Our pre-steady state kinetic analysis shows that the Q151L mutant is fully sensitive to tenofovir-DP. Selectivity values for WT RT and Q151L are almost identical; thus, these findings do not explain the hypersusceptible phenotype observed in cell culture [261]. However, resistance-conferring mutations may not only discriminate against the inhibitor at the level of incorporation, as thymidine analogue associated mutations (TAMs) in HIV-1 RT have also been shown to increase rates of excision in the presence of PPi or the pyrophosphate donor ATP to mediate NRTI resistance [101; 102]. Conversely, many other known mutations, including M184V (lamivudine resistance) [269], L74V (didanosine resistance) [145; 146], and K65R (resistance to multiple nucleotide analogues) [136; 204; 219] have been shown to diminish the efficiency of excision and cause hypersusceptibility to the thymidine analogue zidovudine [204].

Therefore, we assessed the ability of WT RT, K65R, and Q151L to perform ATP- and PPi-mediated excision of tenofovir with the hypothesis that hypersusceptibility could be mediated through decreased efficiency of the excision reaction. Of note, GS-9148-DP was not excised at physiologically relevant concentrations of 3.2 mM ATP;

neither with WT RT, nor with K65R or Q151L (data not shown). The rate of ATP-mediated excision of tenofovir-DP was seen to be very similar between WT and Q151L at 0.010 ± 3.6 $x10^{-4}$ min^{-1} and 0.011 ± 3.2 x 10^{-4} min^{-1}, respectively. With a rate of 9.8 x 10^{-4} ± $1.1x10^{-4}$ min^{-1} K65R was compromised relative to WT and Q151L. In contrast to the results obtained with ATP, similar time course experiments with PPi revealed differences in excision between WT RT and Q151L. We further examined these differences using the same analysis as employed for the forward reaction to determine the maximum rates of pyrophosphorolysis, k_{pyro}, and the equilibrium binding constant, $K_{d\text{-}PPi}$. While WT RT, K65R, and Q151L show similar values for the rate constant (k_{pyro}), Q151L and K65R show 5-fold and 8-fold reductions in affinity (K_d) to PPi (Table 2). With no difference in the rate constant, this decreased affinity to PPi translates directly to an overall reduction in efficiency of the excision reaction of 5-fold for Q151L and explains the observed hypersensitivity to tenofovir.

4.6 Discussion

The aim of this study was to elucidate the biochemical mechanisms of resistance to GS-9148 utilized by the HIV-1 Q151L mutant RT. The related Q151M mutation is known to confer resistance to multiple nucleoside analogues, with the exception of tenofovir [13]. Q151M is often associated with changes at position 62, 75, 77, and 116 that appear to correct for deficiencies in replication capacity [155]. Cell-based assays revealed that Q151L confers resistance to GS-9148 and hypersusceptibility to tenofovir [261]. Both compounds share the same base and phosphonate moieties, suggesting that structural differences between the sugar and the acyclic linker, respectively, can affect the phenotype. We have utilized primarily pre-steady state kinetic tools to study whether these findings can be translated into biochemical terms.

Q151L shows an approximately 8-fold reduction in the efficiency of incorporation of the natural substrate dATP. This deficiency is driven by an increase in K_d values that translate into a reduction in substrate affinity. Similar values are determined with the Q151M mutation, which provides an explanation for the diminished replication capacity of corresponding viruses [154; 155]. By comparison, K65R shows a 2-fold reduction that is driven by subtle differences in k_{pol} values that translate into a deficiency of the rate of conformational closing of the thumb and fingers loop domain [260]. The exact values may change, depending on the nature of the nucleotide substrate and the nature of the primer/template; however, similar trends have been reported for K65R and Q151M [136; 138; 156].

Changes in kinetic parameters for the nucleotide analogues reveal a more complex picture. For instance, K65R shows decreases in k_{pol} values for GS-9148 and tenofovir-DP. The sharp decline in k_{pol} values for tenofovir translates into more efficient discrimination against this inhibitor (6-fold versus 3-fold). Q151M shows both decreases in k_{pol} and increases in K_d values for each of GS-9148-DP, tenofovir, and ddATP, with the greatest effect being a 6-fold decrease in k_{pol} for ddATP. The overall effects of the Q151M mutation on the various inhibitors are generally subtle, however, after adjusting for changes seen with the natural dNTP substrate.

The effect seen with Q151L on the incorporation of GS-9148 is the most striking observation. The inhibitor is not incorporated under single turnover conditions. This effect is highly specific, as the efficiency of incorporation of tenofovir is not reduced. Subtle decreases in k_{pol} values and increases in K_d values appear to be in balance. An interference experiment provides a plausible mechanism for the lack of incorporation of GS-9148. The presence of GS-9148-DP does not interfere with the efficiency of incorporation of dATP. Both kinetic parameters k_{pol} and K_d are almost identical when measured in the absence or presence of the inhibitor. Any increase in the K_d value would have pointed to a certain degree of competition, and, in turn, binding of the inhibitor to the active site. The insignificant change in the K_d value for dATP suggests that Q151L severely compromises binding of the inhibitor.

In an attempt to characterize the structural reasons for this type of discrimination, we studied the effects of Q151L on the kinetic efficiency of related compounds. The phosphonate in place of a phosphoester, the 2'-fluoro group, and the unsaturated 2',3'-double bond of the sugar moiety are the three structural determinants that distinguish GS-9148-DP from its natural counterpart dATP. We ruled out the phosphonate as an important factor in this regard, given that tenofovir is still efficiently incorporated by Q151L. We have therefore limited this analysis to several commercially available compounds with modifications at the 2'-position of the ribose sugar. Y115 in HIV-1 RT appears to play an important role in discriminating between ribonucleotides and deoxyribonucleotides, and structural models suggest that the 2'-OH group appears to cause steric problems [270]. As a consequence, incorporation of ATP requires high concentrations, and is inefficient when the preferred substrate dATP is present. We have made similar observations with ara-ATP, 2'-azido-2'-deoxy-dATP, and 2'-fluoro-2'-deoxy-dATP. The bulky 2'-azido group shows the strongest effect in this regard and incorporation is severely compromised by K65R, Q151L, and Q151M. Low levels of incorporation are solely seen with WT RT. In contrast, the pattern obtained with 2'-fluoro-2'-deoxy-dATP is reminiscent of the data obtained with GS-9148-DP. Both K65R and Q151M show subtle reductions in GS-9148 incorporation, while Q151L completely prevents incorporation of the inhibitor. Together these data point to a certain degree of structural homology between GS-9148 and 2'-fluoro-2'-deoxy-dATP. The planar character of GS-9148 appears to bypass the steric problem with Y115 and facilitates its incorporation. The crystal structure of a complex of WT HIV-1 RT with primer/template and GS-9148-

DP bound at the active site supports this notion and shows favorable interaction between the dihydrofuran ring of the inhibitor and the aromatic sidechain of Y115 [267]. Although structures of Q151L, alone or with GS-9148-DP, are not available, modeling based on the structure of WT RT in complex with GS-9148-DP point to a steric clash between Q151L and the 2'-fluoro group of GS-9148-DP (Figure 4.3). A steric clash is evident only with Q151L and is not seen in the Q151M model, which could explain why Q151M displays near wild-type selectivity for GS-9148-DP.

The observed hypersusceptibility of Q151L to tenofovir is not explained by changes in incorporation as both WT RT and Q151L display similar selectivity to the inhibitor relative to the natural substrate. Results from excision experiments with PPi suggest that hypersusceptibility is instead mediated through diminished excision of incorporated tenofovir. This is likely due to reduced binding of PPi with Q151L. The lack of any significant difference between WT RT and the mutants in the presence of ATP as the PPi-donor could be the result of additional contacts, which dilutes the subtle effect on excision [141].

Taken together, our biochemical studies show that resistance-conferring mutations at position Q151 in HIV-1 RT display only subtle reductions in the efficiency of incorporation of a structurally diverse set of adenosine analogues. The exception is the inability of Q151L to incorporate GS-9148. We present strong evidence to demonstrate that specificity is mediated through steric hindrance caused by modifications at the 2'-position of the sugar moiety. However, the development of

high-level resistance to GS-9148 in the context of Q151L is associated with a price in that the efficiency of incorporation of the natural dATP substrate is reduced to a similar extent as seen with the related Q151M mutation. These findings help to explain the rare selection of the Q151L mutation in cell culture. The high barrier to resistance warrants further investigation into novel nucleotide analogues that are modified at the 2'-position. Of note, potent 2'-modified nucleotides are currently being developed to target the RNA-dependent RNA polymerase of the hepatitis C virus (HCV) [271]. By analogy, the emergence of the signature mutation S282T is also associated with a high barrier in cell culture and in the clinic. To test whether the emergence of Q151L can be further reduced or even prevented, it is likewise of interest to study the interaction of Q151L in conjunction with other mutations that are selected in the presence of established drugs.

Acknowledgments: We would like to thank Dr. Egor Tchesnokov for inspiring discussions and Suzanne McCormick for excellent technical assistant. This study was supported in part by Gilead Sciences, Inc., and by a grant from the Canadian Institutes for Health Research (CIHR) to MG. MG is recipient of a career award from the Fonds de la recherche en santé du Québec (FRSQ). BS is the recipient of CIHR's HIV/AIDS Research Initiative Doctoral Research Award.

4.7 Figures and Tables

Figure 4.1. **The active metabolites of the phosphonate containing NtRTIs tenofovir and GS-9148, and the natural substrate dATP.** Structural differences between the NtRTIs studied are seen between the acyclic linker of tenofovir and the sugar moeity of GS-9148-DP.

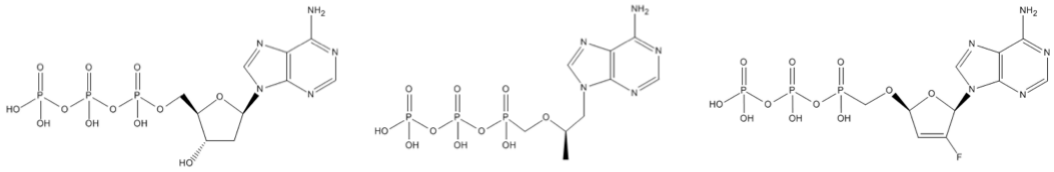

Figure 4. 1

Figure 4.2. **Inhibition of DNA synthesis by adenosine analogues.** Extension of a ^{32}P-radiolabeled primer to the full length product is equal for each of WT, K65R, Q151L, and Q151M mutant RT enzymes (1μM dNTPs). Addition of 10 μM of the adenosine analogues GS-9148-DP, tenofovir-DP, and ddATP results in chain termination at positions of adenosine incorporation on the template strand (underlined).

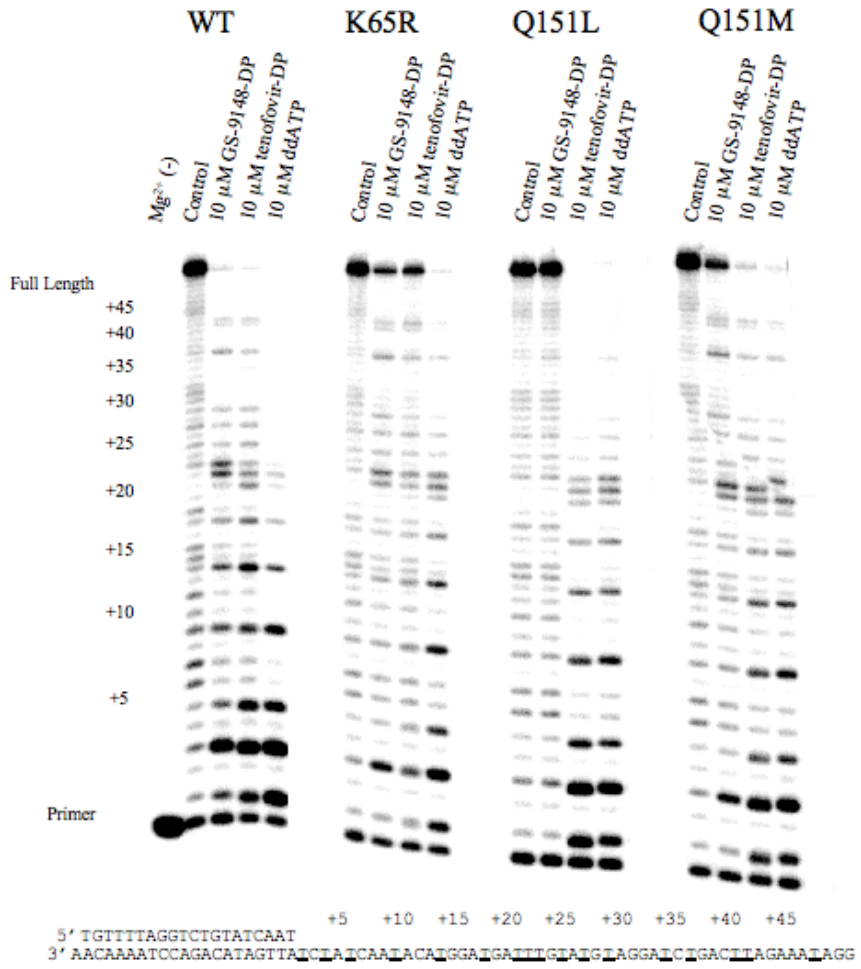
WT
K65R
Q151L
Q151M
Mg2+ (-)
Control
10 μM GS-9148-DP
10 μM tenofovir-DP
10 μM ddATP
Full Length
+45
+40
+35
+30
+25
+20
+15
+10
+5
Primer
+5 +10 +15 +20 +25 +30 +35 +40 +45
5′ TGTTTTAGGTCTGTATCAAT
3′ AACAAAATCCAGACATAGTTA

Figure 4. 2

Figure 4.3. **Molecular models of WT and mutant RT enzymes bound to primer/template and GS-9148-DP.** (A) The structure of WT HIV-1 RT bound to primer/template and GS-9148-DP served as a basis for models with mutations at position Q151 [267]. Models of mutants Q151L (B) and Q151M (C) were generated as described under materials and methods. A steric clash between the 2'-fluoro moiety of GS-9148-DP and the side chain of Q151L is highlighted.

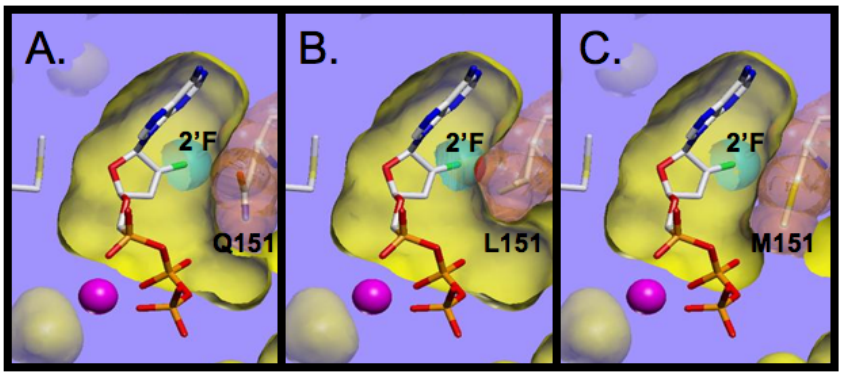

Figure 4. 3

Figure 4.4. **Structure Activity Relationships (SAR) with 2'Modified Adenosine Analogues.** (A) Structures of 2'modified adenosine analogues used in SAR experiments. (B) Incorporation of 2' modified adenosine analogues (1 mM) at 10 s by WT and K65R, Q151L, and Q151M mutant RT normalized to incorporation of the natural substrate dATP (1 μM) under the same conditions.

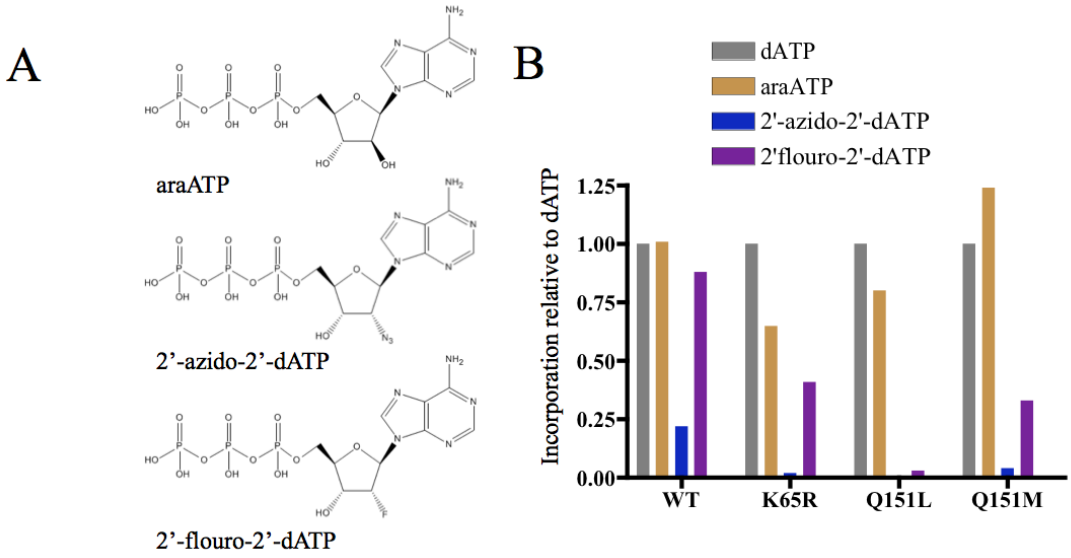

Figure 4. 4

Table 4.1. **Pre-steady state kinetic constants for incorporation of nucleotide analogues**

Enzyme	Substrate	k_{pol} (s^{-1}) [a]	K_d (μM) [a]	k_{pol}/K_d ($\mu M^{-1}s^{-1}$)	Selectivity[b]	ΔSelectivity[c]
WT	dATP	82.2 ± 4.2	6.18 ± 1.0	13.30	1	-
	GS-9148-DP	46.8 ± 2.4	57.9 ± 7.4	0.81	16.5	-
	tenofovir-DP	27.2 ± 0.65	22.1 ± 1.7	1.23	10.8	-
	ddATP	12.8 ± 0.35	4.79 ± 0.44	2.67	5.0	-
K65R	dATP	26.6 ± 0.49	3.68 ± 0.28	7.23	1	-
	GS-9148-DP	7.59 ± 0.086	50.4 ± 1.5	0.15	48.0	2.9
	tenofovir-DP	2.37 ± 0.18	21.5 ± 5.4	0.11	65.6	6.1
	ddATP	3.72 ± 0.11	3.10 ± 0.39	1.20	6.0	1.2
Q151L	dATP	42.9 ± 2.35	25.3 ± 3.6	1.70	1	-
	GS-9148-DP	n.d.				
	dATP + 60μM GS-9148-DP	44.9 ± 0.99	31.9 ± 1.9	1.41	1.2	-
	tenofovir-DP	16.2 ± 0.45	97.7 ± 5.6	0.17	10.2	0.90
	ddATP	0.356 ± 0.013	2.67 ± 0.45	0.13	12.7	2.6
Q151M	dATP	72.0 ± 2.6	36.0 ± 2.9	2.00	1	-
	GS-9148-DP	23.4 ± 1.3	267 ± 22	0.09	22.9	1.4
	tenofovir-DP	6.17 ± 0.23	67.7 ± 6.0	0.09	21.9	2.0
	ddATP	2.04 ± 0.17	10.5 ± 2.4	0.19	10.3	2.1

[a] Errors reported represent the deviation of points from the curve fit generated by GraphPad Prism (Version 5.0)
[b] Ratio of (k_{pol}/K_D) dATP/(k_{pol}/K_D), [c] Ratio of $Selectivity_{mut}/Selectivity_{WT}$, n.d. not determined

Table 4. 1

Table 4.2. **PPi-mediated excision of tenofovir by WT, K65R and Q151L RT**

Enzyme	k_{pyro} (min^{-1}) [a]	K_d (μM) [a]	K_{pyro}/K_d ($\mu M^{-1}min^{-1}$)
WT	2.00 ± 0.089	70.0 ± 7.2	0.029
K65R	1.22 ± 0.30	580 ± 180	0.0021
Q151L	2.15 ± 0.098	360 ± 23	0.0060

[a] Errors reported represent the deviation of points from the curve fit generated by GraphPad Prism (Version 5.0)

Table 4. 2

Chapter 5

Discussion

By the work contained in this thesis I have contributed to our understanding of determinants of the translocational equilibrium of RT and its functional consequences. These findings have implications for both the general mechanism of translocation as well as its role in drug resistance and susceptibility. These findings have implications for future work, both with regard to studies related to translocation as well as implications of nucleic acid sequence choice. I have also determined the mechanism of resistance of the novel mutation Q151L, and while this mechanism of resistance does not relate to changes in the translocational equilibrium, it can be seen as generally related to my studies of RT.

At the onset of my work, the development of site-specific footprinting techniques had recently created novel opportunities to study the translocational equilibrium of RT. My first endeavor was to expand our understanding of molecular determinants of this equilibrium. Interactions between the nucleic acid substrate and the enzyme had been shown to impact the translocational equilibrium in the case of E89K, which caused the enzyme to slide beyond the typical pre- and post-translocation register [104]. My study of the interactions between the template overhang and the fingers subdomain mutations F61A and A62V revealed that this subdomain significantly affected the translocational equilibrium [188]. For the first time it was shown that the loss of a stacking interaction between F61 and the template overhang led to the loss of sequence dependant pre-translocation complex formation. This was seen to significantly affect the activity of the translocation specific inhibitor PFA.

Increases in the proportion of post-translocation complexes, as seen with F61A, led to significant resistance to PFA, while increases in the proportion of pre-translocation complexes, as seen with A62V-containing enzymes, led to increased susceptibility.

Though my characterization of F61A resistance to PFA is unlikely to have direct clinical implications, as F61A does not appear in the clinic, it serves as a general mechanism that may be observed in the context of other mutations. Resistance to PFA has previously been described for amino acid changes that directly affect the binding of PPi or PFA, such as K65R [220] and R72A [221]. Like E89K, F61A represents a distinct mechanism of resistance that acts away from the site of PFA binding. These mutations act through the translocational equilibrium, to disrupt access to the pre-translocation conformation required for PFA activity. In addition to a simple reduced access to the pre-translocation conformation, I determined that the mechanism of F61A was related to decreased closed complex formation. The relationship between closed complex formation and the translocational equilibrium described in chapter two of this thesis may have important implications for the general mechanism of translocation.

The closure of the fingers domain was shown to be required for both PFA activity as well as sequence dependant pre-translocation bias. This was an important finding that relates to my study of the role of the nucleic acid sequence as a determinant of the translocational equilibrium. The observation of heavy post-translocation bias, in the context of F61A, led us to predict that the post-translocation conformation represented the general conformation of the enzyme. Analysis of a large number of consecutive positions by site-specific footprinting confirmed this

prediction. This work represents the first time that the nature of the translocational equilibrium has been determined in such a way that it may be extrapolated to other sequence contexts. We may now say that a sequence chosen at random is likely to exist in the post-translocation conformation, while pre-translocation bias is observed in a small portion of sequences. Attempts to determine a consensus sequence relating these effects to individual contacts between the enzyme and its substrate failed to reach significance. As the translocational equilibrium is affected by several distinct contacts, different sequences may be differentially affected, which would complicate the establishment of a single consensus sequence. In general, however, my characterization of effects of the nucleic acid sequence on the translocational equilibrium has implications for both nucleic acid sequence choice in future studies as well as the general mechanism of nucleotide incorporation and excision.

First, the use of divergent nucleic acid sequences in different studies can significantly alter the results, and creates difficulty in comparing data between groups. As discussed in chapter three, these differences can manifest as greater than 100-fold differences in observed rates of incorporation [100; 137]. Although these differences do not necessarily make one study more or less correct, per se, the use of an agreed upon reference sequence, or series of reference sequences, would aid in comparisons. The use of different sequences can lead to very different conclusions, for example, the characterization of the kinetic contributions to the drug resistance mechanism of M184V. The use of divergent sequences led opposing groups to determine the effect as either decreased rate of incorporation [168; 272] or reduced binding [167]. Interestingly, in these studies only modest differences were observed in

the kinetics of incorporation by WT, making it all the more difficult to assign a particular sequence as the "correct" sequence to be used. My findings that differences in the translocational equilibrium significantly affect kinetic parameters of both nucleotide incorporation and excision would support the use of reference sequences to aid in comparison of results between groups.

Secondly, as it relates to the general mechanisms of nucleotide incorporation and excision, my finding that the majority of sequences exist in the post-translocation conformation supports the primary role of RT as a DNA polymerase. Although the two conformations may freely interconvert when found in the open conformation, the increased proportion of post-translocation complexes, for most sequences, favors nucleotide binding and incorporation over the reverse reaction.

Differences observed between sequences that favor either pre- or post-translocation conformations, specifically with regard to the rate of nucleotide incorporation, suggest that the two conformations may not always interconvert so freely. In chapter three, my findings that post-translocation bias was associated primarily with increased rates of incorporation, rather than improved nucleotide binding, could not immediately be explained by differences in access to the n-site. If the translocational equilibrium were truly kinetically invisible then the process of translocation should not affect the rate of incorporation, which is determined by a conformational change that occurs upon nucleotide binding [107; 112]. I have proposed that the reduced rate of incorporation, observed in the context of pre-translocation bias, could be the result of a second conformational change, that is needed to free a partitioned sub-population of pre-translocation complexes, from the closed to open

configuration, allowing translocation to occur. Support for this model exists in the form of a recently published crystal structure showing a pre-translocation binary complex of RT with the fingers domain in the closed conformation [141] as well as reduced dissociation kinetics associated with pre-translocation complexes, indicating increased complex stability [114].

My observations of decreased rates of incorporation associated with pre-translocation bias may separately be explained by sequence dependent changes within the active site. The apparent requirement of a thymidine at the 3' primer terminus for strong pre-translocation bias lends support to the notion that changes within the active site affecting the translocational equilibrium could also affect the chemistry of incorporation. It is unclear if these changes are related to interactions between RT and the thymidine at the 3' primer terminus or the template adenosine at position n, however. Structure activity relationship experiments with modified substrates will allow for a more detailed assessment of the individual contributions of different contacts, in the absence of crystal structure data of pre- and post-translocation complexes in the appropriate sequence contexts.

Sequence dependant differences within the active site related to the translocational equilibrium, as predicted by this work, could have further consequences with respect to the fidelity of RT. The fidelity of RT was shown to be affected by the use of either RNA or DNA templates, with higher fidelity observed for RNA templates [255]. Fidelity is also affected by the specific sequence used, with high fidelity and low extension efficiency observed at the initiation of (+) strand synthesis [273]. Increased constraints within the active site, in the form of either

modifications to the sugar of the incorporated substrate, or amino acid substitutions at the active site, are also seen to dramatically increase fidelity [163]. I would predict that sequences biased to the pre-translocation conformation, with lower rates of incorporation, would have higher fidelity owing to reduced efficiency of incorporation.

Results presented in chapter three, with respect to the pyrophosphorolytic excision of chain terminating nucleotides by RT, highlight the complementary roles of the pre- and post-translocation conformations of RT with respect to nucleotide incorporation and excision. While the post-translocation conformation favors the incorporation of nucleotides, the pre-translocation conformation is seen to favor the reverse reaction. Similar to incorporation of nucleotides, the effect of translocation bias on the excision reaction is seen in both the catalytic rate and binding affinity of the substrate, in this case PPi. Here, PPi has been used as a tool to probe the functional consequences of the translocational equilibrium, in much the same way that the PPi-analogue PFA was used to explore the effects of the translocational equilibrium in chapter two. With respect to excision-based mechanisms of drug resistance, the biologically relevant substrate is more likely ATP.

The selection of TAMs near the active site of RT, namely M41L, D67N, K70R, L210W, T215Y, T215F, K219Q and K219E leads to the enhancement of the excision of chain terminators, usually AZT, by ATP-mediated excision [242]. The excision of AZT by ATP leads to the production of a dinucleotide tetraphosphate (AZTppppA). The effect of these mutations does not appear to be on the translocational equilibrium, but rather in creating a high-affinity binding site for ATP,

through extensive interactions between primary mutations K70R and T215Y [141]. Crystallographic snap shots of the binding of ATP in the form of the excision product AZTppppA reveals that all of the TAMs, except M41L cluster around the base of the ATP molecule [141]. Results of chapter three relate to the TAMs mechanism of drug resistance by my finding that strong bias toward the pre-translocation conformation is associated with thymidine at the 3' primer terminus. The thymidine moeity of AZT may therefore be involved in promoting the pre-translocation conformation required for the excision reaction. This is supported by previous work that points to the importance of the nucleobase rather than the 3' azido group in conferring resistance via the TAMs mechanism [181].

Additionally, my finding that the presence of a thymidine at the 3' primer terminus is necessary for strong pre-translocation bias would have implications to the suppression of excision by dead-end complex formation (DEC). I observed that both strong pre-translocation bias and mixed translocation states elicited the same effects on the kinetics of PPi-mediated excision, for ddTTP and ddATP substrates, respectively. TAMs do not confer high-level resistance to other NRTIs, which is believed to be due to the formation of DECs at physiological concentrations of nucleotides [102; 182; 187]. While the full benefit of access to the pre-translocation conformation appears to be met by ddATP in the context of mixed translocation bias, increased opportunity for DEC formation would be expected to interfere with excision. This reaction would be predicted, based on previous studies, to be inhibited at lower concentrations of the next nucleotide than the reaction of ddTTP with strong pre-translocation bias [125; 126]. The general mechanism of increased excision efficiency

associated with the pre-translocation conformation can be extended from my work with PPi and would apply in the context of ATP as well.

PPi-mediated excision may also be directly relevant to mechanisms of resistance and NRTI susceptibility in the absence of TAMs. In chapter four I described the mechanism of drug resistance and hypersusceptibility of the novel mutation Q151L to the investigational inhibitor GS-9148 and tenofovir, respectively. Using pre-steady state kinetics, I determined that the mechanism of drug resistance of Q151L to GS-9148 was increased discrimination as a result of reduced binding of the inhibitor. Extremely low levels of incorporation of GS-9148 by Q151L under pre-steady state conditions, preventing a straightforward kinetic analysis, complicated this work. The use of a competition experiment allowed me to overcome this obstacle. By incorporating the natural substrate dATP in the presence of GS-9148, which I knew would not be incorporated, I was able to determine that GS-9148 was not bound unproductively to the active site of the enzyme, as its presence did not interfere with the incorporation of dATP. SAR experiments with modified substrates and modeling, indicate that this mechanism is mediated through a steric clash between the 2' flouro group of GS-9148 and the sidechain of 151L. The mechanism of hypersusceptibility of Q151L to tenofovir was shown by pre-steady state kinetics to not be related to increased incorporation. Instead this mechanism was shown to be related to decreased excision of the inhibitor by Q151L in PPi-mediated excision assays.

As this mechanism involves excision in general and does not involve the high affinity binding of ATP seen in TAMs, the use of either ATP or PPi as an acceptor

substrate would be relevant *in vivo*. The decreased excision of tenofovir by Q151L would lead to hypersusceptibility by increasing the effective inhibition of this NtRTI once incorporated. This is conceptually important for future work involving the study of excision mechanisms by RT. The role or PPi as a substrate for novel mechanisms of resistance or hypersusceptibility based on an excision mechanism should be considered.

The subject of novel mechanisms of hypersusceptibility to inhibitors of RT relates back to my work presented in chapter two. In this chapter I described for the first time, to our knowledge, a mechanism of hypersusceptibility to PFA related to an increase in the proportion of pre-translocation complexes for A62V-containing RTs. This finding was made possible by the use of the robust and highly reproducible site-specific footprinting assay. This technique allowed me to tease out small differences in the translocational equilibrium, related to the presence of the A62V mutation, that were statistically significant. Though these differences were small they were seen to correlate with increased susceptibility to PFA in both binding and filter based IC50 assays. My study of a panel of A62V containing drug resistance-conferring mutations also lead to the identification of additional determinants of the translocational equilibrium that further increased this effect. For example, the presence of V75I, F77L and F116Y in the context of Q151M and A62V led to an additional increase in the proportion of pre-translocation complexes. Of these, it has recently been shown that the V75I mutation exerts a bias toward the pre-translocation conformation in certain mutational backgrounds [150]. Additional studies of the individual contributions of F77L and F116Y are warranted.

Finally, though the common theme of hypersusceptibility to RT inhibitors, seen in both my study of Q151L and tenovir and A62V-containing RTs and PFA, holds clinical promise, this concept should be approached with caution. The introduction of hypersusceptibility to a class of RT inhibitors also imposes a strong selective pressure on the virus toward alternative pathways of resistance. In the context of inhibition of RT by GS-9148, Q151L creates high-level selective inhibition, however, resistance may also be established through a combination of K70E, D123N and T165I [265]. Alternatively, low-level resistance may occur in the presence of the classical Q151M mutation [185]. K70E is shown to be antagonistic to the K65R mutation commonly associated with tenofovir resistance [274], however, resistance to tenofovir is maintained in the context of K70E [135]. The Q151M mutation is not usually associated with cross-resistance to tenofovir, however, recent reports suggest that the addition of K70Q to this complex would expand resistance to include tenofovir [158]. In the context of hypersusceptibility toward PFA, reports of long term PFA use in salvage therapy indicate that extensive remodeling of TAMs leads to the establishment of PFA resistance [217]. In particular this pathway involved the selection of K70G, V75T, K219R and L228R. Although patients in this study did not possess the A62V mutation at baseline, it is conceivable that similar pathways of resistance would develop in that context. It would be interesting to explore the role of these novel mutations on PFA resistance, in terms of potential contributions to the translocational equilibrium or directly related to the binding of the inhibitor.

In conclusion, my work has added to our understanding of molecular determinants and functional consequences of the translocational equilibrium of RT. I

have described a novel mechanism of hypersusceptibility to PFA relating the translocational equilibrium to the closure of the fingers subdomian. This relationship aided in my characterization of the role of the nucleic acid sequence context on translocation, which I have advanced to a level allowing extrapolation beyond the small number of sequences previously described. The possible closure of the fingers domain, as I have proposed relates to the partitioning of a population of binary pre-translocation complexes, opens the door to continued research in this field. Studies of the stability of these complexes in conjunction with SAR experiments designed to probe the effect of a thymidine nucleobase at the 3' primer terminus will expand our understanding of this equilibrium. Lastly, my characterization of the mechanism of resistance of Q151L to the investigational inhibitor GS-9148 serves to inform future developments of NtRTI based therapies.

References

1. World Health Organization, U. A. (2009). Global Summay of the AIDS epidemic.
2. (1981). Kaposi's sarcoma and Pneumocystis pneumonia among homosexual men--New York City and California. *MMWR Morb Mortal Wkly Rep* **30**, 305-8.
3. Barre-Sinoussi, F., Chermann, J. C., Rey, F., Nugeyre, M. T., Chamaret, S., Gruest, J., Dauguet, C., Axler-Blin, C., Vezinet-Brun, F., Rouzioux, C., Rozenbaum, W. & Montagnier, L. (1983). Isolation of a T-lymphotropic retrovirus from a patient at risk for acquired immune deficiency syndrome (AIDS). *Science* **220**, 868-71.
4. Gallo, R. C., Sarin, P. S., Gelmann, E. P., Robert-Guroff, M., Richardson, E., Kalyanaraman, V. S., Mann, D., Sidhu, G. D., Stahl, R. E., Zolla-Pazner, S., Leibowitch, J. & Popovic, M. (1983). Isolation of human T-cell leukemia virus in acquired immune deficiency syndrome (AIDS). *Science* **220**, 865-7.
5. Levy, J. A., Hoffman, A. D., Kramer, S. M., Landis, J. A., Shimabukuro, J. M. & Oshiro, L. S. (1984). Isolation of lymphocytopathic retroviruses from San Francisco patients with AIDS. *Science* **225**, 840-2.
6. Levy, J. A. & Shimabukuro, J. (1985). Recovery of AIDS-associated retroviruses from patients with AIDS or AIDS-related conditions and from clinically healthy individuals. *J Infect Dis* **152**, 734-8.
7. Cihlar, T. & Ray, A. S. (2010). Nucleoside and nucleotide HIV reverse transcriptase inhibitors: 25 years after zidovudine. *Antiviral Res* **85**, 39-58.
8. De Clercq, E. (2009). Anti-HIV drugs: 25 compounds approved within 25 years after the discovery of HIV. *Int J Antimicrob Agents* **33**, 307-20.
9. Fauci, A. S. (2007). 25 years of HIV/AIDS science: reaching the poor with research advances. *Cell* **131**, 429-32.
10. Brinkman, K. & Kakuda, T. N. (2000). Mitochondrial toxicity of nucleoside analogue reverse transcriptase inhibitors: a looming obstacle for long-term antiretroviral therapy? *Curr Opin Infect Dis* **13**, 5-11.
11. Metzger, D. S., Woody, G. E. & O'Brien, C. P. (2010). Drug treatment as HIV prevention: a research update. *Journal of acquired immune deficiency syndromes* **55 Suppl 1**, S32-6.
12. Geocze, L., Mucci, S., De Marco, M. A., Nogueira-Martins, L. A. & Citero Vde, A. (2010). Quality of life and adherence to HAART in HIV-infected patients. *Revista de saude publica* **44**, 743-9.
13. Menendez-Arias, L. (2008). Mechanisms of resistance to nucleoside analogue inhibitors of HIV-1 reverse transcriptase. *Virus Res* **134**, 124-46.
14. Caceres, W., Cruz-Amy, M. & Diaz-Melendez, V. (2010). AIDS-related malignancies: revisited. *P R Health Sci J* **29**, 70-5.
15. Varbanov, M., Espert, L. & Biard-Piechaczyk, M. (2006). Mechanisms of CD4 T-cell depletion triggered by HIV-1 viral proteins. *AIDS Rev* **8**, 221-36.

16. Torres, B. A., Tanabe, T., Subramaniam, P. S., Yamamoto, J. K. & Johnson, H. M. (1998). Mechanism of HIV pathogenesis: role of superantigens in disease. *Alcohol Clin Exp Res* **22**, 188S-192S.
17. Gisselquist, D. (2008). Denialism undermines AIDS prevention in sub-Saharan Africa. *Int J STD AIDS* **19**, 649-55.
18. Chigwedere, P. & Essex, M. (2010). AIDS denialism and public health practice. *AIDS Behav* **14**, 237-47.
19. O'Brien, S. J. & Goedert, J. J. (1996). HIV causes AIDS: Koch's postulates fulfilled. *Curr Opin Immunol* **8**, 613-8.
20. Jaffe, H. W., Darrow, W. W., Echenberg, D. F., O'Malley, P. M., Getchell, J. P., Kalyanaraman, V. S., Byers, R. H., Drennan, D. P., Braff, E. H., Curran, J. W. & et al. (1985). The acquired immunodeficiency syndrome in a cohort of homosexual men. A six-year follow-up study. *Ann Intern Med* **103**, 210-4.
21. Schechter, M. T., Craib, K. J., Gelmon, K. A., Montaner, J. S., Le, T. N. & O'Shaughnessy, M. V. (1993). HIV-1 and the aetiology of AIDS. *Lancet* **341**, 658-9.
22. Mellors, J. W., Munoz, A., Giorgi, J. V., Margolick, J. B., Tassoni, C. J., Gupta, P., Kingsley, L. A., Todd, J. A., Saah, A. J., Detels, R., Phair, J. P. & Rinaldo, C. R., Jr. (1997). Plasma viral load and CD4+ lymphocytes as prognostic markers of HIV-1 infection. *Ann Intern Med* **126**, 946-54.
23. Hammer, S., Crumpacker, C., D'Aquila, R., Jackson, B., Lathey, J., Livnat, D. & Reichelderfer, P. (1993). Use of virologic assays for detection of human immunodeficiency virus in clinical trials: recommendations of the AIDS Clinical Trials Group Virology Committee. *J Clin Microbiol* **31**, 2557-64.
24. Jackson, J. B., Kwok, S. Y., Sninsky, J. J., Hopsicker, J. S., Sannerud, K. J., Rhame, F. S., Henry, K., Simpson, M. & Balfour, H. H., Jr. (1990). Human immunodeficiency virus type 1 detected in all seropositive symptomatic and asymptomatic individuals. *J Clin Microbiol* **28**, 16-9.
25. Reitz, M. S., Jr., Hall, L., Robert-Guroff, M., Lautenberger, J., Hahn, B. M., Shaw, G. M., Kong, L. I., Weiss, S. H., Waters, D., Gallo, R. C. & et al. (1994). Viral variability and serum antibody response in a laboratory worker infected with HIV type 1 (HTLV type IIIB). *AIDS Res Hum Retroviruses* **10**, 1143-55.
26. Weiss, S. H., Goedert, J. J., Gartner, S., Popovic, M., Waters, D., Markham, P., di Marzo Veronese, F., Gail, M. H., Barkley, W. E., Gibbons, J. & et al. (1988). Risk of human immunodeficiency virus (HIV-1) infection among laboratory workers. *Science* **239**, 68-71.
27. Guo, H. G., Chermann, J. C., Waters, D., Hall, L., Louie, A., Gallo, R. C., Streicher, H., Reitz, M. S., Popovic, M. & Blattner, W. (1991). Sequence analysis of original HIV-1. *Nature* **349**, 745-6.
28. Palca, J. (1992). The case of the Florida dentist. *Science* **255**, 392-4.
29. Palca, J. (1992). AIDS. CDC closes the case of the Florida dentist. *Science* **256**, 1130-1.
30. Barnett, S. W., Murthy, K. K., Herndier, B. G. & Levy, J. A. (1994). An AIDS-like condition induced in baboons by HIV-2. *Science* **266**, 642-6.

31. Mosier, D. E., Gulizia, R. J., Baird, S. M. & Wilson, D. B. (1988). Transfer of a functional human immune system to mice with severe combined immunodeficiency. *Nature* **335**, 256-9.
32. Mosier, D. E., Gulizia, R. J., Baird, S. M., Wilson, D. B., Spector, D. H. & Spector, S. A. (1991). Human immunodeficiency virus infection of human-PBL-SCID mice. *Science* **251**, 791-4.
33. Mosier, D. E., Gulizia, R. J., MacIsaac, P. D., Torbett, B. E. & Levy, J. A. (1993). Rapid loss of CD4+ T cells in human-PBL-SCID mice by noncytopathic HIV isolates. *Science* **260**, 689-92.
34. Deane, K. D., Parkhurst, J. O. & Johnston, D. (2010). Linking migration, mobility and HIV. *Trop Med Int Health* **15**, 1458-63.
35. (CDC), C. f. D. C. (2008). www.cdc.gov/hiv.
36. Pierson, T. C. & Doms, R. W. (2003). HIV-1 entry and its inhibition. *Curr Top Microbiol Immunol* **281**, 1-27.
37. Goudsmit, J., Debouck, C., Meloen, R. H., Smit, L., Bakker, M., Asher, D. M., Wolff, A. V., Gibbs, C. J., Jr. & Gajdusek, D. C. (1988). Human immunodeficiency virus type 1 neutralization epitope with conserved architecture elicits early type-specific antibodies in experimentally infected chimpanzees. *Proc Natl Acad Sci U S A* **85**, 4478-82.
38. Granados-Gonzalez, V., Piedrahita, L. D., Martinez, M., Genin, C., Riffard, S. & Urcuqui-Inchima, S. (2009). [Role of the HIV-1 gp120 V1/V2 domains in the induction of neutralizing antibodies]. *Enferm Infecc Microbiol Clin* **27**, 523-30.
39. Capon, D. J. & Ward, R. H. (1991). The CD4-gp120 interaction and AIDS pathogenesis. *Annu Rev Immunol* **9**, 649-78.
40. Berger, E. A., Murphy, P. M. & Farber, J. M. (1999). Chemokine receptors as HIV-1 coreceptors: roles in viral entry, tropism, and disease. *Annu Rev Immunol* **17**, 657-700.
41. Stein, B. S., Gowda, S. D., Lifson, J. D., Penhallow, R. C., Bensch, K. G. & Engleman, E. G. (1987). pH-independent HIV entry into CD4-positive T cells via virus envelope fusion to the plasma membrane. *Cell* **49**, 659-68.
42. Fletcher, C. V. (2003). Enfuvirtide, a new drug for HIV infection. *Lancet* **361**, 1577-8.
43. Dorr, P., Westby, M., Dobbs, S., Griffin, P., Irvine, B., Macartney, M., Mori, J., Rickett, G., Smith-Burchnell, C., Napier, C., Webster, R., Armour, D., Price, D., Stammen, B., Wood, A. & Perros, M. (2005). Maraviroc (UK-427,857), a potent, orally bioavailable, and selective small-molecule inhibitor of chemokine receptor CCR5 with broad-spectrum anti-human immunodeficiency virus type 1 activity. *Antimicrob Agents Chemother* **49**, 4721-32.
44. Soriano, V., Perno, C. F., Kaiser, R., Calvez, V., Gatell, J. M., di Perri, G., Pillay, D., Rockstroh, J. & Geretti, A. M. (2009). When and how to use maraviroc in HIV-infected patients. *AIDS* **23**, 2377-85.
45. Cameron, E. C., Gotte, M., Raney, K.D., Ed. (2009). Viral Genome Replication. University of Arkansas for Medical Sciences, Little Rock, AR: Springer.

46. Heinzinger, N. K., Bukinsky, M. I., Haggerty, S. A., Ragland, A. M., Kewalramani, V., Lee, M. A., Gendelman, H. E., Ratner, L., Stevenson, M. & Emerman, M. (1994). The Vpr protein of human immunodeficiency virus type 1 influences nuclear localization of viral nucleic acids in nondividing host cells. *Proc Natl Acad Sci U S A* **91**, 7311-5.
47. Gallay, P., Swingler, S., Song, J., Bushman, F. & Trono, D. (1995). HIV nuclear import is governed by the phosphotyrosine-mediated binding of matrix to the core domain of integrase. *Cell* **83**, 569-76.
48. Hicks, C. & Gulick, R. M. (2009). Raltegravir: the first HIV type 1 integrase inhibitor. *Clin Infect Dis* **48**, 931-9.
49. Margolis, D. M. (2010). Mechanisms of HIV latency: an emerging picture of complexity. *Curr HIV/AIDS Rep* **7**, 37-43.
50. Ashorn, P., McQuade, T. J., Thaisrivongs, S., Tomasselli, A. G., Tarpley, W. G. & Moss, B. (1990). An inhibitor of the protease blocks maturation of human and simian immunodeficiency viruses and spread of infection. *Proc Natl Acad Sci U S A* **87**, 7472-6.
51. De Clercq, E. (2010). Antiretroviral drugs. *Curr Opin Pharmacol*.
52. McKeage, K. & Scott, L. J. (2010). Darunavir: in treatment-experienced pediatric patients with HIV-1 infection. *Paediatr Drugs* **12**, 123-31.
53. Miller, M., Jaskolski, M., Rao, J. K., Leis, J. & Wlodawer, A. (1989). Crystal structure of a retroviral protease proves relationship to aspartic protease family. *Nature* **337**, 576-9.
54. Blair, W. S., Pickford, C., Irving, S. L., Brown, D. G., Anderson, M., Bazin, R., Cao, J., Ciaramella, G., Isaacson, J., Jackson, L., Hunt, R., Kjerrstrom, A., Nieman, J. A., Patick, A. K., Perros, M., Scott, A. D., Whitby, K., Wu, H. & Butler, S. L. (2010). HIV capsid is a tractable target for small molecule therapeutic intervention. *PLoS Pathog* **6**, e1001220.
55. Muesing, M. A., Smith, D. H., Cabradilla, C. D., Benton, C. V., Lasky, L. A. & Capon, D. J. (1985). Nucleic acid structure and expression of the human AIDS/lymphadenopathy retrovirus. *Nature* **313**, 450-8.
56. Bryant, M. & Ratner, L. (1990). Myristoylation-dependent replication and assembly of human immunodeficiency virus 1. *Proc Natl Acad Sci U S A* **87**, 523-7.
57. Gottlinger, H. G., Sodroski, J. G. & Haseltine, W. A. (1989). Role of capsid precursor processing and myristoylation in morphogenesis and infectivity of human immunodeficiency virus type 1. *Proc Natl Acad Sci U S A* **86**, 5781-5.
58. Harrison, G. P. & Lever, A. M. (1992). The human immunodeficiency virus type 1 packaging signal and major splice donor region have a conserved stable secondary structure. *J Virol* **66**, 4144-53.
59. Lapadat-Tapolsky, M., De Rocquigny, H., Van Gent, D., Roques, B., Plasterk, R. & Darlix, J. L. (1993). Interactions between HIV-1 nucleocapsid protein and viral DNA may have important functions in the viral life cycle. *Nucleic Acids Res* **21**, 831-9.
60. Levin, J. G., Mitra, M., Mascarenhas, A. & Musier-Forsyth, K. (2010). Role of HIV-1 nucleocapsid protein in HIV-1 reverse transcription. *RNA Biol* **7**.

61. Paxton, W., Connor, R. I. & Landau, N. R. (1993). Incorporation of Vpr into human immunodeficiency virus type 1 virions: requirement for the p6 region of gag and mutational analysis. *J Virol* **67**, 7229-37.
62. Jacks, T., Power, M. D., Masiarz, F. R., Luciw, P. A., Barr, P. J. & Varmus, H. E. (1988). Characterization of ribosomal frameshifting in HIV-1 gag-pol expression. *Nature* **331**, 280-3.
63. Hwang, S. S., Boyle, T. J., Lyerly, H. K. & Cullen, B. R. (1991). Identification of the envelope V3 loop as the primary determinant of cell tropism in HIV-1. *Science* **253**, 71-4.
64. Geijtenbeek, T. B., Kwon, D. S., Torensma, R., van Vliet, S. J., van Duijnhoven, G. C., Middel, J., Cornelissen, I. L., Nottet, H. S., KewalRamani, V. N., Littman, D. R., Figdor, C. G. & van Kooyk, Y. (2000). DC-SIGN, a dendritic cell-specific HIV-1-binding protein that enhances trans-infection of T cells. *Cell* **100**, 587-97.
65. Ruben, S., Perkins, A., Purcell, R., Joung, K., Sia, R., Burghoff, R., Haseltine, W. A. & Rosen, C. A. (1989). Structural and functional characterization of human immunodeficiency virus tat protein. *J Virol* **63**, 1-8.
66. Roy, S., Delling, U., Chen, C. H., Rosen, C. A. & Sonenberg, N. (1990). A bulge structure in HIV-1 TAR RNA is required for Tat binding and Tat-mediated trans-activation. *Genes Dev* **4**, 1365-73.
67. Feinberg, M. B., Baltimore, D. & Frankel, A. D. (1991). The role of Tat in the human immunodeficiency virus life cycle indicates a primary effect on transcriptional elongation. *Proc Natl Acad Sci U S A* **88**, 4045-9.
68. Zapp, M. L. & Green, M. R. (1989). Sequence-specific RNA binding by the HIV-1 Rev protein. *Nature* **342**, 714-6.
69. Kim, S. Y., Byrn, R., Groopman, J. & Baltimore, D. (1989). Temporal aspects of DNA and RNA synthesis during human immunodeficiency virus infection: evidence for differential gene expression. *J Virol* **63**, 3708-13.
70. Malim, M. H., Hauber, J., Le, S. Y., Maizel, J. V. & Cullen, B. R. (1989). The HIV-1 rev trans-activator acts through a structured target sequence to activate nuclear export of unspliced viral mRNA. *Nature* **338**, 254-7.
71. Felber, B. K., Drysdale, C. M. & Pavlakis, G. N. (1990). Feedback regulation of human immunodeficiency virus type 1 expression by the Rev protein. *J Virol* **64**, 3734-41.
72. Hope, T. J., McDonald, D., Huang, X. J., Low, J. & Parslow, T. G. (1990). Mutational analysis of the human immunodeficiency virus type 1 Rev transactivator: essential residues near the amino terminus. *Journal of virology* **64**, 5360-6.
73. Zapp, M. L., Hope, T. J., Parslow, T. G. & Green, M. R. (1991). Oligomerization and RNA binding domains of the type 1 human immunodeficiency virus Rev protein: a dual function for an arginine-rich binding motif. *Proc Natl Acad Sci U S A* **88**, 7734-8.
74. Wen, W., Meinkoth, J. L., Tsien, R. Y. & Taylor, S. S. (1995). Identification of a signal for rapid export of proteins from the nucleus. *Cell* **82**, 463-73.

75. Fischer, U., Huber, J., Boelens, W. C., Mattaj, I. W. & Luhrmann, R. (1995). The HIV-1 Rev activation domain is a nuclear export signal that accesses an export pathway used by specific cellular RNAs. *Cell* **82**, 475-83.
76. Aiken, C., Konner, J., Landau, N. R., Lenburg, M. E. & Trono, D. (1994). Nef induces CD4 endocytosis: requirement for a critical dileucine motif in the membrane-proximal CD4 cytoplasmic domain. *Cell* **76**, 853-64.
77. Garcia, J. V. & Miller, A. D. (1992). Downregulation of cell surface CD4 by nef. *Res Virol* **143**, 52-5.
78. Goldsmith, M. A., Warmerdam, M. T., Atchison, R. E., Miller, M. D. & Greene, W. C. (1995). Dissociation of the CD4 downregulation and viral infectivity enhancement functions of human immunodeficiency virus type 1 Nef. *J Virol* **69**, 4112-21.
79. Lama, J., Mangasarian, A. & Trono, D. (1999). Cell-surface expression of CD4 reduces HIV-1 infectivity by blocking Env incorporation in a Nef- and Vpu-inhibitable manner. *Curr Biol* **9**, 622-31.
80. Schwartz, O., Marechal, V., Le Gall, S., Lemonnier, F. & Heard, J. M. (1996). Endocytosis of major histocompatibility complex class I molecules is induced by the HIV-1 Nef protein. *Nat Med* **2**, 338-42.
81. Baur, A. S., Sawai, E. T., Dazin, P., Fantl, W. J., Cheng-Mayer, C. & Peterlin, B. M. (1994). HIV-1 Nef leads to inhibition or activation of T cells depending on its intracellular localization. *Immunity* **1**, 373-84.
82. Vodicka, M. A., Koepp, D. M., Silver, P. A. & Emerman, M. (1998). HIV-1 Vpr interacts with the nuclear transport pathway to promote macrophage infection. *Genes Dev* **12**, 175-85.
83. Schwartz, S., Felber, B. K., Fenyo, E. M. & Pavlakis, G. N. (1990). Env and Vpu proteins of human immunodeficiency virus type 1 are produced from multiple bicistronic mRNAs. *J Virol* **64**, 5448-56.
84. Neil, S. J., Zang, T. & Bieniasz, P. D. (2008). Tetherin inhibits retrovirus release and is antagonized by HIV-1 Vpu. *Nature* **451**, 425-30.
85. Schubert, U., Bour, S., Ferrer-Montiel, A. V., Montal, M., Maldarell, F. & Strebel, K. (1996). The two biological activities of human immunodeficiency virus type 1 Vpu protein involve two separable structural domains. *J Virol* **70**, 809-19.
86. Willey, R. L., Maldarelli, F., Martin, M. A. & Strebel, K. (1992). Human immunodeficiency virus type 1 Vpu protein induces rapid degradation of CD4. *J Virol* **66**, 7193-200.
87. Klimkait, T., Strebel, K., Hoggan, M. D., Martin, M. A. & Orenstein, J. M. (1990). The human immunodeficiency virus type 1-specific protein vpu is required for efficient virus maturation and release. *J Virol* **64**, 621-9.
88. Strebel, K., Daugherty, D., Clouse, K., Cohen, D., Folks, T. & Martin, M. A. (1987). The HIV 'A' (sor) gene product is essential for virus infectivity. *Nature* **328**, 728-30.
89. Romani, B., Engelbrecht, S. & Glashoff, R. H. (2009). Antiviral roles of APOBEC proteins against HIV-1 and suppression by Vif. *Arch Virol* **154**, 1579-88.

90. Schwartz, S., Felber, B. K., Benko, D. M., Fenyo, E. M. & Pavlakis, G. N. (1990). Cloning and functional analysis of multiply spliced mRNA species of human immunodeficiency virus type 1. *J Virol* **64**, 2519-29.
91. Hope, T. J. & Trono, D. (2000). HIV InSite Knowledge Base Chapter, Structure, Expression, and Regulation of the HIV Geneome, Vol. 2011.
92. Jonckheere, H., Anne, J. & De Clercq, E. (2000). The HIV-1 reverse transcription (RT) process as target for RT inhibitors. *Med Res Rev* **20**, 129-54.
93. Nabel, G. & Baltimore, D. (1987). An inducible transcription factor activates expression of human immunodeficiency virus in T cells. *Nature* **326**, 711-3.
94. Garcia, J. A., Harrich, D., Soultanakis, E., Wu, F., Mitsuyasu, R. & Gaynor, R. B. (1989). Human immunodeficiency virus type 1 LTR TATA and TAR region sequences required for transcriptional regulation. *EMBO J* **8**, 765-78.
95. Karn, J. (2011). The molecular biology of HIV latency: breaking and restoring the Tat-dependent transcriptional circuit. *Current opinion in HIV and AIDS* **6**, 4-11.
96. Kao, S. Y., Calman, A. F., Luciw, P. A. & Peterlin, B. M. (1987). Anti-termination of transcription within the long terminal repeat of HIV-1 by tat gene product. *Nature* **330**, 489-93.
97. Schwartz, S., Felber, B. K. & Pavlakis, G. N. (1992). Mechanism of translation of monocistronic and multicistronic human immunodeficiency virus type 1 mRNAs. *Mol Cell Biol* **12**, 207-19.
98. Martin, J. C., Hitchcock, M. J., De Clercq, E. & Prusoff, W. H. (2010). Early nucleoside reverse transcriptase inhibitors for the treatment of HIV: a brief history of stavudine (D4T) and its comparison with other dideoxynucleosides. *Antiviral research* **85**, 34-8.
99. Rittinger, K., Divita, G. & Goody, R. S. (1995). Human immunodeficiency virus reverse transcriptase substrate-induced conformational changes and the mechanism of inhibition by nonnucleoside inhibitors. *Proc Natl Acad Sci U S A* **92**, 8046-9.
100. Spence, R. A., Kati, W. M., Anderson, K. S. & Johnson, K. A. (1995). Mechanism of inhibition of HIV-1 reverse transcriptase by nonnucleoside inhibitors. *Science* **267**, 988-93.
101. Arion, D., Kaushik, N., McCormick, S., Borkow, G. & Parniak, M. A. (1998). Phenotypic mechanism of HIV-1 resistance to 3'-azido-3'-deoxythymidine (AZT): increased polymerization processivity and enhanced sensitivity to pyrophosphate of the mutant viral reverse transcriptase. *Biochemistry* **37**, 15908-17.
102. Meyer, P. R., Matsuura, S. E., So, A. G. & Scott, W. A. (1998). Unblocking of chain-terminated primer by HIV-1 reverse transcriptase through a nucleotide-dependent mechanism. *Proc Natl Acad Sci U S A* **95**, 13471-6.
103. Jochmans, D., Deval, J., Kesteleyn, B., Van Marck, H., Bettens, E., De Baere, I., Dehertogh, P., Ivens, T., Van Ginderen, M., Van Schoubroeck, B., Ehteshami, M., Wigerinck, P., Gotte, M. & Hertogs, K. (2006). Indolopyridones inhibit human immunodeficiency virus reverse transcriptase with a novel mechanism of action. *J Virol* **80**, 12283-92.

104. Marchand, B., Tchesnokov, E. P. & Gotte, M. (2007). The pyrophosphate analogue foscarnet traps the pre-translocational state of HIV-1 reverse transcriptase in a Brownian ratchet model of polymerase translocation. *J Biol Chem* **282**, 3337-46.
105. Kohlstaedt, L. A., Wang, J., Friedman, J. M., Rice, P. A. & Steitz, T. A. (1992). Crystal structure at 3.5 A resolution of HIV-1 reverse transcriptase complexed with an inhibitor. *Science* **256**, 1783-90.
106. Beilhartz, G. L., Wendeler, M., Baichoo, N., Rausch, J., Le Grice, S. & Gotte, M. (2009). HIV-1 reverse transcriptase can simultaneously engage its DNA/RNA substrate at both DNA polymerase and RNase H active sites: implications for RNase H inhibition. *J Mol Biol* **388**, 462-74.
107. Huang, H., Chopra, R., Verdine, G. L. & Harrison, S. C. (1998). Structure of a covalently trapped catalytic complex of HIV-1 reverse transcriptase: implications for drug resistance. *Science* **282**, 1669-75.
108. Kaushik, N., Harris, D., Rege, N., Modak, M. J., Yadav, P. N. & Pandey, V. N. (1997). Role of glutamine-151 of human immunodeficiency virus type-1 reverse transcriptase in RNA-directed DNA synthesis. *Biochemistry* **36**, 14430-8.
109. Liu, S., Abbondanzieri, E. A., Rausch, J. W., Le Grice, S. F. & Zhuang, X. (2008). Slide into action: dynamic shuttling of HIV reverse transcriptase on nucleic acid substrates. *Science* **322**, 1092-7.
110. Steitz, T. A. (1998). A mechanism for all polymerases. *Nature* **391**, 231-2.
111. Steitz, T. A. (1999). DNA polymerases: structural diversity and common mechanisms. *J Biol Chem* **274**, 17395-8.
112. Kati, W. M., Johnson, K. A., Jerva, L. F. & Anderson, K. S. (1992). Mechanism and fidelity of HIV reverse transcriptase. *J Biol Chem* **267**, 25988-97.
113. Wohrl, B. M., Krebs, R., Goody, R. S. & Restle, T. (1999). Refined model for primer/template binding by HIV-1 reverse transcriptase: pre-steady-state kinetic analyses of primer/template binding and nucleotide incorporation events distinguish between different binding modes depending on the nature of the nucleic acid substrate. *J Mol Biol* **292**, 333-44.
114. Ignatov, M. E., Berdis, A. J., Le Grice, S. F. & Barkley, M. D. (2005). Attenuation of DNA replication by HIV-1 reverse transcriptase near the central termination sequence. *Biochemistry* **44**, 5346-56.
115. Ding, J., Das, K., Hsiou, Y., Sarafianos, S. G., Clark, A. D., Jr., Jacobo-Molina, A., Tantillo, C., Hughes, S. H. & Arnold, E. (1998). Structure and functional implications of the polymerase active site region in a complex of HIV-1 RT with a double-stranded DNA template-primer and an antibody Fab fragment at 2.8 A resolution. *J Mol Biol* **284**, 1095-111.
116. Patel, P. H., Jacobo-Molina, A., Ding, J., Tantillo, C., Clark, A. D., Jr., Raag, R., Nanni, R. G., Hughes, S. H. & Arnold, E. (1995). Insights into DNA polymerization mechanisms from structure and function analysis of HIV-1 reverse transcriptase. *Biochemistry* **34**, 5351-63.
117. Li, Y., Korolev, S. & Waksman, G. (1998). Crystal structures of open and closed forms of binary and ternary complexes of the large fragment of

Thermus aquaticus DNA polymerase I: structural basis for nucleotide incorporation. *EMBO J* **17**, 7514-25.
118. Yin, Y. W. & Steitz, T. A. (2004). The structural mechanism of translocation and helicase activity in T7 RNA polymerase. *Cell* **116**, 393-404.
119. Gnatt, A. L., Cramer, P., Fu, J., Bushnell, D. A. & Kornberg, R. D. (2001). Structural basis of transcription: an RNA polymerase II elongation complex at 3.3 A resolution. *Science* **292**, 1876-82.
120. Gong, X. Q., Zhang, C., Feig, M. & Burton, Z. F. (2005). Dynamic error correction and regulation of downstream bubble opening by human RNA polymerase II. *Mol Cell* **18**, 461-70.
121. Bar-Nahum, G., Epshtein, V., Ruckenstein, A. E., Rafikov, R., Mustaev, A. & Nudler, E. (2005). A ratchet mechanism of transcription elongation and its control. *Cell* **120**, 183-93.
122. Foster, J. E., Holmes, S. F. & Erie, D. A. (2001). Allosteric binding of nucleoside triphosphates to RNA polymerase regulates transcription elongation. *Cell* **106**, 243-52.
123. Sarafianos, S. G., Clark, A. D., Jr., Das, K., Tuske, S., Birktoft, J. J., Ilankumaran, P., Ramesha, A. R., Sayer, J. M., Jerina, D. M., Boyer, P. L., Hughes, S. H. & Arnold, E. (2002). Structures of HIV-1 reverse transcriptase with pre- and post-translocation AZTMP-terminated DNA. *EMBO J* **21**, 6614-24.
124. Rothwell, P. J., Berger, S., Kensch, O., Felekyan, S., Antonik, M., Wohrl, B. M., Restle, T., Goody, R. S. & Seidel, C. A. (2003). Multiparameter single-molecule fluorescence spectroscopy reveals heterogeneity of HIV-1 reverse transcriptase:primer/template complexes. *Proc Natl Acad Sci U S A* **100**, 1655-60.
125. Marchand, B. & Gotte, M. (2003). Site-specific footprinting reveals differences in the translocation status of HIV-1 reverse transcriptase. Implications for polymerase translocation and drug resistance. *J Biol Chem* **278**, 35362-72.
126. Marchand, B., White, K. L., Ly, J. K., Margot, N. A., Wang, R., McDermott, M., Miller, M. D. & Gotte, M. (2007). Effects of the translocation status of human immunodeficiency virus type 1 reverse transcriptase on the efficiency of excision of tenofovir. *Antimicrob Agents Chemother* **51**, 2911-9.
127. Meyer, P. R., Rutvisuttinunt, W., Matsuura, S. E., So, A. G. & Scott, W. A. (2007). Stable complexes formed by HIV-1 reverse transcriptase at distinct positions on the primer-template controlled by binding deoxynucleoside triphosphates or foscarnet. *J Mol Biol* **369**, 41-54.
128. Gotte, M., Maier, G., Gross, H. J. & Heumann, H. (1998). Localization of the active site of HIV-1 reverse transcriptase-associated RNase H domain on a DNA template using site-specific generated hydroxyl radicals. *J Biol Chem* **273**, 10139-46.
129. Gao, H. Q., Boyer, P. L., Sarafianos, S. G., Arnold, E. & Hughes, S. H. (2000). The role of steric hindrance in 3TC resistance of human immunodeficiency virus type-1 reverse transcriptase. *J Mol Biol* **300**, 403-18.

130. Valer, L., Martin-Carbonero, L., de Mendoza, C., Corral, A. & Soriano, V. (2004). Predictors of selection of K65R: tenofovir use and lack of thymidine analogue mutations. *AIDS* **18**, 2094-6.
131. White, K. L., Margot, N. A., Ly, J. K., Chen, J. M., Ray, A. S., Pavelko, M., Wang, R., McDermott, M., Swaminathan, S. & Miller, M. D. (2005). A combination of decreased NRTI incorporation and decreased excision determines the resistance profile of HIV-1 K65R RT. *AIDS* **19**, 1751-60.
132. Selmi, B., Boretto, J., Sarfati, S. R., Guerreiro, C. & Canard, B. (2001). Mechanism-based suppression of dideoxynucleotide resistance by K65R human immunodeficiency virus reverse transcriptase using an alpha-boranophosphate nucleoside analogue. *J Biol Chem* **276**, 48466-72.
133. Deval, J., White, K. L., Miller, M. D., Parkin, N. T., Courcambeck, J., Halfon, P., Selmi, B., Boretto, J. & Canard, B. (2004). Mechanistic basis for reduced viral and enzymatic fitness of HIV-1 reverse transcriptase containing both K65R and M184V mutations. *J Biol Chem* **279**, 509-16.
134. Feng, J. Y., Myrick, F. T., Margot, N. A., Mulamba, G. B., Rimsky, L., Borroto-Esoda, K., Selmi, B. & Canard, B. (2006). Virologic and enzymatic studies revealing the mechanism of K65R- and Q151M-associated HIV-1 drug resistance towards emtricitabine and lamivudine. *Nucleosides Nucleotides Nucleic Acids* **25**, 89-107.
135. Sluis-Cremer, N., Sheen, C. W., Zelina, S., Torres, P. S., Parikh, U. M. & Mellors, J. W. (2007). Molecular mechanism by which the K70E mutation in human immunodeficiency virus type 1 reverse transcriptase confers resistance to nucleoside reverse transcriptase inhibitors. *Antimicrob Agents Chemother* **51**, 48-53.
136. Parikh, U. M., Zelina, S., Sluis-Cremer, N. & Mellors, J. W. (2007). Molecular mechanisms of bidirectional antagonism between K65R and thymidine analog mutations in HIV-1 reverse transcriptase. *AIDS* **21**, 1405-14.
137. Svarovskaia, E. S., Feng, J. Y., Margot, N. A., Myrick, F., Goodman, D., Ly, J. K., White, K. L., Kutty, N., Wang, R., Borroto-Esoda, K. & Miller, M. D. (2008). The A62V and S68G Mutations in HIV-1 Reverse Transcriptase Partially Restore the Replication Defect Associated With the K65R Mutation. *J Acquir Immune Defic Syndr* **48**, 428-36.
138. Frangeul, A., Bussetta, C., Deval, J., Barral, K., Alvarez, K. & Canard, B. (2008). Gln151 of HIV-1 reverse transcriptase acts as a steric gate towards clinically relevant acyclic phosphonate nucleotide analogues. *Antivir Ther* **13**, 115-24.
139. K Das, X. T., R Bandwar, S Sarafianos, S Tuske, P Boyer, K White, M Miller, S Hughes, E Arnold. (2009). Structural Basis for HIV-1 Reverse Transcriptase Drug Resistance to Zidovudine and Tenofovir. In *CROI*, Vol. 67, Boston, MA.
140. Delaugerre, C., Flandre, P., Marcelin, A. G., Descamps, D., Tamalet, C., Cottalorda, J., Schneider, V., Yerly, S., LeGoff, J., Morand-Joubert, L., Chaix, M. L., Costagliola, D. & Calvez, V. (2008). National survey of the prevalence

and conditions of selection of HIV-1 reverse transcriptase K70E mutation. *J Med Virol* **80**, 762-5.
141. Tu, X., Das, K., Han, Q., Bauman, J. D., Clark, A. D., Jr., Hou, X., Frenkel, Y. V., Gaffney, B. L., Jones, R. A., Boyer, P. L., Hughes, S. H., Sarafianos, S. G. & Arnold, E. (2010). Structural basis of HIV-1 resistance to AZT by excision. *Nat Struct Mol Biol* **17**, 1202-9.
142. McColl, D. J., Chappey, C., Parkin, N. T. & Miller, M. D. (2008). Prevalence, genotypic associations and phenotypic characterization of K65R, L74V and other HIV-1 RT resistance mutations in a commercial database. *Antivir Ther* **13**, 189-97.
143. Margot, N. A., Lu, B., Cheng, A. & Miller, M. D. (2006). Resistance development over 144 weeks in treatment-naive patients receiving tenofovir disoproxil fumarate or stavudine with lamivudine and efavirenz in Study 903. *HIV Med* **7**, 442-50.
144. Deval, J., Navarro, J. M., Selmi, B., Courcambeck, J., Boretto, J., Halfon, P., Garrido-Urbani, S., Sire, J. & Canard, B. (2004). A loss of viral replicative capacity correlates with altered DNA polymerization kinetics by the human immunodeficiency virus reverse transcriptase bearing the K65R and L74V dideoxynucleoside resistance substitutions. *J Biol Chem* **279**, 25489-96.
145. Miranda, L. R., Gotte, M., Liang, F. & Kuritzkes, D. R. (2005). The L74V mutation in human immunodeficiency virus type 1 reverse transcriptase counteracts enhanced excision of zidovudine monophosphate associated with thymidine analog resistance mutations. *Antimicrob Agents Chemother* **49**, 2648-56.
146. Frankel, F. A., Marchand, B., Turner, D., Gotte, M. & Wainberg, M. A. (2005). Impaired rescue of chain-terminated DNA synthesis associated with the L74V mutation in human immunodeficiency virus type 1 reverse transcriptase. *Antimicrob Agents Chemother* **49**, 2657-64.
147. McMahon, M. A., Siliciano, J. D., Lai, J., Liu, J. O., Stivers, J. T., Siliciano, R. F. & Kohli, R. M. (2008). The antiherpetic drug acyclovir inhibits HIV replication and selects the V75I reverse transcriptase multidrug resistance mutation. *J Biol Chem* **283**, 31289-93.
148. Ueno, T., Shirasaka, T. & Mitsuya, H. (1995). Enzymatic characterization of human immunodeficiency virus type 1 reverse transcriptase resistant to multiple 2',3'-dideoxynucleoside 5'-triphosphates. *J Biol Chem* **270**, 23605-11.
149. Feng, J. Y., Myrick, F., Selmi, B., Deval, J., Canard, B. & Borroto-Esoda, K. (2005). Effects of HIV Q151M-associated multi-drug resistance mutations on the activities of (-)-beta-D-1',3'-dioxolan guanine. *Antiviral Res* **66**, 153-8.
150. Matamoros, T., Nevot, M., Martinez, M. A. & Menendez-Arias, L. (2009). Thymidine analogue resistance suppression by V75I of HIV-1 reverse transcriptase: effects of substituting valine 75 on stavudine excision and discrimination. *J Biol Chem* **284**, 32792-802.
151. Tchesnokov, E. P., Obikhod, A., Massud, I., Lisco, A., Vanpouille, C., Brichacek, B., Balzarini, J., McGuigan, C., Derudas, M., Margolis, L., Schinazi, R. F. & Gotte, M. (2009). Mechanisms associated with HIV-1

resistance to acyclovir by the V75I mutation in reverse transcriptase. *J Biol Chem* **284**, 21496-504.
152. Lacey, S. F. & Larder, B. A. (1994). Novel mutation (V75T) in human immunodeficiency virus type 1 reverse transcriptase confers resistance to 2',3'-didehydro-2',3'-dideoxythymidine in cell culture. *Antimicrob Agents Chemother* **38**, 1428-32.
153. Selmi, B., Boretto, J., Navarro, J. M., Sire, J., Longhi, S., Guerreiro, C., Mulard, L., Sarfati, S. & Canard, B. (2001). The valine-to-threonine 75 substitution in human immunodeficiency virus type 1 reverse transcriptase and its relation with stavudine resistance. *J Biol Chem* **276**, 13965-74.
154. Maeda, Y., Venzon, D. J. & Mitsuya, H. (1998). Altered drug sensitivity, fitness, and evolution of human immunodeficiency virus type 1 with pol gene mutations conferring multi-dideoxynucleoside resistance. *J Infect Dis* **177**, 1207-13.
155. Kosalaraksa, P., Kavlick, M. F., Maroun, V., Le, R. & Mitsuya, H. (1999). Comparative fitness of multi-dideoxynucleoside-resistant human immunodeficiency virus type 1 (HIV-1) in an In vitro competitive HIV-1 replication assay. *J Virol* **73**, 5356-63.
156. Deval, J., Selmi, B., Boretto, J., Egloff, M. P., Guerreiro, C., Sarfati, S. & Canard, B. (2002). The molecular mechanism of multidrug resistance by the Q151M human immunodeficiency virus type 1 reverse transcriptase and its suppression using alpha-boranophosphate nucleotide analogues. *J Biol Chem* **277**, 42097-104.
157. Garcia-Lerma, J. G., Gerrish, P. J., Wright, A. C., Qari, S. H. & Heneine, W. (2000). Evidence of a role for the Q151L mutation and the viral background in development of multiple dideoxynucleoside-resistant human immunodeficiency virus type 1. *J Virol* **74**, 9339-46.
158. Hachiya, A., Kodama, E. N., Schuckmann, M. M., Kirby, K. A., Michailidis, E., Sakagami, Y., Oka, S., Singh, K. & Sarafianos, S. G. (2011). K70Q Adds High-Level Tenofovir Resistance to "Q151M Complex" HIV Reverse Transcriptase through the Enhanced Discrimination Mechanism. *PLoS One* **6**, e16242.
159. Catucci, M., Venturi, G., Romano, L., Riccio, M. L., De Milito, A., Valensin, P. E. & Zazzi, M. (1999). Development and significance of the HIV-1 reverse transcriptase M184V mutation during combination therapy with lamivudine, zidovudine, and protease inhibitors. *J Acquir Immune Defic Syndr* **21**, 203-8.
160. Miller, V., Ait-Khaled, M., Stone, C., Griffin, P., Mesogiti, D., Cutrell, A., Harrigan, R., Staszewski, S., Katlama, C., Pearce, G. & Tisdale, M. (2000). HIV-1 reverse transcriptase (RT) genotype and susceptibility to RT inhibitors during abacavir monotherapy and combination therapy. *AIDS* **14**, 163-71.
161. Kawamoto, A., Kodama, E., Sarafianos, S. G., Sakagami, Y., Kohgo, S., Kitano, K., Ashida, N., Iwai, Y., Hayakawa, H., Nakata, H., Mitsuya, H., Arnold, E. & Matsuoka, M. (2008). 2'-deoxy-4'-C-ethynyl-2-halo-adenosines active against drug-resistant human immunodeficiency virus type 1 variants. *Int J Biochem Cell Biol* **40**, 2410-20.

162. Pandey, V. N., Kaushik, N., Rege, N., Sarafianos, S. G., Yadav, P. N. & Modak, M. J. (1996). Role of methionine 184 of human immunodeficiency virus type-1 reverse transcriptase in the polymerase function and fidelity of DNA synthesis. *Biochemistry* **35**, 2168-79.
163. Cramer, J., Strerath, M., Marx, A. & Restle, T. (2002). Exploring the effects of active site constraints on HIV-1 reverse transcriptase DNA polymerase fidelity. *J Biol Chem* **277**, 43593-8.
164. Turner, D., Brenner, B. G., Routy, J. P., Petrella, M. & Wainberg, M. A. (2004). Rationale for maintenance of the M184v resistance mutation in human immunodeficiency virus type 1 reverse transcriptase in treatment experienced patients. *The new microbiologica : official journal of the Italian Society for Medical, Odontoiatric, and Clinical Microbiology* **27**, 31-9.
165. Petrella, M. & Wainberg, M. A. (2002). Might the M184V substitution in HIV-1 RT confer clinical benefit? *AIDS reviews* **4**, 224-32.
166. Feng, J. Y. & Anderson, K. S. (1999). Mechanistic studies comparing the incorporation of (+) and (-) isomers of 3TCTP by HIV-1 reverse transcriptase. *Biochemistry* **38**, 55-63.
167. Wilson, J. E., Aulabaugh, A., Caligan, B., McPherson, S., Wakefield, J. K., Jablonski, S., Morrow, C. D., Reardon, J. E. & Furman, P. A. (1996). Human immunodeficiency virus type-1 reverse transcriptase. Contribution of Met-184 to binding of nucleoside 5'-triphosphate. *J Biol Chem* **271**, 13656-62.
168. Krebs, R., Immendorfer, U., Thrall, S. H., Wohrl, B. M. & Goody, R. S. (1997). Single-step kinetics of HIV-1 reverse transcriptase mutants responsible for virus resistance to nucleoside inhibitors zidovudine and 3-TC. *Biochemistry* **36**, 10292-300.
169. Kellam, P., Boucher, C. A. & Larder, B. A. (1992). Fifth mutation in human immunodeficiency virus type 1 reverse transcriptase contributes to the development of high-level resistance to zidovudine. *Proc Natl Acad Sci U S A* **89**, 1934-8.
170. Hooker, D. J., Tachedjian, G., Solomon, A. E., Gurusinghe, A. D., Land, S., Birch, C., Anderson, J. L., Roy, B. M., Arnold, E. & Deacon, N. J. (1996). An in vivo mutation from leucine to tryptophan at position 210 in human immunodeficiency virus type 1 reverse transcriptase contributes to high-level resistance to 3'-azido-3'-deoxythymidine. *J Virol* **70**, 8010-8.
171. Boucher, C. A., O'Sullivan, E., Mulder, J. W., Ramautarsing, C., Kellam, P., Darby, G., Lange, J. M., Goudsmit, J. & Larder, B. A. (1992). Ordered appearance of zidovudine resistance mutations during treatment of 18 human immunodeficiency virus-positive subjects. *J Infect Dis* **165**, 105-10.
172. Larder, B. A. & Kemp, S. D. (1989). Multiple mutations in HIV-1 reverse transcriptase confer high-level resistance to zidovudine (AZT). *Science* **246**, 1155-8.
173. Richman, D. D., Guatelli, J. C., Grimes, J., Tsiatis, A. & Gingeras, T. (1991). Detection of mutations associated with zidovudine resistance in human immunodeficiency virus by use of the polymerase chain reaction. *J Infect Dis* **164**, 1075-81.

174. St Clair, M. H., Martin, J. L., Tudor-Williams, G., Bach, M. C., Vavro, C. L., King, D. M., Kellam, P., Kemp, S. D. & Larder, B. A. (1991). Resistance to ddI and sensitivity to AZT induced by a mutation in HIV-1 reverse transcriptase. *Science* **253**, 1557-9.
175. Lafeuillade, A. & Tardy, J. C. (2003). Stavudine in the face of cross-resistance between HIV-1 nucleoside reverse transcriptase inhibitors: a review. *AIDS Rev* **5**, 80-6.
176. Boyer, P. L., Sarafianos, S. G., Arnold, E. & Hughes, S. H. (2001). Selective excision of AZTMP by drug-resistant human immunodeficiency virus reverse transcriptase. *J Virol* **75**, 4832-42.
177. Dharmasena, S., Pongracz, Z., Arnold, E., Sarafianos, S. G. & Parniak, M. A. (2007). 3'-Azido-3'-deoxythymidine-(5')-tetraphospho-(5')-adenosine, the product of ATP-mediated excision of chain-terminating AZTMP, is a potent chain-terminating substrate for HIV-1 reverse transcriptase. *Biochemistry* **46**, 828-36.
178. Ray, A. S., Murakami, E., Basavapathruni, A., Vaccaro, J. A., Ulrich, D., Chu, C. K., Schinazi, R. F. & Anderson, K. S. (2003). Probing the molecular mechanisms of AZT drug resistance mediated by HIV-1 reverse transcriptase using a transient kinetic analysis. *Biochemistry* **42**, 8831-41.
179. Sarafianos, S. G., Clark, A. D., Jr., Tuske, S., Squire, C. J., Das, K., Sheng, D., Ilankumaran, P., Ramesha, A. R., Kroth, H., Sayer, J. M., Jerina, D. M., Boyer, P. L., Hughes, S. H. & Arnold, E. (2003). Trapping HIV-1 reverse transcriptase before and after translocation on DNA. *J Biol Chem* **278**, 16280-8.
180. Tong, W., Lu, C. D., Sharma, S. K., Matsuura, S., So, A. G. & Scott, W. A. (1997). Nucleotide-induced stable complex formation by HIV-1 reverse transcriptase. *Biochemistry* **36**, 5749-57.
181. Sluis-Cremer, N., Arion, D., Parikh, U., Koontz, D., Schinazi, R. F., Mellors, J. W. & Parniak, M. A. (2005). The 3'-azido group is not the primary determinant of 3'-azido-3'-deoxythymidine (AZT) responsible for the excision phenotype of AZT-resistant HIV-1. *J Biol Chem* **280**, 29047-52.
182. Meyer, P. R., Matsuura, S. E., Schinazi, R. F., So, A. G. & Scott, W. A. (2000). Differential removal of thymidine nucleotide analogues from blocked DNA chains by human immunodeficiency virus reverse transcriptase in the presence of physiological concentrations of 2'-deoxynucleoside triphosphates. *Antimicrob Agents Chemother* **44**, 3465-72.
183. Margot, N. A., Isaacson, E., McGowan, I., Cheng, A. K., Schooley, R. T. & Miller, M. D. (2002). Genotypic and phenotypic analyses of HIV-1 in antiretroviral-experienced patients treated with tenofovir DF. *AIDS* **16**, 1227-35.
184. Scarth, B. J., White, K. L., Miller, M. D. & Gotte, M. (2009). Differences in Incorporation and Excision of Adenosine Analogues GS-9148 and Tenofovir by HIV-1 Reverse Transcriptase: Abstract 626. In *16th Conference on Retroviruses and Opportunistic Infections*, Montreal.
185. Cihlar, T., Ray, A. S., Boojamra, C. G., Zhang, L., Hui, H., Laflamme, G., Vela, J. E., Grant, D., Chen, J., Myrick, F., White, K. L., Gao, Y., Lin, K. Y.,

Douglas, J. L., Parkin, N. T., Carey, A., Pakdaman, R. & Mackman, R. L. (2008). Design and profiling of GS-9148, a novel nucleotide analog active against nucleoside-resistant variants of human immunodeficiency virus type 1, and its orally bioavailable phosphonoamidate prodrug, GS-9131. *Antimicrob Agents Chemother* **52**, 655-65.

186. Smith, A. J., Meyer, P. R., Asthana, D., Ashman, M. R. & Scott, W. A. (2005). Intracellular substrates for the primer-unblocking reaction by human immunodeficiency virus type 1 reverse transcriptase: detection and quantitation in extracts from quiescent- and activated-lymphocyte subpopulations. *Antimicrob Agents Chemother* **49**, 1761-9.
187. Smith, A. J. & Scott, W. A. (2006). The influence of natural substrates and inhibitors on the nucleotide-dependent excision activity of HIV-1 reverse transcriptase in the infected cell. *Curr Pharm Des* **12**, 1827-41.
188. Scarth, B., McCormick, S. & Gotte, M. (2010). Effects of Mutations F61A and A62V in the Fingers Subdomain of HIV-1 Reverse Transcriptase on the Translocational Equilibrium. *J Mol Biol* **405**, 349-60.
189. Meyer, P. R., Smith, A. J., Matsuura, S. E. & Scott, W. A. (2004). Effects of primer-template sequence on ATP-dependent removal of chain-terminating nucleotide analogues by HIV-1 reverse transcriptase. *J Biol Chem* **279**, 45389-98.
190. Scarth, B. J. & Gotte, M. (2008). High Phenotypic Resistance to AZT Correlates with an Increased Availability of Pre-translocated Complexes throughout the Viral Genome: Abstract 848. In *15th Conference on Retroviruses and Opportunistic Infections*, Boston.
191. Briones, C., Mas, A., Gomez-Mariano, G., Altisent, C., Menendez-Arias, L., Soriano, V. & Domingo, E. (2000). Dynamics of dominance of a dipeptide insertion in reverse transcriptase of HIV-1 from patients subjected to prolonged therapy. *Virus Res* **66**, 13-26.
192. Mas, A., Parera, M., Briones, C., Soriano, V., Martinez, M. A., Domingo, E. & Menendez-Arias, L. (2000). Role of a dipeptide insertion between codons 69 and 70 of HIV-1 reverse transcriptase in the mechanism of AZT resistance. *Embo J* **19**, 5752-61.
193. Boyer, P. L., Sarafianos, S. G., Arnold, E. & Hughes, S. H. (2002). Nucleoside analog resistance caused by insertions in the fingers of human immunodeficiency virus type 1 reverse transcriptase involves ATP-mediated excision. *J Virol* **76**, 9143-51.
194. Quinones-Mateu, M. E., Tadele, M., Parera, M., Mas, A., Weber, J., Rangel, H. R., Chakraborty, B., Clotet, B., Domingo, E., Menendez-Arias, L. & Martinez, M. A. (2002). Insertions in the reverse transcriptase increase both drug resistance and viral fitness in a human immunodeficiency virus type 1 isolate harboring the multi-nucleoside reverse transcriptase inhibitor resistance 69 insertion complex mutation. *J Virol* **76**, 10546-52.
195. Meyer, P. R., Lennerstrand, J., Matsuura, S. E., Larder, B. A. & Scott, W. A. (2003). Effects of dipeptide insertions between codons 69 and 70 of human immunodeficiency virus type 1 reverse transcriptase on primer unblocking,

deoxynucleoside triphosphate inhibition, and DNA chain elongation. *J Virol* **77**, 3871-7.

196. Matamoros, T., Franco, S., Vazquez-Alvarez, B. M., Mas, A., Martinez, M. A. & Menendez-Arias, L. (2004). Molecular determinants of multi-nucleoside analogue resistance in HIV-1 reverse transcriptases containing a dipeptide insertion in the fingers subdomain: effect of mutations D67N and T215Y on removal of thymidine nucleotide analogues from blocked DNA primers. *J Biol Chem* **279**, 24569-77.
197. White, K. L., Chen, J. M., Margot, N. A., Wrin, T., Petropoulos, C. J., Naeger, L. K., Swaminathan, S. & Miller, M. D. (2004). Molecular mechanisms of tenofovir resistance conferred by human immunodeficiency virus type 1 reverse transcriptase containing a diserine insertion after residue 69 and multiple thymidine analog-associated mutations. *Antimicrob Agents Chemother* **48**, 992-1003.
198. Cases-Gonzalez, C. E., Franco, S., Martinez, M. A. & Menendez-Arias, L. (2007). Mutational patterns associated with the 69 insertion complex in multi-drug-resistant HIV-1 reverse transcriptase that confer increased excision activity and high-level resistance to zidovudine. *J Mol Biol* **365**, 298-309.
199. Eggink, D., Huigen, M. C., Boucher, C. A., Gotte, M. & Nijhuis, M. (2007). Insertions in the beta3-beta4 loop of reverse transcriptase of human immunodeficiency virus type 1 and their mechanism of action, influence on drug susceptibility and viral replication capacity. *Antiviral Res* **75**, 93-103.
200. Tachedjian, G., Mellors, J., Bazmi, H., Birch, C. & Mills, J. (1996). Zidovudine resistance is suppressed by mutations conferring resistance of human immunodeficiency virus type 1 to foscarnet. *J Virol* **70**, 7171-81.
201. Boyer, P. L., Sarafianos, S. G., Arnold, E. & Hughes, S. H. (2002). The M184V mutation reduces the selective excision of zidovudine 5'-monophosphate (AZTMP) by the reverse transcriptase of human immunodeficiency virus type 1. *J Virol* **76**, 3248-56.
202. Parikh, U. M., Bacheler, L., Koontz, D. & Mellors, J. W. (2006). The K65R mutation in human immunodeficiency virus type 1 reverse transcriptase exhibits bidirectional phenotypic antagonism with thymidine analog mutations. *J Virol* **80**, 4971-7.
203. Parikh, U. M., Barnas, D. C., Faruki, H. & Mellors, J. W. (2006). Antagonism between the HIV-1 reverse-transcriptase mutation K65R and thymidine-analogue mutations at the genomic level. *J Infect Dis* **194**, 651-60.
204. White, K. L., Chen, J. M., Feng, J. Y., Margot, N. A., Ly, J. K., Ray, A. S., Macarthur, H. L., McDermott, M. J., Swaminathan, S. & Miller, M. D. (2006). The K65R reverse transcriptase mutation in HIV-1 reverses the excision phenotype of zidovudine resistance mutations. *Antivir Ther* **11**, 155-63.
205. Maag, H., Rydzewski, R. M., McRoberts, M. J., Crawford-Ruth, D., Verheyden, J. P. & Prisbe, E. J. (1992). Synthesis and anti-HIV activity of 4'-azido- and 4'-methoxynucleosides. *J Med Chem* **35**, 1440-51.
206. Michailidis, E., Marchand, B., Kodama, E. N., Singh, K., Matsuoka, M., Kirby, K. A., Ryan, E. M., Sawani, A. M., Nagy, E., Ashida, N., Mitsuya, H.,

Parniak, M. A. & Sarafianos, S. G. (2009). Mechanism of inhibition of HIV-1 reverse transcriptase by 4'-Ethynyl-2-fluoro-2'-deoxyadenosine triphosphate, a translocation-defective reverse transcriptase inhibitor. *J Biol Chem* **284**, 35681-91.

207. Boyer, P. L., Julias, J. G., Marquez, V. E. & Hughes, S. H. (2005). Fixed conformation nucleoside analogs effectively inhibit excision-proficient HIV-1 reverse transcriptases. *J Mol Biol* **345**, 441-50.
208. Soriano, V., Vispo, E., Labarga, P. & Barreiro, P. (2008). A low antiretroviral activity of the antihepatitis B drug entecavir may be enough to select for M184V in HIV-1. *AIDS* **22**, 911-2.
209. Tchesnokov, E. P., Obikhod, A., Schinazi, R. F. & Gotte, M. (2008). Delayed chain termination protects the anti-hepatitis B virus drug entecavir from excision by HIV-1 reverse transcriptase. *J Biol Chem* **283**, 34218-28.
210. Magee, W. C., Aldern, K. A., Hostetler, K. Y. & Evans, D. H. (2008). Cidofovir and (S)-9-[3-hydroxy-(2-phosphonomethoxy)propyl]adenine are highly effective inhibitors of vaccinia virus DNA polymerase when incorporated into the template strand. *Antimicrob Agents Chemother* **52**, 586-97.
211. Magee, W. C., Hostetler, K. Y. & Evans, D. H. (2005). Mechanism of inhibition of vaccinia virus DNA polymerase by cidofovir diphosphate. *Antimicrob Agents Chemother* **49**, 3153-62.
212. De Clercq, E. (1997). Acyclic nucleoside phosphonates in the chemotherapy of DNA virus and retrovirus infections. *Intervirology* **40**, 295-303.
213. Hostetler, K. Y., Aldern, K. A., Wan, W. B., Ciesla, S. L. & Beadle, J. R. (2006). Alkoxyalkyl esters of (S)-9-[3-hydroxy-2-(phosphonomethoxy)propyl]adenine are potent inhibitors of the replication of wild-type and drug-resistant human immunodeficiency virus type 1 in vitro. *Antimicrob Agents Chemother* **50**, 2857-9.
214. Noormohamed, F. H., Youle, M. S., Higgs, C. J., Martin-Munley, S., Gazzard, B. G. & Lant, A. F. (1998). Pharmacokinetics and absolute bioavailability of oral foscarnet in human immunodeficiency virus-seropositive patients. *Antimicrobial agents and chemotherapy* **42**, 293-7.
215. Gerard, L. & Salmon-Ceron, D. (1995). Pharmacology and clinical use of foscarnet. *International journal of antimicrobial agents* **5**, 209-17.
216. Canestri, A., Ghosn, J., Wirden, M., Marguet, F., Ktorza, N., Boubezari, I., Dominguez, S., Bossi, P., Caumes, E., Calvez, V. & Katlama, C. (2006). Foscarnet salvage therapy for patients with late-stage HIV disease and multiple drug resistance. *Antivir Ther* **11**, 561-6.
217. Mathiesen, S., Dam, E., Roge, B., Joergensen, L. B., Laursen, A. L., Gerstoft, J. & Clavel, F. (2007). Long-term foscarnet therapy remodels thymidine analogue mutations and alters resistance to zidovudine and lamivudine in HIV-1. *Antivir Ther* **12**, 335-43.
218. Arion, D., Sluis-Cremer, N. & Parniak, M. A. (2000). Mechanism by which phosphonoformic acid resistance mutations restore 3'-azido-3'-deoxythymidine (AZT) sensitivity to AZT-resistant HIV-1 reverse transcriptase. *J Biol Chem* **275**, 9251-5.

219. Meyer, P. R., Matsuura, S. E., Zonarich, D., Chopra, R. R., Pendarvis, E., Bazmi, H. Z., Mellors, J. W. & Scott, W. A. (2003). Relationship between 3'-azido-3'-deoxythymidine resistance and primer unblocking activity in foscarnet-resistant mutants of human immunodeficiency virus type 1 reverse transcriptase. *J Virol* **77**, 6127-37.
220. Hammond, J. L., Koontz, D. L., Bazmi, H. Z., Beadle, J. R., Hostetler, S. E., Kini, G. D., Aldern, K. A., Richman, D. D., Hostetler, K. Y. & Mellors, J. W. (2001). Alkylglycerol prodrugs of phosphonoformate are potent in vitro inhibitors of nucleoside-resistant human immunodeficiency virus type 1 and select for resistance mutations that suppress zidovudine resistance. *Antimicrob Agents Chemother* **45**, 1621-8.
221. Sarafianos, S. G., Pandey, V. N., Kaushik, N. & Modak, M. J. (1995). Site-directed mutagenesis of arginine 72 of HIV-1 reverse transcriptase. Catalytic role and inhibitor sensitivity. *J Biol Chem* **270**, 19729-35.
222. Fisher, T. S. & Prasad, V. R. (2002). Substitutions of Phe61 located in the vicinity of template 5'-overhang influence polymerase fidelity and nucleoside analog sensitivity of HIV-1 reverse transcriptase. *J Biol Chem* **277**, 22345-52.
223. Fisher, T. S., Darden, T. & Prasad, V. R. (2003). Substitutions at Phe61 in the beta3-beta4 hairpin of HIV-1 reverse transcriptase reveal a role for the Fingers subdomain in strand displacement DNA synthesis. *J Mol Biol* **325**, 443-59.
224. Mandal, D., Dash, C., Le Grice, S. F. & Prasad, V. R. (2006). Analysis of HIV-1 replication block due to substitutions at F61 residue of reverse transcriptase reveals additional defects involving the RNase H function. *Nucleic Acids Res* **34**, 2853-63.
225. Upadhyay, A. K., Talele, T. T. & Pandey, V. N. (2010). Impact of template overhang-binding region of HIV-1 RT on the binding and orientation of the duplex region of the template-primer. *Mol Cell Biochem* **338**, 19-33.
226. Jochmans, D., kesteleyn, B., Marchand, B., Gotte, M., Ivens, T., Dehertogh, P., Peeters, A., Pauwels, R., Wigerinck, P., and Hertogs, K. . (2005). Identification and Biochemical Characterization of a New Class of HIV Inhibitors: Nucleotide-competing Reverse Transcriptase Inhibitors. In *Conference of Retroviruses and Opportunistic Infections*, Vol. Abstratc 156.
227. Ehteshami, M., Scarth, B. J., Tchesnokov, E. P., Dash, C., Le Grice, S. F., Hallenberger, S., Jochmans, D. & Gotte, M. (2008). Mutations M184V and Y115F in HIV-1 reverse transcriptase discriminate against "nucleotide-competing reverse transcriptase inhibitors". *J Biol Chem* **283**, 29904-11.
228. Zhou, Z., Lin, X. & Madura, J. D. (2006). HIV-1 RT nonnucleoside inhibitors and their interaction with RT for antiviral drug development. *Infect Disord Drug Targets* **6**, 391-413.
229. Sluis-Cremer, N., Temiz, N. A. & Bahar, I. (2004). Conformational changes in HIV-1 reverse transcriptase induced by nonnucleoside reverse transcriptase inhibitor binding. *Curr HIV Res* **2**, 323-32.
230. Ren, J. & Stammers, D. K. (2008). Structural basis for drug resistance mechanisms for non-nucleoside inhibitors of HIV reverse transcriptase. *Virus Res* **134**, 157-70.

231. Yap, S. H., Sheen, C. W., Fahey, J., Zanin, M., Tyssen, D., Lima, V. D., Wynhoven, B., Kuiper, M., Sluis-Cremer, N., Harrigan, P. R. & Tachedjian, G. (2007). N348I in the connection domain of HIV-1 reverse transcriptase confers zidovudine and nevirapine resistance. *PLoS Med* **4**, e335.
232. Biondi, M. J., Beilhartz, G. L., McCormick, S. & Gotte, M. (2010). N348I in HIV-1 reverse transcriptase can counteract the nevirapine-mediated bias toward RNase H cleavage during plus-strand initiation. *J Biol Chem*.
233. de Bethune, M. P. (2010). Non-nucleoside reverse transcriptase inhibitors (NNRTIs), their discovery, development, and use in the treatment of HIV-1 infection: a review of the last 20 years (1989-2009). *Antiviral Res* **85**, 75-90.
234. Das, K., Clark, A. D., Jr., Lewi, P. J., Heeres, J., De Jonge, M. R., Koymans, L. M., Vinkers, H. M., Daeyaert, F., Ludovici, D. W., Kukla, M. J., De Corte, B., Kavash, R. W., Ho, C. Y., Ye, H., Lichtenstein, M. A., Andries, K., Pauwels, R., De Bethune, M. P., Boyer, P. L., Clark, P., Hughes, S. H., Janssen, P. A. & Arnold, E. (2004). Roles of conformational and positional adaptability in structure-based design of TMC125-R165335 (etravirine) and related non-nucleoside reverse transcriptase inhibitors that are highly potent and effective against wild-type and drug-resistant HIV-1 variants. *J Med Chem* **47**, 2550-60.
235. Das, K., Bauman, J. D., Clark, A. D., Jr., Frenkel, Y. V., Lewi, P. J., Shatkin, A. J., Hughes, S. H. & Arnold, E. (2008). High-resolution structures of HIV-1 reverse transcriptase/TMC278 complexes: strategic flexibility explains potency against resistance mutations. *Proc Natl Acad Sci U S A* **105**, 1466-71.
236. Girardet, J. L., Koh, Y. H., De La Rosa, M., Gunic, E., Zhang, Z., Hamatake, R. & Yeh, L. T. (2007). The discovery of RDEA806, a Potent New HIV NNRTI in Phase 1 Clinical Trials. In *47th ICAAC Conference*, Chicago.
237. Maga, G., Radi, M., Zanoli, S., Manetti, F., Cancio, R., Hubscher, U., Spadari, S., Falciani, C., Terrazas, M., Vilarrasa, J. & Botta, M. (2007). Discovery of non-nucleoside inhibitors of HIV-1 reverse transcriptase competing with the nucleotide substrate. *Angew Chem Int Ed Engl* **46**, 1810-3.
238. Freisz, S., Bec, G., Radi, M., Wolff, P., Crespan, E., Angeli, L., Dumas, P., Maga, G., Botta, M. & Ennifar, E. (2010). Crystal structure of HIV-1 reverse transcriptase bound to a non-nucleoside inhibitor with a novel mechanism of action. *Angew Chem Int Ed Engl* **49**, 1805-8.
239. Coffin, J. (1996). Retroviridae: The viruses and their replication. In *Fundamental virology.*, pp. 763–843. Lippincott-Raven, Philadelphia.
240. Gotte, M. (2006). Effects of nucleotides and nucleotide analogue inhibitors of HIV-1 reverse transcriptase in a ratchet model of polymerase translocation. *Curr Pharm Des* **12**, 1867-77.
241. Mathiesen, S., Roge, B. T., Weis, N., Lundgren, J. D., Obel, N. & Gerstoft, J. (2004). Foscarnet used in salvage therapy of HIV-1 patients harbouring multiple nucleotide excision mutations. *AIDS* **18**, 1076-8.
242. Meyer, P. R., Matsuura, S. E., Mian, A. M., So, A. G. & Scott, W. A. (1999). A mechanism of AZT resistance: an increase in nucleotide-dependent primer unblocking by mutant HIV-1 reverse transcriptase. *Mol Cell* **4**, 35-43.

243. Sarafianos, S. G., Das, K., Ding, J., Boyer, P. L., Hughes, S. H. & Arnold, E. (1999). Touching the heart of HIV-1 drug resistance: the fingers close down on the dNTP at the polymerase active site. *Chem Biol* **6**, R137-46.
244. Garforth, S. J., Kim, T. W., Parniak, M. A., Kool, E. T. & Prasad, V. R. (2007). Site-directed mutagenesis in the fingers subdomain of HIV-1 reverse transcriptase reveals a specific role for the beta3-beta4 hairpin loop in dNTP selection. *J Mol Biol* **365**, 38-49.
245. Shirasaka, T., Kavlick, M. F., Ueno, T., Gao, W. Y., Kojima, E., Alcaide, M. L., Chokekijchai, S., Roy, B. M., Arnold, E., Yarchoan, R. & et al. (1995). Emergence of human immunodeficiency virus type 1 variants with resistance to multiple dideoxynucleosides in patients receiving therapy with dideoxynucleosides. *Proc Natl Acad Sci U S A* **92**, 2398-402.
246. Mas, A., Vazquez-Alvarez, B. M., Domingo, E. & Menendez-Arias, L. (2002). Multidrug-resistant HIV-1 reverse transcriptase: involvement of ribonucleotide-dependent phosphorolysis in cross-resistance to nucleoside analogue inhibitors. *J Mol Biol* **323**, 181-97.
247. Deval, J., Alvarez, K., Selmi, B., Bermond, M., Boretto, J., Guerreiro, C., Mulard, L. & Canard, B. (2005). Mechanistic insights into the suppression of drug resistance by human immunodeficiency virus type 1 reverse transcriptase using alpha-boranophosphate nucleoside analogs. *J Biol Chem* **280**, 3838-46.
248. Le Grice, S. F. & Gruninger-Leitch, F. (1990). Rapid purification of homodimer and heterodimer HIV-1 reverse transcriptase by metal chelate affinity chromatography. *Eur J Biochem* **187**, 307-14.
249. Sharma, B., Kaushik, N., Upadhyay, A., Tripathi, S., Singh, K. & Pandey, V. N. (2003). A positively charged side chain at position 154 on the beta8-alphaE loop of HIV-1 RT is required for stable ternary complex formation. *Nucleic Acids Res* **31**, 5167-74.
250. Tuske, S., Sarafianos, S. G., Clark, A. D., Jr., Ding, J., Naeger, L. K., White, K. L., Miller, M. D., Gibbs, C. S., Boyer, P. L., Clark, P., Wang, G., Gaffney, B. L., Jones, R. A., Jerina, D. M., Hughes, S. H. & Arnold, E. (2004). Structures of HIV-1 RT-DNA complexes before and after incorporation of the anti-AIDS drug tenofovir. *Nat Struct Mol Biol* **11**, 469-74.
251. Zhang, Z., Walker, M., Xu, W., Shim, J. H., Girardet, J. L., Hamatake, R. K. & Hong, Z. (2006). Novel nonnucleoside inhibitors that select nucleoside inhibitor resistance mutations in human immunodeficiency virus type 1 reverse transcriptase. *Antimicrob Agents Chemother* **50**, 2772-81.
252. Gotte, M., Rausch, J. W., Marchand, B., Sarafianos, S. & Le Grice, S. F. (2010). Reverse transcriptase in motion: conformational dynamics of enzyme-substrate interactions. *Biochim Biophys Acta* **1804**, 1202-12.
253. Jochmans, D. (2008). Novel HIV-1 reverse transcriptase inhibitors. *Virus Res* **134**, 171-85.
254. Huang, J. & Sousa, R. (2000). T7 RNA polymerase elongation complex structure and movement. *Journal of molecular biology* **303**, 347-58.
255. Kerr, S. G. & Anderson, K. S. (1997). RNA dependent DNA replication fidelity of HIV-1 reverse transcriptase: evidence of discrimination between DNA and RNA substrates. *Biochemistry* **36**, 14056-63.

256. Reardon, J. E. (1993). Human immunodeficiency virus reverse transcriptase. A kinetic analysis of RNA-dependent and DNA-dependent DNA polymerization. *The Journal of biological chemistry* **268**, 8743-51.
257. Svarovskaia, E. S., Feng, J. Y., Margot, N. A., Myrick, F., Goodman, D., Ly, J. K., White, K. L., Kutty, N., Wang, R., Borroto-Esoda, K. & Miller, M. D. (2008). The A62V and S68G mutations in HIV-1 reverse transcriptase partially restore the replication defect associated with the K65R mutation. *Journal of acquired immune deficiency syndromes* **48**, 428-36.
258. Thrall, S. H., Krebs, R., Wohrl, B. M., Cellai, L., Goody, R. S. & Restle, T. (1998). Pre-steady-state kinetic characterization of RNA-primed initiation of transcription by HIV-1 reverse transcriptase and analysis of the transition to a processive DNA-primed polymerization mode. *Biochemistry* **37**, 13349-58.
259. Zinnen, S., Hsieh, J. C. & Modrich, P. (1994). Misincorporation and mispaired primer extension by human immunodeficiency virus reverse transcriptase. *The Journal of biological chemistry* **269**, 24195-202.
260. Das, K., Bandwar, R. P., White, K. L., Feng, J. Y., Sarafianos, S. G., Tuske, S., Tu, X., Clark, A. D., Jr., Boyer, P. L., Hou, X., Gaffney, B. L., Jones, R. A., Miller, M. D., Hughes, S. H. & Arnold, E. (2009). Structural basis for the role of the K65R mutation in HIV-1 reverse transcriptase polymerization, excision antagonism, and tenofovir resistance. *J Biol Chem* **284**, 35092-100.
261. Kulkarni, R., Margot, N. A., Myrick, F., Svarovskaia, J., Chen, J., Landson, E., Ray, A. S., Cihlar, T., Swaminathan, S., Miller, M. D. & White, K. L. (2009). The HIV-1 RT mutant Q151L shows decreased replication capacity, selective high-level resistance to GS-9148 and hypersusceptibility to tenofovir and zidovudine. *Antiviral Therapy* **14 Suppl 1** A20.
262. Cihlar, T., Laflamme, G., Fisher, R., Carey, A. C., Vela, J. E., Mackman, R. & Ray, A. S. (2009). Novel nucleotide human immunodeficiency virus reverse transcriptase inhibitor GS-9148 with a low nephrotoxic potential: characterization of renal transport and accumulation. *Antimicrob Agents Chemother* **53**, 150-6.
263. Ray, A. S., Vela, J. E., Boojamra, C. G., Zhang, L., Hui, H., Callebaut, C., Stray, K., Lin, K. Y., Gao, Y., Mackman, R. L. & Cihlar, T. (2008). Intracellular metabolism of the nucleotide prodrug GS-9131, a potent anti-human immunodeficiency virus agent. *Antimicrob Agents Chemother* **52**, 648-54.
264. Boojamra, C. G., Mackman, R. L., Markevitch, D. Y., Prasad, V., Ray, A. S., Douglas, J., Grant, D., Kim, C. U. & Cihlar, T. (2008). Synthesis and anti-HIV activity of GS-9148 (2'-Fd4AP), a novel nucleoside phosphonate HIV reverse transcriptase inhibitor. *Bioorg Med Chem Lett* **18**, 1120-3.
265. Laflamme, G., Grant, D., White, K. L., Stray, K., Boojamra, C. G., Zhang, L., Mackman, R., Ray, A. S., Miller, M. D. & Cihlar, T. (2007). Novel Nucleotide Inhibitor GS-9148 Selects for a K70E Mutation in HIV-1 Reverse Transcriptase and Low-Level Resistance In Vitro. In *Interscience Conference on Antimicrobial Agents and Chemotherapy*, Chicago, Illinois.
266. Domaoal, R. A., McMahon, M., Thio, C. L., Bailey, C. M., Tirado-Rives, J., Obikhod, A., Detorio, M., Rapp, K. L., Siliciano, R. F., Schinazi, R. F. &

Anderson, K. S. (2008). Pre-steady-state kinetic studies establish entecavir 5'-triphosphate as a substrate for HIV-1 reverse transcriptase. *J Biol Chem* **283**, 5452-9.

267. Lansdon, E. B., Samuel, D., Lagpacan, L., Brendza, K. M., White, K. L., Hung, M., Liu, X., Boojamra, C. G., Mackman, R. L., Cihlar, T., Ray, A. S., McGrath, M. E. & Swaminathan, S. (2010). Visualizing the molecular interactions of a nucleotide analog, GS-9148, with HIV-1 reverse transcriptase-DNA complex. *J Mol Biol* **397**, 967-78.
268. Ly, J. K., Margot, N. A., MacArthur, H. L., Hung, M., Miller, M. D. & White, K. L. (2007). The balance between NRTI discrimination and excision drives the susceptibility of HIV-1 RT mutants K65R, M184V and K65r+M184V. *Antivir Chem Chemother* **18**, 307-16.
269. Gotte, M., Arion, D., Parniak, M. A. & Wainberg, M. A. (2000). The M184V mutation in the reverse transcriptase of human immunodeficiency virus type 1 impairs rescue of chain-terminated DNA synthesis. *J Virol* **74**, 3579-85.
270. Cases-Gonzalez, C. E., Gutierrez-Rivas, M. & Menendez-Arias, L. (2000). Coupling ribose selection to fidelity of DNA synthesis. The role of Tyr-115 of human immunodeficiency virus type 1 reverse transcriptase. *J Biol Chem* **275**, 19759-67.
271. Powdrill, M. H., Bernatchez, J. A. & Gotte, M. (2010). Inhibitors of the Hepatitis C Virus RNA-Dependent RNA Polymerase NS5B. *Viruses* **2**, 2169-2195.
272. Feng, J. Y. & Anderson, K. S. (1999). Mechanistic studies examining the efficiency and fidelity of DNA synthesis by the 3TC-resistant mutant (184V) of HIV-1 reverse transcriptase. *Biochemistry* **38**, 9440-8.
273. Gotte, M., Kameoka, M., McLellan, N., Cellai, L. & Wainberg, M. A. (2001). Analysis of efficiency and fidelity of HIV-1 (+)-strand DNA synthesis reveals a novel rate-limiting step during retroviral reverse transcription. *J Biol Chem* **276**, 6711-9.
274. Kagan, R. M., Lee, T. S., Ross, L., Lloyd, R. M., Jr., Lewinski, M. A. & Potts, S. J. (2007). Molecular basis of antagonism between K70E and K65R tenofovir-associated mutations in HIV-1 reverse transcriptase. *Antiviral research* **75**, 210-8.